

Hadronic atoms in QCD + QED

November 16, 2007

J. Gasser ^a, V.E. Lyubovitskij ^{b,†} and A. Rusetsky ^{c,‡}

^a Institut für theoretische Physik, Universität Bern
Sidlerstr. 5, CH–3012 Bern, Switzerland

^b Institut für Theoretische Physik, Universität Tübingen
Auf der Morgenstelle 14, D–72076 Tübingen, Germany

^c Helmholtz–Institut für Strahlen– und Kernphysik,
Universität Bonn, Nussallee 14–16, D–53115 Bonn, Germany

[†] On leave of absence from: Department of Physics,
Tomsk State University, 634050 Tomsk, Russia

[‡] On leave of absence from: High Energy Physics Institute,
Tbilisi State University, University St. 9, 380086 Tbilisi, Georgia

Abstract

We review the theory of hadronic atoms in QCD + QED, based on a non-relativistic effective Lagrangian framework. We first provide an introduction to the theory, and then describe several applications: meson–meson, meson–nucleon atoms and meson–deuteron compounds. Finally, we compare the quantum field theory framework used here with the traditional approach, which is based on quantum–mechanical potential scattering.

Pacs: 36.10.Gv, 12.39.Fe, 11.10.St
Keywords: Hadronic atoms, QCD, QED, Chiral perturbation theory,
Non-relativistic effective Lagrangians

Corresponding Author: Akaki Rusetsky
Tel: +49 228 732372, Fax: +49 228 733728
Email: rusetsky@itkp.uni-bonn.de

Contents

1	Introduction	4
2	Physics background	9
2.1	Pionium	10
2.2	πK atom	12
2.3	Pionic hydrogen and pionic deuterium	13
2.4	Kaonic hydrogen and kaonic deuterium	15
3	Non-relativistic effective theories: strong sector	17
3.1	Introductory remarks	17
3.2	The Lagrangian and the reduction formulae	18
3.3	Matching condition	21
3.4	Tree level	22
3.5	Loops	22
3.6	Relation to the effective range expansion	25
4	Non-relativistic effective theories: including photons	26
4.1	The Lagrangian	26
4.2	Perturbation theory	28
4.3	Coulomb photons	29
4.4	Transverse photons and the threshold expansion	31
4.5	Matching	34
5	Bound states	37
5.1	Introductory remarks	37
5.2	Coulomb problem	37
5.3	Feshbach formalism and the Rayleigh-Schrödinger perturbation theory	39
5.4	Energy levels	41
5.5	Decay into 2 photons	44
5.6	Vacuum polarization due to electrons	45
5.7	Energy shift and width: summary	47
6	On DGBT formulae in ChPT	48
6.1	Electromagnetic corrections in scalar QED	48
6.2	Isospin breaking effects in ChPT	50
7	Hadronic atoms and scattering lengths:	
	General observations	53
7.1	Counting rules for the widths	53
7.2	Spectrum and scattering lengths	55

8 Pionium	56
8.1 DIRAC experiment at CERN	56
8.2 Two-channel problem	57
8.3 DGBT formula and numerical analysis	60
8.4 Two-photon decay of pionium	63
9 πK atom	64
10 Pionic hydrogen	67
10.1 Pionic hydrogen experiments at PSI	67
10.2 Effective theory and counting rules	70
10.3 Matching	72
10.4 Bound state – electromagnetic shift	74
10.5 DGBT formula for πH	76
10.6 Isospin breaking corrections and data analysis	77
11 Kaonic hydrogen	82
11.1 The kaonic hydrogen and kaonic deuterium experiments at DAΦNE	82
11.2 DGBT-type formulae for kaonic hydrogen	83
11.3 Analysis of the DEAR data	87
12 Pionic and kaonic deuterium	91
12.1 Introductory remarks and DGBT formulae	91
12.2 Pion–deuteron scattering	93
12.3 Isospin breaking in the πd scattering length	95
12.4 Kaon–deuteron scattering	100
13 Potential scattering theory	103
14 Summary and outlook	105
A Notation	109
A.1 General	109
A.2 Coulombic bound states	109
A.3 Master equation	111
A.4 Energy shift of the atom	111
A.5 Threshold amplitude	112
A.6 Real part of the threshold amplitudes	114
A.7 Two-particle phase space	115
A.8 Panofsky ratio	115
B Generalized unitarity	116
C Matching and unitarity	117

1 Introduction

Consider a hydrogen atom, and replace the electron with a negatively charged pion. This compound is called *pionic hydrogen* and is the simplest example of a *hadronic atom*. In many aspects, the properties of hadronic atoms are similar to those of the hydrogen atom, because both bound states are predominantly formed by the static Coulomb force. The typical size of pionic hydrogen e.g. is characterized by its Bohr radius

$$r_B = (\alpha\mu_c)^{-1}, \quad \mu_c = m_p M_\pi (m_p + M_\pi)^{-1}, \quad (1.1)$$

where $\alpha \simeq 1/137$ denotes the fine-structure constant, and where μ_c is the reduced mass of the system. The mass of the proton and of the charged pion are denoted by m_p and M_π , respectively. The distance $r_B \simeq 220$ fm is much smaller than the hydrogen radius, but still much larger than the range of strong interactions, which is typically of the order of a few fm. It is for this reason that strong interactions do not change the structure of the bound-state spectrum in a profound manner. At leading order in an expansion in α , the energy of *S*-wave states of pionic hydrogen is still given by the standard quantum-mechanical formula

$$E_n = m_p + M_\pi - \frac{\mu_c \alpha^2}{2n^2}, \quad n = 1, 2, \dots \quad (1.2)$$

However, in distinction to ordinary hydrogen, the ground state of pionic hydrogen is unstable. It decays mainly via the charge-exchange reaction $\pi^- p \rightarrow \pi^0 n$, and via the electromagnetic channel $\pi^- p \rightarrow \gamma n$, with width $\Gamma_1 \sim 1$ eV [1]. This corresponds to a lifetime $\tau_1 \sim 10^{-15}$ s, which is much smaller than the lifetime of the charged pion, $\tau_\pi \sim 10^{-8}$ s, so that the pion in the atom can be considered a practically stable particle. Despite of its short lifetime, pionic hydrogen can be considered a quasi-stable bound state, since the pion travels many times around the proton before decaying, as the ratio $\frac{1}{2} \mu_c \alpha^2 / \Gamma_1 \sim 10^3$ indicates.

To understand the significance of experiments performed with hadronic atoms, we imagine a simplified picture, where the interaction between the constituents of a hadronic atom consists of only two terms: the long-range Coulomb part and the short-range strong interaction. Equation (1.2) describes the bound-state spectrum only approximately, at leading order in an expansion in α . The leading correction to Eq. (1.2), which emerges at order α^3 , is due to strong interactions only – there is no interference between Coulomb and strong interactions at this order. Consequently, measuring very accurately the difference between the true energy levels of pionic hydrogen and their pure Coulomb values Eq. (1.2), one can extract information about the strong interactions between the pion and the proton. Because the size of the atom is much larger than the characteristic radius of strong interactions, the bound-state observables can feel only the low-momentum behavior of the strong pion-nucleon *S*-matrix – in other words,

the energy shift must be expressed in terms of the threshold parameters of the pion–nucleon scattering amplitude: the scattering lengths, effective ranges, etc. Because the characteristic 3-momenta of the hadrons within the atom are of size $|\mathbf{p}_{\text{av}}| \simeq r_B^{-1} = \alpha\mu_c \propto \alpha$, the relative strength of the corrections which contain scattering lengths, effective ranges, \dots should be ordered according to $1 : \alpha^2 : \dots$. As a result of this, the leading–order energy shift depends only on the pion–nucleon scattering lengths. The situation closely resembles a well–known example in classical electrodynamics, which tells us that an arbitrarily complicated charge distribution can be characterized by a few parameters of the multipole expansion, if the distance to the system is much larger than the size of the system itself. It is also clear, why the observables of the atom cannot depend on anything else but on the threshold parameters of the pion–nucleon amplitude: the distances characteristic for the atom are already asymptotic for the pion–nucleon system, where nothing but the S -matrix elements can be observed. In other words, the measurement of the observables of the pionic hydrogen does not probe the inner region of the pion–nucleon interaction.

The insensitivity of the pionic hydrogen observables to the short–range details of the pion–nucleon interaction is very fortunate: it provides us with the possibility to directly extract the values of the pion–nucleon scattering lengths from atomic experiments. A different method for determining the same quantities is to measure the scattering cross sections at different energies, and to extrapolate the result to threshold [2–7]. The former method, however, is free from the difficulties which are related to this extrapolation procedure. This property is even more important in other hadronic systems, where the scattering amplitude near threshold is hardly accessible by other experimental technique.

Deser, Goldberger, Baumann and Thirring (DGBT) were the first who derived the model–independent relation between the (complex) energy shift of the ground state in pionic hydrogen and the strong pion–nucleon scattering amplitude at leading order in α [8]. The result reads¹

$$\Delta E_1^{\text{str}} - \frac{i}{2} \Gamma_1 = -\frac{2\pi}{\mu_c} |\tilde{\Psi}_{10}(0)|^2 A(\pi^- p \rightarrow \pi^- p) + O(\alpha^4), \quad (1.3)$$

where $|\tilde{\Psi}_{10}(0)|^2 = \alpha^3 \mu_c^3 / \pi$ denotes the square of the Coulomb wave function of the atom at the origin and is, therefore, a measure of the probability that the charged pion and the proton in the atom come very close to each other. Further, $A(\pi^- p \rightarrow \pi^- p)$ is the $\pi^- p$ elastic scattering amplitude at threshold, which describes strong interactions between these particles after they come close. The scattering amplitude is normalized so that

$$A(\pi^- p \rightarrow \pi^- p) = a_{0+}^+ + a_{0+}^- + \dots \quad (1.4)$$

¹We use throughout the Landau symbols $O(x)$ [$o(x)$] for quantities that vanish like x [faster than x] when x tends to zero. Furthermore, it is understood that this holds modulo logarithmic terms, i.e. we write also $O(x)$ for $x \ln x$.

Here, the quantities on the r.h.s. denote the S -wave πN isospin even/odd scattering lengths, which are defined according to Ref. [2], and the ellipsis stands for isospin breaking terms.

The imaginary part of the quantity $A(\pi^- p \rightarrow \pi^- p)$ is given by unitarity. For simplicity, let us assume for a moment that the atom decays only into the strong channel $\pi^- p \rightarrow \pi^0 n$. Then, the imaginary part is²

$$\text{Im} A(\pi^- p \rightarrow \pi^- p) = 2p^* |A(\pi^- p \rightarrow \pi^0 n)|^2, \quad (1.5)$$

where p^* is the CM momentum of the outgoing π^0 in the scattering process $\pi^- p \rightarrow \pi^0 n$ at threshold. The normalization is chosen such that, in the isospin limit, the threshold amplitude is $A(\pi^- p \rightarrow \pi^0 n) = -a_{0+}^-$. Finally, the decay width Γ_1 of the ground state is calculated from Eqs. (1.3, 1.5). Therefore, measuring the spectrum of pionic atoms provides information on the pion–nucleon scattering lengths.

Hadronic scattering lengths are important low–energy characteristics of quantum chromodynamics (QCD) for the following reason. At small momenta of order of the pion mass, QCD can be described by a low–energy effective field theory (EFT), which contains only hadronic degrees of freedom – the approach goes under the name chiral perturbation theory (ChPT) [9]. The crucial point is that, in certain cases, (e.g., for $\pi\pi$ scattering [10–15]), it is possible to obtain a very accurate prediction for the hadronic scattering lengths in ChPT and, consequently, comparing the theoretical values with the results obtained in the experiment, one can perform a direct study of the properties of the low–energy QCD. For a method which does not make use of chiral symmetry to determine the scattering lengths, see Refs. [16]. Scattering lengths in the framework of pure QCD can now also be determined from numerical simulations of QCD on a lattice [17], see also the reviews by Leutwyler [18] and Colangelo [19]. Last but not least, the hadronic scattering lengths often serve as an input in the determination of other important low–energy characteristics of strong interactions (like the pion–nucleon σ -term [20] or the πNN coupling constant [21–23] in the case of the pion–nucleon scattering lengths). Below, we discuss the fundamental physics content of various hadronic scattering lengths. Here we merely note that the knowledge of the exact values of these quantities would greatly advance our knowledge of the fundamental features of strong interactions, allowing for a variety of high–precision tests of QCD at low energy.

²Note that, as we shall see below, adding the second decay channel $\pi^- p \rightarrow \gamma n$ merely leads to the replacement $\text{Im} A(\pi^- p \rightarrow \pi^- p) \rightarrow (1 + P^{-1}) \text{Im} A(\pi^- p \rightarrow \pi^- p)$, where $P = \sigma(\pi^- p \rightarrow \pi^0 n)/\sigma(\pi^- p \rightarrow \gamma n)$ is the so–called Panofsky ratio $P \simeq 1.546$, which describes the relative probability for the “strong” and “electromagnetic” decay channels. Since the value of the Panofsky ratio is taken from other measurements and is thus considered to be an input in the analysis of the pionic hydrogen data, this analysis proceeds exactly similar to the 1-channel case.

In order to carry out the comparison of the experimentally determined hadronic scattering lengths with the theoretical predictions, the accuracy of the lowest-order formulae, analogous to Eq. (1.3), is not sufficient in most cases. For this reason, there have been numerous attempts to improve the accuracy in these relations by including electromagnetic corrections and strong isospin breaking effects. These investigations had first been carried out within the framework of potential scattering theory: strong interactions are described by potentials, assumed to be isospin symmetric. Isospin violation then stems from Coulomb corrections, from the mass differences in the free Green functions (masses of all particles involved are put equal to their physical masses), from the coupling to the electromagnetic channels, etc. Unfortunately, the results of potential-model-based calculations turned out to be not unique – in some cases, they even differ to an extent that matters at the level of the experimental precision.

The following two comments are in order at this point.

- i) The scattering lengths which one attempts to extract from the investigation of hadronic atoms are the ones in pure QCD, in the isospin symmetry limit $m_u = m_d$. In particular, the electromagnetic effects are switched off. In potential scattering theory, the Coulomb potential can be easily turned on or off. It is however well known that splitting off electromagnetic effects in quantum field theory (QFT) is ambiguous and leads in general to scale dependent results.
- ii) Whereas the relation of hadronic atom observables to the threshold parameters in the hadron-hadron scattering amplitude is universal, the relation of these threshold parameters to the purely hadronic scattering lengths is not universal and depends on a complicated interplay of strong and electromagnetic interactions. Potential models do not include the full content of isospin breaking effects *ab initio* and therefore do not, in general, suffice to work out this relation. For example, the effects due to the short-range electromagnetic interactions and the quark mass dependence of the hadronic scattering amplitudes – which naturally emerge in ChPT – are omitted in simple hadronic potentials. On the other hand, in many cases the bulk of the total correction is provided exactly by these omitted terms.

These two points illustrate the major challenge to any theoretical investigation: in order to be able to fully exploit the high-precision data from present and future experiments on hadronic atoms, one needs a systematic framework to relate hadronic atom characteristics to observables of the underlying theory. Chiral perturbation theory is an obvious candidate for such a framework. However, despite remarkable progress in describing low-energy scattering processes with *elementary hadrons* in ChPT, the study of *bound states* within the same theory remained terra incognita for a long time. In certain cases, the problem could be solved by brute force with the use of methods of QFT, namely, Bethe-Salpeter

equation or quasipotential reductions thereof [24–30]. On the other hand, the matter turned out to be very involved in general – it became obvious that new ideas are needed to overcome the difficulties on the way towards a general theory of hadronic atoms in QCD+QED.

A crucial observation was that the calculation of the spectrum of hadronic atoms can be treated separately from the chiral expansion [31–36]. The reason for this consists in the large difference of the pertinent momentum scales: whereas the characteristic momenta in ChPT are of order of the pion mass, the typical bound–state momentum is the inverse of the Bohr radius. This difference in scales prompts using a non–relativistic effective Lagrangian approach to bound states, which has first been introduced by Caswell and Lepage in the framework of QED [37].

Let us shortly describe the pertinent low–energy EFT, which is valid at typical momenta of size $|\mathbf{p}| \ll M_\pi$. The structure of this EFT is much simpler than the structure of ChPT, for the following reasons. i) As just mentioned, the system can be described by means of an effective non–relativistic Lagrangian. Relativistic corrections are included in a perturbative manner. In bound–states, these corrections will obviously contribute at higher orders in α , because \mathbf{p} is a quantity of order α . ii) The bound states in the non–relativistic theory are described by a Schrödinger equation, instead of the Bethe–Salpeter equation. This leads to dramatic simplifications and allows one to design a systematic perturbative approach to the calculation of the bound–state observables on the basis of the Feshbach formalism [38, 39]. Finally, the parameters of the effective Lagrangian are determined by matching this theory to ChPT in the scattering sector. At the end of the calculation, the reference to the (auxiliary) non–relativistic EFT completely disappears from the final results, which express the observables of hadronic atoms in terms of the parameters of ChPT.

The application of the above simple idea for the description of hadronic atoms turned out to be very fruitful. Indeed, within a few years, most of the (theoretically) relevant hadronic bound states have been revisited using this approach (see, e.g., Refs. [36, 40–49]. For calculations using field theoretical methods different from the ones just described, see Refs. [50–62]). Data analysis now rests on the basis of low–energy effective field theories of QCD+QED, and is in general free of any model assumptions³.

The article is organized as follows. In section 2 we start with a detailed discussion of the fundamental physics background behind hadronic atom experiments. In sections 3, 4, 5 and 6, we construct the general theory of hadronic atoms in QCD+QED. We keep this part rather self–contained, avoiding extensive references to existing literature. For this reason, these sections also contain the

³Non–relativistic Lagrangians in the spirit of Ref. [37] are heavily used for the description of heavy quark bound states in QCD, see Ref. [63] for the introduction of the method. Two recent reviews on the subject are Refs. [64, 65].

Atom	Name	Symbol
$\pi^+\pi^-$	pionium	$A_{2\pi}$
$\pi^\mp K^\pm$	πK atom	$A_{\pi K}$
π^-p	pionic hydrogen	πH
K^-p	kaonic hydrogen	$\bar{K}H$
π^-d	pionic deuterium	πD
K^-d	kaonic deuterium	$\bar{K}D$

Table 1: Hadronic atoms investigated in this report. The corresponding names and symbols used in the text are also displayed.

essentials of non-relativistic effective field theories, to an extent that is needed for understanding the material related to hadronic atoms. In section 7 we collect useful general information on the relation between spectra and scattering lengths. We then describe in sections 8–12 several hadronic atoms, which have been treated so far in the framework of QFT, see Table 1.

In section 13 we briefly discuss the relation of our approach to conventional potential models. Finally, section 14 contains a summary and concluding remarks. Appendix A collects some notation, appendix B discusses the unitarity condition for non hermitian Hamiltonians, and in appendix C we discuss matching for non-relativistic coupling constants in πH , using unitarity.

We note that it was not our aim to cover the large number of articles concerned with the rich and well-developed phenomenology of hadronic atoms within the traditional quantum-mechanical setting, based on hadronic potentials, or to provide a complete bibliography on this issue. There are excellent textbooks (see, e.g., Refs. [66–68]) or review articles (e.g. Ref. [69]), which should be considered as complementary to the present work. In addition, the issue of deeply bound exotic atoms lies beyond the scope of the present review and will not be discussed at all. In order to follow the developments in this field, we refer the interested reader e.g. to the EXA05 proceedings [70]. For a short review, see, e.g., Ref. [71] and references therein.

2 Physics background

As already mentioned, experiments on hadronic atoms can provide stringent information on fundamental properties of QCD. In this section we consider in some detail the potential of individual experiments in this respect.

2.1 Pionium

Pionium is presently investigated by the DIRAC collaboration at CERN [72–78]. The experiment is a very challenging one: the lifetime of pionium in the ground state is of the order $\tau_1 \simeq 3 \times 10^{-15}$ s. Because the ratio of the binding energy with the width is of order 10^4 , one concludes that pionium is a quasi-stable bound state as well. At present, it is not possible to measure this lifetime directly. Instead, one first measures the ionization probability of pionium into a charged pion pair in different targets. From the calculated relation [79, 80] between this probability and the lifetime of pionium (which in vacuum almost exclusively decays into a $\pi^0\pi^0$ pair), one obtains the lifetime. The DIRAC collaboration has reported [77] the result

$$\tau_1 = 2.91_{-0.38}^{+0.45} (\text{stat})_{-0.49}^{+0.19} (\text{syst}) \times 10^{-15} \text{ s} = 2.91_{-0.62}^{+0.49} \times 10^{-15} \text{ s}. \quad (2.1)$$

Efforts to reduce the experimental uncertainty are ongoing [81].

The decay width of pionium in the ground state into a $2\pi^0$ pair is related to the S -wave $\pi\pi$ scattering lengths⁴ a_I with total isospin $I = 0, 2$,

$$\Gamma_{1,2\pi^0} = \frac{2}{9} \alpha^3 p_1^* (a_0 - a_2)^2 + \dots, \quad (2.2)$$

where $p_1^* = (M_\pi^2 - M_{\pi^0}^2 - \frac{1}{4} M_\pi^2 \alpha^2)^{1/2}$ denotes the magnitude of the 3-momentum of the $\pi^0\pi^0$ pair in the final state (with higher order terms in α ignored), and the ellipses stand for the isospin breaking corrections. In the derivation of Eq. (2.2) one has not used chiral symmetry: this relation is universal and holds – at leading order in isospin breaking – as long as the scale of strong interactions is much smaller than characteristic atomic distances. The DIRAC collaboration plans to measure $\Gamma_{1,2\pi^0}$ with an accuracy of 10%. Once a reliable evaluation of the isospin breaking corrections in the relation Eq. (2.2) is carried out, this measurement enables one to determine the value of $|a_0 - a_2|$ with 5% accuracy. As we shall see later, these isospin breaking corrections are of the order of 6% and therefore not at all negligible at the accuracy one is interested here.

What makes the above enterprise particularly interesting is the fact that the difference $a_0 - a_2$ is very sensitive to the value of the quark condensate in QCD [82], and thus to the manner in which chiral symmetry is spontaneously broken. The so-called “standard” scenario is based on the assumption that the condensate is large. This, for example, signifies that in the expansion of the pion mass in terms of the quark mass,

$$M_\pi^2 = M^2 - \frac{\bar{l}_3}{32\pi^2 F^2} M^4 + O(M^6), \quad M^2 = 2\hat{m}B, \quad \hat{m} = \frac{1}{2}(m_u + m_d), \quad (2.3)$$

the first term is dominant [83]. Here, F stands for the pion decay constant F_π in the chiral limit⁵, and \bar{l}_3 denotes a particular low-energy constant (LEC) that

⁴We use a convention where $\pi\pi$ scattering lengths a_I are dimensionless.

⁵We use $F_\pi = 92.4$ MeV.

appears in the $O(p^4)$ Lagrangian of ChPT, whereas B is related to the quark condensate in the chiral limit [84, 85]. Assuming the standard scenario of chiral symmetry breaking, a very accurate prediction of scattering lengths was achieved by merging two-loop ChPT with Roy equations [13, 14],

$$a_0 = 0.220 \pm 0.005, \quad a_2 = -0.0444 \pm 0.0010, \quad a_0 - a_2 = 0.265 \pm 0.004. \quad (2.4)$$

If the experimental value of $a_0 - a_2$ does not agree with this prediction, this would unambiguously indicate that chiral symmetry breaking in QCD proceeds differently from the standard picture [82]. As a result of this, the first term in the expansion Eq. (2.3) would be non-leading, and the chiral expansion must be reordered [82].

Measuring the energy levels of ponium [86, 87] enables one to extract a different combination of the S -wave scattering lengths. Indeed, the strong energy shift of S -states is given by [44]

$$\Delta E_n^{\text{str}} = -\frac{\alpha^3 M_\pi}{6n^3} (2a_0 + a_2) + \dots, \quad (2.5)$$

where n denotes the principal quantum number, and where the ellipsis stands for isospin breaking corrections. Hence, measuring both, $\Gamma_{1,2\pi^0}$ and ΔE_n , and assuming $a_0 - a_2 > 0$, one may extract the values of a_0 and a_2 separately and compare them with the prediction Eq. (2.4).

The present situation concerning the verification of the prediction Eq. (2.4) is the following. Lattice results [17–19], the data from DIRAC [77] on ponium lifetime and from NA48 on the cusp in $K \rightarrow 3\pi$ decays [88–93] neatly confirm the prediction, although partly with considerably larger error bars. On the other hand, preliminary NA48/2 data on K_{e4} apparently preferred larger values [94] of a_0 than the one displayed in Eq. (2.4). This puzzle was very recently resolved by the following observation [95, 96]. The electromagnetic corrections applied in the NA48/2 K_{e4} data were calculated using the PHOTOS Monte Carlo code [97], and by applying in addition the Sommerfeld factor [98]. However, this does not yet take care of all isospin breaking effects in this decay [99]. Indeed, the kaon can first decay into a $\pi^0\pi^0$ or $\pi^0\eta$ pair, that then re-scatter into the outgoing charged pions, through $\pi^0\pi^0 \rightarrow \pi^+\pi^-$ and $\pi^0\eta \rightarrow \pi^0\pi^0 \rightarrow \pi^+\pi^-$. Since the charged pion is heavier than the neutral one by about 4.6 MeV, these intermediate states generate a cusp in the *phase* of the relevant form factor. As a result of this, the phase is pushed upwards by about half a degree, and does not vanish at the threshold for $\pi^+\pi^-$ production. Once this is taken into account, the K_{e4} data from NA48/2 are in nice agreement with Eq. (2.4). There is, however, a discrepancy with the E865 data [100, 101]: the isospin corrections just mentioned spoil the good agreement with the prediction Eq. (2.4). We refer to Refs. [18, 19, 95, 102] for more details.

2.2 πK atom

The DIRAC collaboration at CERN plans [78] to measure the πK atoms in continuation of the already running experiment on pionium. From the measurements of the energy shift and decay width of the ground state, one would in principle extract the two independent isospin combinations a_0^+ and a_0^- of the S -wave πK scattering lengths, because the strong energy shifts and decay widths of πK atoms in their S -states are related to these scattering lengths in a manner very analogous to pionium,

$$\begin{aligned}\Delta E_n^{\text{str}} &= -\frac{2\alpha^3\mu_c^2}{n^3}(a_0^+ + a_0^-) + \dots, \\ \Gamma_n &= \frac{8\alpha^3\mu_c^2}{n^3}p_n^*(a_0^-)^2 + \dots.\end{aligned}\tag{2.6}$$

Here the ellipses stand for isospin breaking effects.

The theoretical interest in these scattering lengths is twofold at least. First, we mention that there exists a low-energy theorem [103], which states that the expansion of the isospin odd scattering length a_0^- is of the form

$$a_0^- = \frac{M_\pi M_K}{8\pi F_\pi^2(M_\pi + M_K)}(1 + O(M_\pi^2)).\tag{2.7}$$

Here, M_π, M_K and F_π denote the physical meson masses and the pion decay constant in the isospin symmetry limit. The theorem Eq. (2.7) states that the corrections to the leading current algebra result are proportional to powers of the pion mass – they vanish in the chiral limit $m_u = m_d = 0$.⁶ Since there is no strong final state interaction in this channel, one expects that these corrections are modest. On the other hand, the two-loop calculation performed in Ref. [105] suggests that the correction at order p^6 is substantial, and moreover larger than the one at order p^4 . The numerical result obtained in Ref. [105] for the scattering length a_0^- agrees with an analysis [106] based on Roy equations⁷.

The situation is puzzling – how can it be that higher orders are larger than low-order contributions? As was shown by Schweizer [107], in the present case, the large two-loop correction stems mostly from counterterms at order p^6 , estimated with resonance saturation in Ref. [105], see also Ref. [108] in this connection. Is this resonance estimate correct? If yes, ChPT is turned upside down. If no, ChPT does not agree with the result from the Roy equation analysis.

Second, the scattering length do also depend on certain LECs at order p^4 , whose values would be interesting to know in light of the large/small condensate

⁶Implicitly, this result is contained in the explicit expressions of the πK amplitudes given in Ref. [104].

⁷Note, however, that the available experimental data below 1 GeV are, in general, inconsistent with the solution of Roy equations, where the data above 1 GeV are used as phenomenological input.

question [82]. So, in case one does have a precise value of the scattering lengths, the first point could be clarified in the sense that one knows what is right and what is wrong. Concerning the second point, it remains to be seen whether this would indeed allow one to pin down those LECs which play a dominant role in connection with the large/small condensate issue. A detailed analysis of this point remains to be performed.

2.3 Pionic hydrogen and pionic deuterium

Measurements of the energy shift and decay width of the ground state of πH and πD were carried out by the Pionic Hydrogen Collaboration at PSI [1, 109–114]. The pionic hydrogen experiment was upgraded in 1998 [115], followed by an increased accuracy in particular of the width measurement [116] (for a review, see, e.g., Ref. [117]). The preliminary values of the strong shift and width of the ground state of πH obtained in the upgrade [115] are [118]

$$\begin{aligned}\Delta E_1^{\text{str}} &= -7.120 \pm 0.011 \text{ eV}, \\ \Gamma_1 &= 0.823 \pm 0.019 \text{ eV}.\end{aligned}\tag{2.8}$$

The announced aim [119] of the collaboration is to extract S -wave πN scattering lengths from this experiment with 1% precision. This will be a unique experimental result for hadron physics. Of course, in order to achieve this goal by measuring πH alone, one should remove possible sources of theoretical uncertainties related to isospin breaking effects, at an accuracy that matches the experimental precision. At present, this seems to be a very difficult task, as we will show later in this report.

The measured shift and width of πD are [112]

$$\Delta E_1^{\text{str,d}} = 2.46 \pm 0.048 \text{ eV}, \quad \Gamma_1^{\text{d}} = 1.194 \pm 0.105 \text{ eV}.\tag{2.9}$$

This accuracy is expected to improve in the near future [120, 121].

We will show in later sections that, using multiple-scattering theory [22, 66, 68, 122–130] or chiral EFT in the two-nucleon sector [47, 131–143], one can relate the value of the πd scattering length, which can be extracted from the experimental data, to the πN scattering lengths. This results in additional constraints on the values of a_{0+}^+ and a_{0+}^- .

Let us assume that one indeed is able to extract the exact values of the πN scattering lengths from the experiment with high precision. What information about the fundamental properties of QCD are contained in these precise values? Of course, πN scattering lengths are quantities of fundamental importance in low-energy hadronic physics by themselves, since they test the QCD symmetries and the exact pattern of the chiral symmetry breaking (see, e.g., Refs. [144–146]). Moreover, since the knowledge of these scattering lengths places a constraint on

the πN interactions at low energy, it also affects our understanding of more complicated systems where πN interaction serves as an input, e.g. NN interaction, π -nucleus scattering, three-nucleon forces, etc.

In addition to this, the high-precision values of the πN scattering lengths are used as an input for the determination of different basic parameters of QCD at low energies more accurately. One example is the πNN coupling constant $g_{\pi NN}$, which is obtained from the Goldberger–Myazawa–Oehme (GMO) sum rule [21], where a particular combination of scattering lengths enters as a subtraction constant,

$$\begin{aligned} \frac{g_{\pi NN}^2}{4\pi} &= \left(\left(\frac{2m_N}{M_\pi} \right)^2 - 1 \right) \left\{ \left(1 + \frac{M_\pi}{m_N} \right) \frac{M_\pi}{4} (a_{\pi^- p} - a_{\pi^+ p}) \right. \\ &\quad \left. - \frac{M_\pi^2}{8\pi^2} \int_0^\infty \frac{dk}{\sqrt{M_\pi^2 + k^2}} (\sigma_{\pi^- p}(k) - \sigma_{\pi^+ p}(k)) \right\}, \end{aligned} \quad (2.10)$$

where m_N is the nucleon mass in the isospin symmetry limit, $\sigma_{\pi^\pm p}(k)$ denotes the total elastic cross section for the scattering of π^+ (π^-) on the proton, and $a_{\pi^\pm p}$ stand for isospin combinations of S -wave πN scattering lengths, $a_{\pi^\mp p} = a_{0+}^\pm \pm a_{0+}^\mp$. For recent investigations of the GMO sum rule, see Refs. [22, 23].

Other important quantities, which can be obtained by using the S -wave πN scattering lengths as an input, are the so-called πN σ -term and the strangeness content of the nucleon [20]. The σ -term, which measures the explicit breaking of chiral symmetry in the one-nucleon sector due to the u - and d -quark masses, is given by the matrix element of the chiral symmetry-breaking Hamiltonian $\hat{m}(\bar{u}u + \bar{d}d)$ between the one-nucleon states. The latter quantity is expressed through the value of the scalar form factor of the nucleon at $t = (p' - p)^2 = 0$,

$$\bar{u}(p', s') \sigma_{\pi N}(t) u(p, s) = \langle p' s' | \hat{m}(\bar{u}u + \bar{d}d) | p s \rangle, \quad \sigma_{\pi N} \doteq \sigma_{\pi N}(0), \quad (2.11)$$

where the Dirac spinors are normalized to $\bar{u}u = 2m_N$. The σ -term is related to the strangeness content of the nucleon y and the $SU(3)$ symmetry breaking piece of the strong Hamiltonian,

$$\begin{aligned} \frac{m_s - \hat{m}}{2m_N} \langle ps | \bar{u}u + \bar{d}d - 2\bar{s}s | ps \rangle &= \left(\frac{m_s}{\hat{m}} - 1 \right) (1 - y) \sigma_{\pi N}, \\ y &= \frac{2\langle ps | \bar{s}s | ps \rangle}{\langle ps | \bar{u}u + \bar{d}d | ps \rangle}. \end{aligned} \quad (2.12)$$

An analysis of the experimental data, carried out some time ago [147], gives

$$\sigma_{\pi N} \simeq 45 \text{ MeV}, \quad y \simeq 0.2. \quad (2.13)$$

Note that in this analysis, one has used S -wave πN scattering lengths as input in the dispersion relations which provide the extrapolation of the isospin even

pion–nucleon scattering amplitude from threshold down to the Cheng–Dashen point. The σ -term, which is obtained as a result of the above analysis, is rather sensitive to these scattering lengths, see, e.g., Ref. [148, Fig. 1]. Consequently, an accurate measurement of the scattering lengths will have a large impact on the values of $\sigma_{\pi N}$ and y . For an analysis that finds a substantially larger value of $\sigma_{\pi N}$ than the one quoted above, see Pavan et al. [20].

2.4 Kaonic hydrogen and kaonic deuterium

The DEAR collaboration at LNF–INFN [149–152] has performed a measurement of the energy level shift and width of the $\bar{K}H$ ground state with a considerably better accuracy than the earlier KpX experiment at KEK [153]. The present experimental values of these quantities are [154]

$$\begin{aligned}\Delta E_1^{\text{str}} &= 193 \pm 37 \text{ (stat)} \pm 6 \text{ (syst)} \text{ eV}, \\ \Gamma_1 &= 249 \pm 111 \text{ (stat)} \pm 30 \text{ (syst)} \text{ eV}.\end{aligned}\tag{2.14}$$

As can be seen from the above result, the uncertainty is still tens of eV in the energy shift and more than 100 eV in the width. Now DEAR is being followed by the SIDDHARTA experiment that features new silicon drift detectors [154, 155]. The plans of the SIDDHARTA collaboration include the measurement of both, the energy shift and width of $\bar{K}H$, with a precision of several eV, i.e. at the few percent level, by 2008. Moreover, SIDDHARTA will attempt the first ever measurement of the energy shift of $\bar{K}D$ with a comparable accuracy and possibly, kaonic helium and sigmonic atoms. Eventually, these experiments will allow one to extract the values of the K^-p and K^-d threshold scattering amplitudes by using the pertinent DGBT–type formulae. Because these amplitudes depend on the other hand on the S -wave $\bar{K}N$ scattering lengths a_0 and a_1 , one can in principle determine these.

The necessity to perform measurements of $\bar{K}D$ energy shift and width of the ground state is also due to the fact that, unlike in the case of pionic atoms, the measurement of the $\bar{K}H$ spectrum alone does not allow one – even in principle – to extract independently a_0 and a_1 . This happens because the imaginary parts of the threshold amplitudes do not vanish in the isospin limit, being determined by the decays into inelastic strong channels $\pi\Sigma, \pi^0\Lambda, \dots$ – in other words, the separation of thresholds is governed by the breaking of $SU(3)$ symmetry. Consequently, one attempts here to determine four independent quantities (real and imaginary parts of a_0 and a_1) that requires performing four independent measurements – e.g., the energy level shifts and widths of $\bar{K}H$ and $\bar{K}D$. Note however that, even though it is clear that a_0 and a_1 cannot be determined separately without measuring kaonic deuterium, it is still not evident whether it is possible to do so if one performs such a measurement. The reason is that the (complex) kaon–deuteron

amplitude at threshold, which is directly determined from the experiment and which is expressed in terms of a_0 and a_1 through a multiple-scattering series, is generally plagued by systematic uncertainties due to a poor knowledge of the low-energy kaon-nucleon dynamics. Thus, one needs to know whether these uncertainties are small enough not to hinder a determination of a_0 and a_1 from the SIDDHARTA experiment.

In order to answer this question, a detailed analysis of the problem has been performed in Ref. [49]. This investigation revealed that – at least, within the lowest-order approximation – a combined analysis of DEAR/SIDDHARTA data on $\bar{K}H$ and $\bar{K}D$ turns out to be more restrictive than one would *a priori* expect, see also the discussion in section 12 of this report. The combined analysis imposes stringent constraints on the theoretical description of the kaon-deuteron interactions at low energies and provides a tool for determining a_0 and a_1 with reasonable accuracy from the forthcoming SIDDHARTA data. It remains to be seen, whether this conclusion stays intact, if higher-order corrections are systematically included.

What fundamental physical information can be gained from the values of a_0 and a_1 ? We believe that it could be very useful to carry out a comparison of the $\bar{K}N$ scattering lengths measured in the DEAR/SIDDHARTA experiment with different theoretical predictions based on the unitarization of the lowest order ChPT amplitude [156–169]. It turns out that even the data from $\bar{K}H$ alone impose rather stringent constraints on the values of the $\bar{K}N$ scattering lengths – namely, in certain cases there emerge difficulties to make DEAR data compatible with the scattering sector [46, 160–169]. It is clear that imposing additional constraints from $\bar{K}D$ data makes the issue of compatibility even more pronounced. In our opinion, it will be important to check whether the unitarization approach passes this test.

Finally we wish to note that the original physics program of the DEAR/SIDDHARTA experiment was largely a direct extension of the πH experiment to the strange quark sector, including, in addition, the measurement of the kaon-nucleon σ -term and the strangeness content of the nucleon [150, 151]. On the other hand, there are significant differences between these systems [170, 171]:

- i) There are much less data on $\bar{K}N$ scattering than in the πN case.
- ii) There are open strong channels below threshold.
- iii) There is a sub-threshold resonance $\Lambda(1405)$.
- iv) The distance between the threshold and the Cheng–Dashen point is much larger than in the πN case.

It will therefore be very difficult to extract the experimental value of the $\bar{K}N$ σ -term [150, 151].

3 Non-relativistic effective theories: strong sector

3.1 Introductory remarks

In relativistic quantum field theories, the number of particles is not a conserved quantity. As a result of this, S -matrix elements have a complicated analytic structure. In particular, they contain branch points at each energy that corresponds to a threshold for a newly allowed physical process [172].

This feature renders the description of bound states very complicated. On the other hand, recall that we are concerned with loosely bound states which generate poles in the complex energy plane. The poles are located close to the elastic threshold and thus far away from any inelastic and crossed channel singularities. Further, the magnitudes of the characteristic momenta are much smaller than the particle masses, and the characteristic kinetic energies lie far below the inelastic thresholds generated by the presence of additional massive particles in the final state. This suggests that a framework where all singularities are treated on an equal footing is counterproductive and superfluous in this case: the physics at low energies can equally well be described by a simpler effective non-relativistic field theory, in which the S -matrix elements possess only the elastic cut and the poles that are located close to this cut, whereas the contributions from distant singularities can be Taylor expanded in external momenta [37]. This (truncated) Taylor series is generated by a finite number of operators in the non-relativistic Lagrangian, multiplied with unknown coupling constants. For properly chosen couplings, the non-relativistic and the relativistic theories are physically equivalent at low energy, up to a certain power in the momentum expansion. This procedure to fix the couplings in the non-relativistic Lagrangian is called *matching*.

In this non-relativistic theory, bound-state dynamics is described by the Schrödinger equation, and the perturbation expansion of the bound-state energies is given by the Rayleigh-Schrödinger series [37]. The crucial property of the non-relativistic theory which makes this calculation simple, is the fact that the production and annihilation of massive particles can be forbidden by construction: the interaction Hamiltonian has vanishing matrix elements between states with different number of massive particles. In the presence of photons, only matrix elements between states that contain the same number of massive particles and an arbitrary number of photons can be non-vanishing.

For the Coulomb bound state, momenta are of order α . As a result of this, the contribution to the bound-state energy from an operator in the interaction Lagrangian which contains n space derivatives is suppressed by α^n as compared to the contribution from an operator with the same field content and without derivatives. Stated differently, one counts each space derivative $\partial_i = O(v) = O(\alpha)$ (here

v stands for the velocity of a massive particle). If one wishes to evaluate the binding energy at a given order in α , one may truncate the non-relativistic Lagrangian at a certain order in v and carry out calculations with the truncated Lagrangian – the error in the bound state occurs at a higher order in α . The method works, provided that the power counting stays intact in higher-order calculations involving loops. This can be achieved by applying threshold expansions, in the scattering sector as well as in the Rayleigh–Schrödinger perturbation series (see, e.g., Refs. [42, 64, 173–182]). For a review on electromagnetic bound states see, e.g., Refs. [183, 184].

We illustrate in this and in the following two sections the procedure in a simple theory: we consider a self-interacting scalar field which is coupled to photons – in the absence of the self interaction, the Lagrangian reduces to the one of scalar electrodynamics. We determine the widths and energy levels of the bound states at next-to-leading order in α , following closely the procedure outlined in Refs. [181, 185]. As we shall see later, the evaluation of the energy levels and widths in hadronic atoms in the framework of ChPT amounts to a rather straightforward generalization of the techniques presented here.

3.2 The Lagrangian and the reduction formulae

We start from a situation where only one hard scale is present, and where the external momenta involved are much smaller than this scale. This situation is described e.g. by a theory that contains solely massive charged scalar particles ϕ^\pm of physical mass M , and where the external momenta are considered to be small in comparison to M . In the relativistic case, we introduce a complex massive self-interacting scalar field ϕ . Photons will be included in the following section. The Lagrangian is given by

$$\mathcal{L} = \partial_\mu \phi (\partial^\mu \phi)^\dagger - M_r^2 \phi \phi^\dagger + \frac{\lambda_r}{4!} (\phi \phi^\dagger)^2 + \text{counterterms}, \quad (3.1)$$

where $\phi = \frac{1}{\sqrt{2}} (\phi_1 + i\phi_2)$ is the charged scalar field, $M_r = M_r(\mu_0)$ and $\lambda_r = \lambda_r(\mu_0)$ stand for the renormalized mass and the quartic coupling, respectively. We use the modified minimal subtraction ($\overline{\text{MS}}$) prescription throughout this paper. The scale of dimensional renormalization is denoted by μ_0 .

In the following, we restrict the discussion to the sector with vanishing total charge and, in particular, consider the scattering of two oppositely charged particles $\phi^+ \phi^- \rightarrow \phi^+ \phi^-$. The pertinent Green function is given by

$$G(p_1, p_2; q_1, q_2) = \int d^4x_1 d^4x_2 d^4y_1 d^4y_2 e^{ip_1x_1 + ip_2x_2 - iq_1y_1 - iq_2y_2} \times i^4 \langle 0 | T \phi(x_1) \phi^\dagger(x_2) \phi^\dagger(y_1) \phi(y_2) | 0 \rangle_c, \quad (3.2)$$

where the subscript c refers to the connected part.

The scattering amplitude

$$\begin{aligned} \langle p_1, p_2 \text{ out} | q_1, q_2 \text{ in} \rangle &= \langle p_1, p_2 \text{ in} | q_1, q_2 \text{ in} \rangle \\ &+ i(2\pi)^4 \delta^4(p_1 + p_2 - q_1 - q_2) T(\mathbf{p}_1, \mathbf{p}_2; \mathbf{q}_1, \mathbf{q}_2) \end{aligned} \quad (3.3)$$

is obtained from the Green function in a standard manner, through amputating external legs and multiplying with appropriate renormalization factors.

Let us now construct the non-relativistic theory, which reproduces this scattering amplitude at small 3-momenta $\mathbf{p}_i^2, \mathbf{q}_j^2 \ll M^2$. We first introduce the non-relativistic field operators $\Phi_{\pm}(x)$ ($\Phi_{\pm}^{\dagger}(x)$) that annihilate (create) a non-relativistic (positive/negative) charged particle from the vacuum. The non-relativistic Lagrangian $\mathcal{L}_{NR}(x)$ consists of an infinite tower of operators which are constructed from the fields $\Phi_{\pm}(x)$, its conjugated fields $\Phi_{\pm}^{\dagger}(x)$ and space derivatives thereof. Time derivatives at order ≥ 2 can be eliminated by using the equations of motion and field redefinitions. The guiding principles for constructing the Lagrangian are the following.

- i) The effective theory must be rotationally invariant and obey P, T discrete symmetries, under which the non-relativistic field transforms as follows,

$$P\Phi_{\pm}(x^0, \mathbf{x})P^{\dagger} = \Phi_{\pm}(x^0, -\mathbf{x}), \quad T\Phi_{\pm}(x^0, \mathbf{x})T^{\dagger} = \Phi_{\pm}(-x^0, \mathbf{x}), \quad (3.4)$$

where T is an anti-unitary operator. Lorentz invariance is realized in form of relations between different low-energy couplings.

- ii) Since the number of the heavy particles is conserved, all vertices in the non-relativistic Lagrangian must contain an equal number of $\Phi_{\pm}(x)$ and $\Phi_{\pm}^{\dagger}(x)$. Particle creation and annihilation, which occurs in the relativistic theory, is implicitly included in the couplings of the non-relativistic Lagrangian. In the case considered in this section, these couplings are real and the Lagrangian is a hermitian operator.

- iii) The T -invariance implies

$$T\mathcal{L}_{NR}(x^0, \mathbf{x})T^{\dagger} = \mathcal{L}_{NR}(-x^0, \mathbf{x}). \quad (3.5)$$

- iv) It is necessary to specify counting rules, which allow one to order different operators in the Lagrangian. We introduce a formal small parameter v – a velocity of the massive particle in units of the speed of light – and count each 3-momentum \mathbf{p} and space derivatives ∇ as $O(v)$. Further, the kinetic energy of the massive particles $p^0 - M$ (or $i\partial_t - M$) is counted at $O(v^2)$. This rule amounts to an expansion in inverse powers of the heavy mass M . All terms in the Lagrangian can be ordered according to the counting in the parameter v . This ordering can be performed separately in each n -particle sector – the sectors with different numbers of massive particles do not mix.

According to the above rules, the non-relativistic effective Lagrangian in the two-particle sector with $Q = 0$ is given by

$$\begin{aligned} \mathcal{L}_{NR} = & \sum_{\pm} \Phi_{\pm}^{\dagger} \left(i\partial_t - M + \frac{\Delta}{2M} + \frac{\Delta^2}{8M^3} + \dots \right) \Phi_{\pm} + \frac{g_1}{M^2} (\Phi_{+}^{\dagger} \Phi_{-}^{\dagger})(\Phi_{+} \Phi_{-}) \\ & + \frac{g_2}{4M^4} \left\{ (\Phi_{+}^{\dagger} \overset{\leftrightarrow}{\Delta} \Phi_{-}^{\dagger})(\Phi_{+} \Phi_{-}) + h.c. \right\} + \frac{g_3}{2M^4} (\Phi_{+}^{\dagger} \Phi_{+}) \overset{\leftrightarrow}{\Delta} (\Phi_{-}^{\dagger} \Phi_{-}) + \dots, \end{aligned} \quad (3.6)$$

where $u \overset{\leftrightarrow}{\Delta} v = u(\Delta v) + (\Delta u)v$ and g_i denote non-relativistic couplings, which are functions of the parameters $\lambda_r(\mu_0)$, $M_r(\mu_0)$ and μ_0 . Ellipses stand for higher derivatives.

The calculation in perturbation theory with the Lagrangian \mathcal{L}_{NR} proceeds as follows. One splits the Lagrangian into a free and an interacting part, $\mathcal{L}_{NR} = \mathcal{L}_{NR}^0 + \mathcal{L}_{NR}^{\text{int}}$ with $\mathcal{L}_{NR}^0 = \sum_{\pm} \Phi_{\pm}^{\dagger} (i\partial_t - M + \Delta/2M) \Phi_{\pm}$. The free propagator is given by

$$i\langle 0|T\Phi_{\pm}(x)\Phi_{\pm}^{\dagger}(0)|0\rangle = \int \frac{d^4p}{(2\pi)^4} \frac{e^{-ipx}}{M + \frac{\mathbf{p}^2}{2M} - p^0 - i0}. \quad (3.7)$$

It vanishes for negative times, which shows that the field $\Phi_{\pm}(x)$ indeed annihilates the vacuum. As expected, the free particle has a non-relativistic dispersion law $p^0 = M + \mathbf{p}^2/2M$. In order to arrive at a relativistic dispersion law, one has to sum up all higher-order relativistic corrections proportional to $\Delta^2/8M^3 \dots$. Taking into account that Δ is of order v^2 , and counting the propagator in momentum space as $O(v^{-2})$, the corresponding series for the propagator is of the form $a/v^2 + b + cv^2 + \dots$ and thus indeed corresponds to an expansion which makes sense.

For later use, we note that the one-particle states in the non-relativistic theory – with the propagator given by Eq. (3.7) – are normalized according to

$$\langle \mathbf{k}|\mathbf{q}\rangle = (2\pi)^3 \delta^3(\mathbf{k} - \mathbf{q}) \quad [\text{non-relativistic}]. \quad (3.8)$$

Calculation of the scattering amplitude of two oppositely charged particles in the non-relativistic theory proceeds analogously to the relativistic framework: one evaluates the connected Green functions

$$\begin{aligned} G_{NR}(p_1, p_2; q_1, q_2) = & \int d^4x_1 d^4x_2 d^4y_1 d^4y_2 e^{ip_1x_1 + ip_2x_2 - iq_1y_1 - iq_2y_2} \\ & \times i^4 \langle 0|T\Phi_{+}(x_1)\Phi_{-}(x_2)\Phi_{+}^{\dagger}(y_1)\Phi_{-}^{\dagger}(y_2)|0\rangle_c. \end{aligned} \quad (3.9)$$

Here, the non-relativistic self-energy corrections in the external legs are summed up, so that the correct relativistic dispersion law $p^0 = w(\mathbf{p}) = (M^2 + \mathbf{p}^2)^{1/2}$ is recovered. Because light (massless) particles are absent here, there are no loop

corrections to the self-energy, and the pertinent wave function renormalization factor $Z_{NR} = 1$. Amputating external legs on the mass shell, we finally obtain

$$\begin{aligned}
& i(2\pi)^4 \delta^4(p_1 + p_2 - q_1 - q_2) T_{NR}(\mathbf{p}_1, \mathbf{p}_2; \mathbf{q}_1, \mathbf{q}_2) \\
&= \prod_i^2 \lim_{p_i^0 \rightarrow w(\mathbf{p}_i)} (w(\mathbf{p}_i) - p_i^0) \prod_j^2 \lim_{q_j^0 \rightarrow w(\mathbf{q}_j)} (w(\mathbf{q}_j) - q_j^0) G_{NR}(p_1, p_2; q_1, q_2). \quad (3.10)
\end{aligned}$$

3.3 Matching condition

The relativistic and non-relativistic theories must be physically equivalent at small momenta. This equivalence is enforced by the matching condition, which enables one to express the non-relativistic couplings g_i in Eq. (3.6) through the parameters λ_r , M_r and the scale μ_0 .

We first formulate the matching condition for the scattering amplitude T_{NR} introduced in Eq. (3.10) and start with the observation that the normalization of the asymptotic states is different in the relativistic and in the non-relativistic theory: in the relativistic case, one has

$$\langle \mathbf{k} | \mathbf{q} \rangle = (2\pi)^3 2w(\mathbf{p}) \delta^3(\mathbf{k} - \mathbf{q}) \quad [\text{relativistic}]. \quad (3.11)$$

From this we conclude that, in order that the cross sections in the relativistic and in the non-relativistic theories are the same, the scattering matrix elements must satisfy

$$T(\mathbf{p}_1, \mathbf{p}_2; \mathbf{q}_1, \mathbf{q}_2) = \prod_{i=1}^2 (2w(\mathbf{p}_i))^{1/2} (2w(\mathbf{q}_i))^{1/2} T_{NR}(\mathbf{p}_1, \mathbf{p}_2; \mathbf{q}_1, \mathbf{q}_2), \quad (3.12)$$

i.e., the non-relativistic scattering amplitude acquires an extra factor $(2w(\mathbf{k}))^{-1/2}$ for each external leg. The equality Eq. (3.12), which goes under the name of *matching condition*, is understood to hold at small 3-momenta, order by order in the expansion in \mathbf{p}_i/M , \mathbf{q}_i/M . This corresponds to an expansion in the formal parameter v introduced in the previous subsection. We will provide illustrations below.

The matching condition for transition amplitudes with more than 4 legs can be formulated in a similar fashion. However, in order to do so explicitly, one must introduce the concept of connected S -matrix elements. As we will not need these higher order transition amplitudes in the present work, we do not go into more details here.

Finally, let us mention that the matching condition does not always determine all couplings g_i separately. This happens, for instance, when one decides to retain a non-minimal set of operators in the non-relativistic Lagrangian. The matching

condition, which is formulated for the scattering amplitudes, then determines only certain combinations of the non-relativistic couplings. The point is that exactly the same combinations then enter all observable quantities that can be calculated from the non-relativistic Lagrangian. Consequently, the non-relativistic effective theory leads to a consistent treatment of the low-energy physics also in this case. Explicit examples and further details can be found in Ref. [181], chapter IIIc.

3.4 Tree level

As an illustration to the matching procedure, consider the scattering process $q_1 + q_2 \rightarrow p_1 + p_2$ in the sector with $Q = 0$. The relativistic scattering amplitude at tree level is $\lambda_r/6$. Using the matching condition Eq. (3.12), and expanding the non-relativistic amplitude in the CM frame ($\mathbf{p}_1 = -\mathbf{p}_2 = \mathbf{p}$, $\mathbf{q}_1 = -\mathbf{q}_2 = \mathbf{q}$, $|\mathbf{p}| = |\mathbf{q}|$) in powers of v , we get

$$\frac{T(\mathbf{p}_1, \mathbf{p}_2; \mathbf{q}_1, \mathbf{q}_2)}{2w(\mathbf{p})2w(\mathbf{q})} = \frac{\lambda_r}{6} \frac{1}{2w(\mathbf{p})2w(\mathbf{q})} = \frac{\lambda_r}{24M^2} - \frac{\lambda_r}{24M^4} \mathbf{p}^2 + O\left(\frac{1}{M^6}\right). \quad (3.13)$$

On the other hand, the non-relativistic amplitude, evaluated from the Lagrangian (3.6) is given by

$$T_{NR}(\mathbf{p}_1, \mathbf{p}_2; \mathbf{q}_1, \mathbf{q}_2) = \frac{g_1}{M^2} - \frac{g_2 \mathbf{p}^2}{M^4} - \frac{g_3 (\mathbf{p} - \mathbf{q})^2}{M^4} + O(\mathbf{p}^4). \quad (3.14)$$

From these relations, we can read off the couplings g_1, g_2, g_3 at tree level,

$$g_1 = \frac{\lambda_r}{24} + O(\lambda_r^2), \quad g_2 = \frac{\lambda_r}{24} + O(\lambda_r^2), \quad g_3 = O(\lambda_r^2). \quad (3.15)$$

The generalization of the tree-level matching procedure to terms containing more field operators, or higher derivatives, is straightforward. Here, we only mention that the many-particle scattering amplitudes contain singular parts that stem from particles traveling near their mass shell between two interactions. These singular parts are exactly reproduced at low energies by the tree graphs in the non-relativistic theory. The remaining part of the relativistic amplitudes is a polynomial in the small external 3-momenta, and can be reproduced by adjusting the couplings in \mathcal{L}_{NR} .

3.5 Loops

At higher order in the low-energy expansion, loops also contribute. In the non-relativistic theory, they reproduce the non-analytic behavior of the relativistic amplitudes at low energy. The polynomial parts can be fixed with the help of the matching condition.

To illustrate the procedure, we again consider the two-particle amplitude. The structure of the perturbation series is particularly simple here, see Fig. 1: at

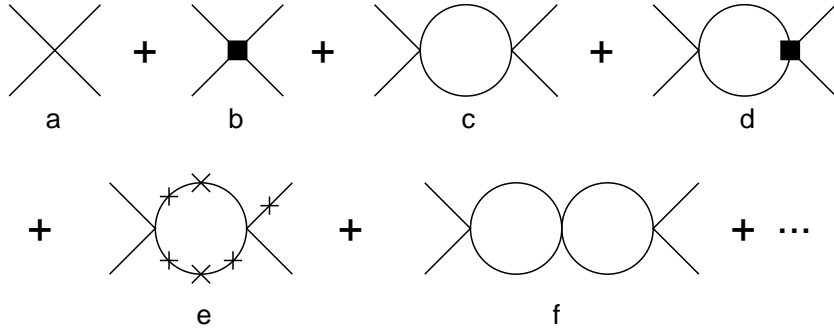


Figure 1: Typical diagrams, contributing to the 2-particle elastic scattering amplitude in the non-relativistic theory. Filled boxes and crosses denote the derivative vertices and the self-energy insertions, respectively.

any order in the loop expansion, only the chain of S -wave bubbles plus relativistic insertions in the internal and external lines plus insertions of derivative 4-particle vertices contribute to the scattering amplitude. The elementary building block to calculate a diagram with any number of bubbles in the CM frame $P^\mu = p_1^\mu + p_2^\mu = (P^0, \mathbf{0})$ is given by

$$\begin{aligned}
 J(P^0) &= \int \frac{d^D l}{(2\pi)^D i} \frac{1}{M + \frac{l^2}{2M} - P^0 + l^0 - i0} \frac{1}{M + \frac{l^2}{2M} - l^0 - i0} \\
 &= \frac{iM}{4\pi} (M(P^0 - 2M))^{1/2}, \quad \text{at } D \rightarrow 4, \quad P^0 > 2M. \quad (3.16)
 \end{aligned}$$

The function $J(P^0)$ is analytic in the complex P^0 plane, cut along the positive real axis for $P^0 > 2M$. The scattering amplitude is obtained by putting $P^0 = 2w(\mathbf{p})$, where \mathbf{p} denotes the relative 3-momentum in the CM frame. Diagrams containing self-energy insertions, or derivative couplings, are evaluated in a similar manner⁸.

The perturbative expansion based on the Lagrangian Eq. (3.6) generates a systematic low-energy expansion of the scattering amplitudes. The single loop $J(P^0)$ is proportional to the magnitude of the small relative momentum $|\mathbf{p}|$. Self-energy insertions and derivative vertices contribute additional powers of $|\mathbf{p}|$. Hence, evaluating loop diagrams with vertices of higher dimension yields contributions at higher order in the expansion in momenta. We conclude that, at any given order in v^n , only a finite number of diagrams contributes. For example, combining two non-derivative vertices through one loop (Fig. 1c) generates a contribution at $O(v)$, and the contribution from the two-loop diagram in Fig. 1f is $O(v^2)$, as is the derivative vertex displayed in Fig. 1b.

⁸Our theory is perturbative in dimensional regularization. We do not consider here the case when some of the non-relativistic couplings are “unnaturally” large, which would lead to the necessity of partial re-summation of the perturbative series (example: the “pionless” effective field theory in the two-nucleon sector [186, 187]).

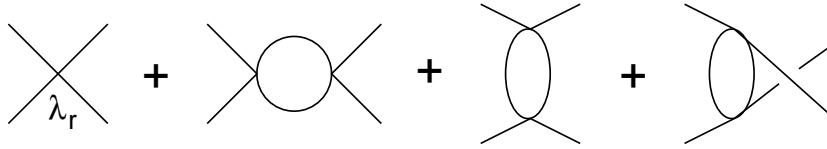


Figure 2: One-loop scattering amplitude in the relativistic $(\phi^\dagger\phi)^2$ theory. Self-energy insertions are not displayed.

From the above discussion one concludes that in the CM frame, the non-relativistic scattering amplitude takes the form

$$T_{NR} = M^{-2} \left(f_0 + f_1 \frac{|\mathbf{p}|}{M} + f_2 \frac{|\mathbf{p}|^2}{M^2} + f_3 \frac{\mathbf{p}\mathbf{q}}{M^2} + \dots \right), \quad (3.17)$$

where the expansion coefficients f_i are polynomials of finite order in the dimensionless couplings g_i . The matching condition Eq. (3.12) fixes these couplings through λ_r, M_r and the scale μ_0 order by order in the perturbative expansion.

As one observes from Eq. (3.17), the analytic structure of the amplitude is particularly simple. The only non-analytic piece of the non-relativistic amplitude at low energy is given by terms containing odd powers of $|\mathbf{p}|$, whereas the rest is a polynomial in the external momenta. As mentioned above, only s -channel bubbles generate non-analytic contributions in the vicinity of the elastic threshold (graphs shown in Figs. 1c,d,e, \dots).

Let us now verify that the relativistic amplitude has the same non-analytic structure at low energy as the non-relativistic one. We consider the relativistic scattering amplitude at one loop (see Fig. 2),

$$T(s, t, u) = T_0 + \frac{\lambda_r^2}{72} (2\bar{J}(s) + 2\bar{J}(t) + \bar{J}(u)) + O(\lambda_r^3), \quad (3.18)$$

where T_0 is a constant, $s = (p_1 + p_2)^2$, $t = (p_1 - q_1)^2$, $u = (p_1 - q_2)^2$ are the usual Mandelstam variables, and where, for $x < 0$,

$$\bar{J}(x) = \frac{1}{16\pi^2} \left(\sigma_x \ln \frac{\sigma_x - 1}{\sigma_x + 1} + 2 \right), \quad \sigma_x = \sqrt{1 - \frac{4M^2}{x}}. \quad (3.19)$$

The amplitude Eq. (3.18) has a more complicated analytic structure than its non-relativistic counterpart Eq. (3.17). For instance, its partial waves contain, in addition to a cut at $s > 4M^2$, a left-hand cut at $s < 0$. However, in the vicinity of the elastic threshold, the contribution from these distant singularities can be approximated by a polynomial. Expanding the functions $\bar{J}(s)$, $\bar{J}(t)$, $\bar{J}(u)$

near $s = 4M^2$, $t = 0$, $u = 0$, we obtain

$$\begin{aligned}
16\pi^2 \bar{J}(s) &= 2 + \frac{i\pi|\mathbf{p}|}{M} - \frac{2|\mathbf{p}|^2}{M^2} + O(v^3), \\
16\pi^2 \bar{J}(t) &= -\frac{(\mathbf{p} - \mathbf{q})^2}{6M^2} + O(v^4), \\
16\pi^2 \bar{J}(u) &= -\frac{(\mathbf{p} + \mathbf{q})^2}{6M^2} + O(v^4).
\end{aligned} \tag{3.20}$$

Substituting this expansion into Eq. (3.18), one immediately sees that the low-energy behavior of the non-relativistic amplitude Eq. (3.17) is reproduced. One may further check that the non-analytic part $\propto \lambda_r^2 |\mathbf{p}|$ in the expression for the amplitude, which is generated by $\bar{J}(s)$, is automatically reproduced in the non-relativistic calculation with the correct coefficient, provided the matching at $O(\lambda_r)$ has been performed.

We end this subsection with a brief discussion of crossing and charge symmetry. In the relativistic theory, the scattering amplitude obeys crossing symmetry. The crossed channels, along with $\phi^+ \phi^- \rightarrow \phi^+ \phi^-$, include also the reactions $\phi^+ \phi^+ \rightarrow \phi^+ \phi^+$ and $\phi^- \phi^- \rightarrow \phi^- \phi^-$. These reactions are described by a single analytic amplitude, derived from the relativistic Lagrangian Eq. (3.1).

In the non-relativistic case, crossing symmetry is apparently lost because, first of all, the non-relativistic expansion is performed in the vicinity of $s = 4M^2$, $t = u = 0$. In difference to the relativistic case, an analytic continuation of the amplitude from the vicinity of the s -channel threshold to the t - or u -channel thresholds cannot be performed, because the distance between these two regions exceeds the radius of the convergence of the pertinent Taylor series (see, e.g. Eq. (3.20)). Furthermore, our non-relativistic Lagrangian describes only the sector with total charge zero, so that the scattering amplitudes for $\phi^+ \phi^+ \rightarrow \phi^+ \phi^+$ and $\phi^- \phi^- \rightarrow \phi^- \phi^-$ vanish in this theory (within the non-relativistic approach, this choice is a consistent procedure). We therefore conclude that crossing symmetry is not present in the non-relativistic approach *ab initio*. At most, one may describe the scattering amplitudes in all crossed channels, including all pertinent terms in the non-relativistic Lagrangian. The couplings, which are determined from matching to the relativistic theory, will then obey the restrictions imposed by crossing symmetry. The same conclusion holds for charge invariance, which in general connects sectors of different total charge.

3.6 Relation to the effective range expansion

There is one property of the non-relativistic theories that makes the use of this framework extremely effective in many areas of hadron physics. The property is related to the expansion parameters in the non-relativistic perturbation series.

Following the line of reasoning outlined in the introduction, we consider a generic hadronic scattering process at momenta which are much smaller than any of hadron masses involved and any of the dynamically generated scales. It is clear that any consistent EFT at such momenta should operate only with observable characteristics (S -matrix parameters) of this process (since the distances involved are already asymptotic). In other words, for e.g. the elastic two-particle scattering process, the expansion parameters in the non-relativistic EFT should be expressible through the parameters of the effective range expansion (scattering length, effective range, shape parameters), rather than directly through the coupling constant λ_r , the running mass M_r , etc. It can be immediately seen that the non-relativistic EFT, which we have constructed here, passes this test: at a given order v^n only a finite number of the non-relativistic loops contribute, and the coefficients f_0, f_1, \dots in Eq. (3.17) can be expressed through a finite number of effective-range parameters of the relativistic theory. For example, the coefficient of the diagram shown in Fig. 1a is proportional to the scattering length a in the relativistic theory to all orders in λ_r and not only at $O(\lambda_r)$, since all other diagrams Fig. 1 give vanishing contributions at threshold. Hence, the contributions Fig. 1c and Fig. 1f are proportional to $a^2|\mathbf{p}|$ and $a^3\mathbf{p}^2$, respectively, so that the expansion in the scattering length a and in the small momenta is correlated. Note that, in order to achieve this convenient ordering of the various contributions, the regularization scheme – which is used to calculate loops – should not contain a mass scale that destroys power-counting. We use dimensional regularization, because it has this property.

4 Non-relativistic effective theories: including photons

4.1 The Lagrangian

Photons are included in the theory through minimal coupling,

$$\mathcal{L} = D_\mu\phi(D^\mu\phi)^\dagger - M_r^2\phi\phi^\dagger + \frac{\lambda_r}{4!}(\phi\phi^\dagger)^2 - \frac{1}{4}F_{\mu\nu}F^{\mu\nu} + \text{counterterms}, \quad (4.1)$$

where ϕ is a charged scalar field as before, A_μ stands for the photon field, $D_\mu\phi = \partial_\mu\phi + ieA_\mu\phi$, $F_{\mu\nu} = \partial_\mu A_\nu - \partial_\nu A_\mu$, and the gauge fixing term is not explicitly shown. The theory described by the Lagrangian Eq. (4.1) contains two coupling constants λ_r and e and thus mimics the hadronic atom problem where an interplay of electromagnetic and strong effects is present. For convenience, we refer to the self-interaction of the scalar field as “strong interactions”.

The non-relativistic effective Lagrangian that describes this theory at low energy is constructed along the same pattern as before. In the presence of photons, a few additional considerations should be taken into account. First, one

starts from a gauge-invariant non-relativistic Lagrangian. Appropriate building blocks are covariant derivatives of the non-relativistic fields, and the electric and magnetic fields \mathbf{E} and \mathbf{B} . Second, the couplings are expressed in units of the *physical* mass M . The infinitely many terms in the Lagrangian are then generated by expanding it in inverse powers of the mass. This amounts to an ordering according to the number of space derivatives, and according to the number of electric and magnetic fields. Third, one may finally use different gauge fixing in the non-relativistic and in the relativistic theories. The Coulomb gauge is a convenient choice for the non-relativistic theory.

The lowest-order terms in the non-relativistic theory are

$$\begin{aligned} \mathcal{L}_{NR} &= -\frac{1}{4} F_{\mu\nu} F^{\mu\nu} + \sum_{\pm} \Phi_{\pm}^{\dagger} \left(iD_t - M + \frac{\mathbf{D}^2}{2M} + \frac{\mathbf{D}^4}{8M^3} + \dots \right. \\ &\quad \left. \mp eh_1 \frac{\mathbf{D}\mathbf{E} - \mathbf{E}\mathbf{D}}{6M^2} + \dots \right) \Phi_{\pm} + \frac{g_1}{M^2} (\Phi_+^{\dagger} \Phi_-^{\dagger}) (\Phi_+ \Phi_-) + \dots, \quad (4.2) \end{aligned}$$

where Φ_{\pm} denotes the non-relativistic field operator for charged particles, $D_t \Phi_{\pm} = \partial_t \Phi_{\pm} \mp ieA_0 \Phi_{\pm}$, $\mathbf{D}\Phi_{\pm} = \nabla\Phi_{\pm} \pm ie\mathbf{A}\Phi_{\pm}$ are the covariant derivatives, $\mathbf{E} = -\nabla A_0 - \dot{\mathbf{A}}$, $\mathbf{B} = \text{rot } \mathbf{A}$ denote the electric and magnetic fields, and h_1, g_1 are non-relativistic effective couplings⁹. For instance, h_1 is related to the electromagnetic charge radius of the particle, see below. The ellipses stand for higher-order derivative terms, as well as for non-minimal terms containing \mathbf{E} and \mathbf{B} .

We add several comments. First, the set of operators in the Lagrangian Eq. (4.2) is not minimal: the term with h_1 could be eliminated in favor of four-particle local terms by using the equations of motion for the Coulomb photon A_0 . As a result of this manipulation, e.g. the operator proportional to g_1 would receive a contribution. This means that the same linear combination of h_1 and g_1 enter the expressions for the two-particle scattering amplitude and for the bound-state energies – one does not need to know h_1 and g_1 separately. We prefer to work with this non-minimal set, because it renders the presentation more transparent and simplifies the comparison with results available in the literature. Second, calculating loops with \mathcal{L}_{NR} generates ultraviolet (UV) and infrared (IR) divergences. Therefore, to obtain UV finite Green functions and S -matrix elements at $d = 3$, counterterms should be introduced. On the other hand, because the final NR amplitudes will be expressed in terms of the UV finite relativistic expressions, such a renormalization is not needed: one simply performs all calculations at $d \neq 3$ whenever needed, then does the matching at $d > 3$ in order to

⁹Unless stated otherwise, we use here and in the following the same symbols for the coupling constants, for the running and physical masses and for the running scale as in the previous section 3, where $e = 0$ (both in the relativistic and non-relativistic theories). This avoids an unnecessary flooding of the text with symbols. Further, to the order considered in the following, we do not need to distinguish between the bare and the renormalized charge, so we keep the symbol e throughout. See also the discussion in subsection 5.6 on vacuum polarization.

avoid infrared divergences that show up in on-shell amplitudes, and sets $d = 3$ at the end. This simplifies the calculation considerably, while the final result is the same. For a detailed discussion of this point, and for explicit examples, see, e.g., Refs. [42, 181].

The LECs in the the effective Lagrangian \mathcal{L}_{NR} depend on the fine-structure constant. Indeed, they can be considered as functions of λ_r, e , of the mass M_r and of the scale μ_0 ,

$$h_1 = \bar{h}_1 + \alpha h'_1 + O(\alpha^2), \quad g_1 = \bar{g}_1 + \alpha g'_1 + O(\alpha^2), \quad (4.3)$$

such that

$$\frac{dh_1}{d\mu_0} = \frac{dg_1}{d\mu_0} = 0. \quad (4.4)$$

The barred quantities refer to the limit $\alpha = 0$.

Further note that, in general, the couplings of the non-relativistic Lagrangian are complex, because they contain contributions from processes of particle creation and annihilation in the relativistic theory. The imaginary part arises, if the threshold for such a process lies below the threshold for two massive particles. In the case which is considered here, the imaginary part of e.g. the coupling g_1 will be determined by the $\phi^+\phi^-$ -annihilation into intermediate states with two or more photons – consequently, $\text{Im} g_1 = O(\alpha^2)$ (a generalized unitarity condition which holds in the presence of complex couplings is briefly discussed in appendix B). For this reason, the general non-relativistic Lagrangian is not a hermitian operator, and T -invariance implies (cf. with Eq. (3.5))

$$T\mathcal{L}_{NR}^\dagger(x^0, \mathbf{x})T^\dagger = \mathcal{L}_{NR}(-x^0, \mathbf{x}). \quad (4.5)$$

4.2 Perturbation theory

To generate the perturbative expansion, one again splits the Lagrangian into a free and an interacting part, $\mathcal{L}_{NR} = \mathcal{L}_{NR}^0 + \mathcal{L}_{NR}^{\text{int}}$ with $\mathcal{L}_{NR}^0 = -\frac{1}{4} F_{\mu\nu} F^{\mu\nu} + \sum_{\pm} \Phi_{\pm}^\dagger (i\partial_t - M + \Delta/2M)\Phi_{\pm}$. In addition to the strong bubbles, relativistic insertions and derivative vertices already discussed in the previous section, diagrams may now contain photon lines. The calculations in the Coulomb gauge are done as follows. First, the non-dynamical field A_0 is removed from the Lagrangian by using the EOM. This procedure generates the non-local operator

$$\Delta^{-1} = -(2\pi)^{-3} \int d^3\mathbf{k} e^{-i\mathbf{k}(\mathbf{x}-\mathbf{y})} / \mathbf{k}^2 \quad (4.6)$$

in the Lagrangian. In the following, for ease of understanding, we keep calling the pertinent diagrams as “generated by the exchange of Coulomb photons”. The propagator of transverse photons in the Coulomb gauge is given by

$$D^{ij}(k) = i \int dx e^{ikx} \langle 0|T A^i(x) A^j(0)|0\rangle = -\frac{1}{k^2} \left(\delta^{ij} - \frac{k^i k^j}{\mathbf{k}^2} \right). \quad (4.7)$$

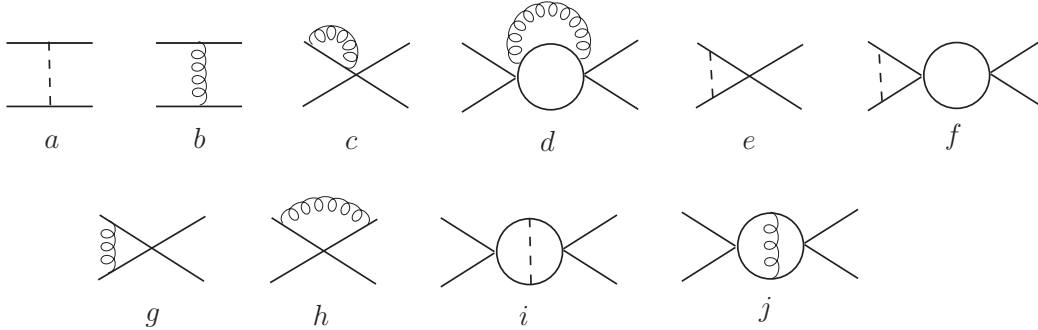


Figure 3: One–photon corrections to the non–relativistic scattering amplitude (representative set of diagrams). Dashed and wiggly lines correspond to Coulomb and to transverse photons, respectively. Diagrams containing non–minimal photon vertices, relativistic insertions and derivative couplings are not shown.

In the following, we restrict ourselves to the first nontrivial order in α , and consider 2-particle scattering in different channels. In Fig. 3, several examples of diagrams with virtual photons are displayed. These are: one–photon exchange in elastic channels (Figs. 3a,b), self–energy corrections in the external and internal legs (Figs. 3c,d), vertex corrections to the external legs (Figs. 3e,f,g,h), internal corrections due to the virtual photon exchange (Figs. 3i,j). At higher orders in the momentum expansion, diagrams containing non–minimal photon couplings occur, generated e.g. by h_1 . These are not shown in Fig. 3.

4.3 Coulomb photons

Here, we investigate diagrams containing Coulomb photons at order α : one–photon exchange (Fig. 3a), vertex correction, where the photon is attached before or after all strong vertices (Figs. 3e,f), and an internal exchange between two strong vertices (Fig. 3i).

The contribution from the graph Fig. 3a to the scattering amplitude of oppositely charged particles is given by

$$T_{NR}^{3a}(\mathbf{p}, \mathbf{q}) = \frac{4\pi\alpha}{|\mathbf{p} - \mathbf{q}|^2}. \quad (4.8)$$

This contribution is non–analytic at $\mathbf{p}, \mathbf{q} \rightarrow 0$, and thus very different from the one encountered in Eq. (3.17).

Next, we consider the vertex correction Fig. 3e. Let $V_c(\mathbf{p}, P^0)$ denote the part of the diagram which stands on the left or on the right of the first strong interaction vertex. After integration over the zeroth component of the loop momentum,

the integral to be evaluated is

$$V_c(\mathbf{p}, P^0) = e^2 \int \frac{d^d \mathbf{l}}{(2\pi)^d} \frac{1}{\mathbf{l}^2} \frac{1}{P^0 - 2M - \frac{(\mathbf{p}-\mathbf{l})^2}{M}}. \quad (4.9)$$

The contribution to the scattering amplitudes is obtained by evaluating this expression at $P^0 = 2w(\mathbf{p})$. The result (singular at $|\mathbf{p}| \rightarrow 0$) is

$$V_c(\mathbf{p}, 2w(\mathbf{p})) = -\frac{\pi\alpha M}{4|\mathbf{p}|} - i\alpha\theta_c + O(|\mathbf{p}|, d-3), \quad (4.10)$$

where

$$\theta_c = \frac{M}{2|\mathbf{p}|} \mu^{d-3} \left\{ \frac{1}{d-3} - \frac{1}{2} [\Gamma'(1) + \ln 4\pi] + \ln \frac{2|\mathbf{p}|}{\mu} \right\} \quad (4.11)$$

denotes the (infrared-divergent) Coulomb phase¹⁰, and μ denotes the scale of dimensional regularization in the non-relativistic theory (not equal to μ_0 in general).

Finally, we consider the two-loop diagram Fig. 3i. Let $B_c(P^0)$ denote the part of the amplitude which corresponds to the diagram with one photon exchange between two strong interaction vertices. Integrating over the zeroth components of the loop momenta, it is given by

$$B_c(P^0) = \frac{e^2}{(2\pi)^{2d}} \int \frac{d^d \mathbf{l}_1}{P^0 - 2M - \frac{\mathbf{l}_1^2}{M}} \frac{1}{|\mathbf{l}_1 - \mathbf{l}_2|^2} \frac{d^d \mathbf{l}_2}{P^0 - 2M - \frac{\mathbf{l}_2^2}{M}}. \quad (4.12)$$

Evaluating this expression at $P^0 = 2w(\mathbf{p})$, we find a result which is again singular at $|\mathbf{p}| \rightarrow \mathbf{0}$,

$$\begin{aligned} B_c(2w(\mathbf{p})) &= -\frac{\alpha M^2}{8\pi} \left\{ \Lambda(\mu) + 2 \ln \frac{2|\mathbf{p}|}{\mu} - 1 - i\pi \right\} + O(|\mathbf{p}|, d-3), \\ \Lambda(\mu) &= \mu^{2(d-3)} \left\{ \frac{1}{d-3} - \ln 4\pi - \Gamma'(1) \right\}. \end{aligned} \quad (4.13)$$

Here, $\Lambda(\mu)$ contains an UV singularity. For the consistency of the method it is important to note that the contributions from diagrams obtained by adding mass insertions and/or using vertices with derivative couplings (not shown explicitly in Fig. 3) are suppressed by powers of momenta with respect to the leading terms B_c and V_c . They are not needed in the following.

¹⁰This phase is identical to the one in the relativistic theory [188] at this order.



Figure 4: NR propagator in the presence of transverse photons.

4.4 Transverse photons and the threshold expansion

The exchange of one transverse photon (Fig. 3b) contributes with

$$T_{NR}^{3b}(\mathbf{p}, \mathbf{q}) = \frac{4\pi\alpha}{|\mathbf{p} - \mathbf{q}|^2} \frac{(\mathbf{p} + \mathbf{q})^2}{4M^2}. \quad (4.14)$$

This term is suppressed by two powers of momenta as compared to the Coulomb contribution Eq. (4.8). This is due to the fact that the transverse photon vertex in the Lagrangian Eq. (4.2) contains a derivative, whereas the corresponding vertex for the Coulomb photon is point-like. In other words, the ordering in the Lagrangian is preserved in the contribution to the amplitude in this case: a term which is suppressed in the Lagrangian by powers of the mass M generates a term in the amplitude which is suppressed by powers of momenta. This feature is called *power counting* in the following.

For the non-relativistic theory to make sense, power-counting should also persist in loops. This is not, however, the case if one uses standard dimensional regularization in the loop calculations. To demonstrate this fact, we consider in detail the virtual photon contribution to the self-energy of the massive particle at one loop. Summing up one-loop diagrams with a transverse photon to all orders (see Fig. 4), one obtains

$$D(p) = \frac{1}{\Omega} + \frac{1}{\Omega} \Sigma_\gamma(\Omega, \mathbf{p}) \frac{1}{\Omega} + \dots = \frac{1}{\Omega - \Sigma_\gamma(\Omega, \mathbf{p})}, \quad (4.15)$$

where $\Omega = M + \frac{\mathbf{p}^2}{2M} - p^0 = O(v^2)$ and $\Sigma_\gamma(\Omega, \mathbf{p})$ denotes the one-loop diagram

$$\Sigma_\gamma(\Omega, \mathbf{p}) = \frac{e^2}{M^2} \int \frac{d^D l}{(2\pi)^{D_i}} \frac{\mathbf{p}^2 - (\mathbf{p}\mathbf{l})^2/l^2}{-l^2(M + \frac{(\mathbf{p}-\mathbf{l})^2}{2M} - p^0 + l^0)}. \quad (4.16)$$

[Coulomb photons do not contribute to the self energy, because the Coulomb photon propagator does not depend on the zeroth component l^0 . Therefore, one may close the contour of integration over l^0 in that half-plane where the propagator of the massive particle has no singularity.]

The self-energy is obviously of order \mathbf{p}^2 ,

$$\Sigma_\gamma(\Omega, \mathbf{p}) = \frac{2e^2\mathbf{p}^2}{M} \tilde{\Sigma}_\gamma(\Omega, \mathbf{p}). \quad (4.17)$$

We combine the denominators by use of the Feynman–Schwinger trick and obtain at $\mathbf{p} = 0$

$$\tilde{\Sigma}_\gamma(\Omega, 0) = -\frac{1}{12\pi^2} \ln \frac{\Omega}{2M} \left(1 - \frac{1}{\sqrt{1 - \frac{2\Omega}{M}}} \right) + \sum_{n=0}^{\infty} a_n \left(\frac{\Omega}{M} \right)^n, \quad a_0 \neq 0. \quad (4.18)$$

The result consists of two parts: a non-analytic piece, which starts with a term proportional to $\Omega \ln \Omega$, and a polynomial part, which starts with a constant. The non-analytic part contributes all in all at order v^4 to the self-energy and therefore respects power counting: its contribution is suppressed by v^2 with respect to the tree contribution Ω in the denominator of the last term in Eq. 4.15. On the other hand, the polynomial part breaks power counting: it generates a term which is of the same order as the tree level one. Considering derivative vertices in Fig. 4, it is seen that the corresponding diagrams contribute at the same order in v , so that the low-energy effective theory is inconsistent in this sense.

It is easy to identify the reason for this failure. First, we note that the integration momenta l^0, \mathbf{l} can vary in wildly different regions. For example, one or both of them can be of order of the hard scale M , be “soft” ($\sim v$) or “ultrasoft” ($\sim v^2$). Consequently, this integral is given by a sum of different terms, where each one corresponds to an integration in a different regime (see, e.g., Ref. [178]. For a detailed investigation of this statement for a specific one-loop diagram in the non-relativistic effective theory, see also Ref. [45]). Therefore, in order to construct a consistent low-energy theory, one should modify the Feynman rules to get rid of the high-energy contribution. In a most general way, this can be done by using the so-called “threshold expansion” [42, 175, 176, 178–182]¹¹. A simple algorithm for the calculation of Feynman diagrams that occur in the present work can be formulated as follows:

- i) Perform contour integrals over the zeroth components of the momenta.
- ii) Assume all 3-momenta (external as well as the integration momenta) to be much smaller than the hard scale M ; expand the integrands in the small 3-momenta.
- iii) Interchange the order of integration and expansion, then perform integrations in dimensional regularization.

After applying the threshold expansion, the integrand becomes a homogeneous function in small kinematic variables, and the counting rules are restored. On the other hand, the high-energy contribution, which is polynomial at low energy, and which upsets power counting, is removed from the result.

¹¹In case of πN scattering at one loop in ChPT, the threshold expansion is obviously equivalent to the infrared regularization introduced in Ref. [146].

Let us see how this procedure works in the present case. The contour integration in Eq. (4.16) gives

$$\Sigma_\gamma(\Omega, \mathbf{p}) = \frac{e^2}{2M^2} \int \frac{d^d l}{(2\pi)^d} \left(\mathbf{p}^2 - \frac{(\mathbf{pl})^2}{l^2} \right) \frac{1}{|l|} \frac{1}{\Omega + |l| - \frac{\mathbf{pl}}{M} + \frac{l^2}{2M}}. \quad (4.19)$$

It is seen that l should scale like $\Omega \sim v^2$, otherwise the expansion of the integrand leads to no-scale integrals that vanish in dimensional regularization. With such scaling assumed, the individual terms in the denominator of the last term in Eq. (4.16) scale like v^2, v^2, v^3, v^4 . Therefore, this denominator is not a homogeneous function in v , leading to a breakdown of the counting rules. Applying the threshold expansion, we obtain (we put a hat on threshold-expanded quantities)

$$\begin{aligned} \hat{\Sigma}_\gamma(\Omega, \mathbf{p}) &= \frac{e^2}{2M^2} \int \frac{d^d \mathbf{l}}{(2\pi)^d} \left(\mathbf{p}^2 - \frac{(\mathbf{pl})^2}{l^2} \right) \frac{1}{|l|} \left\{ \frac{1}{\Omega + |l|} \right. \\ &\quad \left. + \left(\frac{\mathbf{pl}}{M} - \frac{l^2}{2M} \right) \frac{1}{(\Omega + |l|)^2} + \dots \right\}. \end{aligned} \quad (4.20)$$

Performing the remaining integration, we obtain

$$\begin{aligned} \hat{\Sigma}_\gamma(\Omega, \mathbf{p}) &= \frac{e^2}{2M^2} \mathbf{p}^2 \Omega^{d-2} \frac{\Gamma(d)\Gamma(2-d)}{(4\pi)^{d/2}\Gamma(1+\frac{d}{2})} + O(M^{-3}) \\ &= \frac{e^2}{6\pi^2 M^2} \mathbf{p}^2 \Omega \left\{ L(\mu) + \ln \frac{2\Omega}{\mu} - \frac{1}{3} \right\} + O(M^{-3}, d-3), \end{aligned} \quad (4.21)$$

$$L(\mu) = \mu^{d-3} \left(\frac{1}{d-3} - \frac{1}{2} (\Gamma'(1) + \ln 4\pi + 1) \right). \quad (4.22)$$

As expected, the non-analytic piece $\sim \Omega \ln \Omega$ stays unaffected. On the other hand, the part of the polynomial piece which scales like $\sim v^2$ has disappeared from the result. Since the threshold-expanded self-energy is proportional to Ω , the position of the particle pole is not affected by radiative corrections. It is furthermore seen that in the vicinity of the mass shell, the propagator Eq. (4.15) is unaffected,

$$D(p) \rightarrow \frac{1}{\Omega}, \quad \Omega \rightarrow 0 \quad (d > 3), \quad (4.23)$$

as a result of which the external lines are not renormalized (wave function renormalization constant $Z = 1$). Further, it is seen from Eq. (4.21) that the introduction of a counterterm rendering the two-point function finite at $d = 3$ would add a contribution of order \mathbf{p}^2 to Z , which diverges as $d \rightarrow 3$.

We investigate a second example, and consider a diagram that describes the exchange of a transverse photon between the initial pair of charged particles

with momenta $p_{\pm}^{\mu} = (p^0, \pm \mathbf{p})$, see Fig. 3g. The contribution of this diagram is proportional to the integral

$$\begin{aligned}
J_{+-\gamma}(|\mathbf{p}|) &= -\frac{e^2}{M^2} \int \frac{d^D l}{(2\pi)^D i} \left(\mathbf{p}^2 - \frac{(\mathbf{p}\mathbf{l})^2}{\mathbf{l}^2} \right) \frac{1}{\left(M + \frac{(\mathbf{p}-\mathbf{l})^2}{2M} - p^0 + l^0 \right)} \\
&\times \frac{1}{l^2 \left(M + \frac{(\mathbf{p}-\mathbf{l})^2}{2M} - p^0 - l^0 \right)}. \tag{4.24}
\end{aligned}$$

We put the external particles on the mass shell, $p^0 = M + \mathbf{p}^2/(2M) + O(\mathbf{p}^4)$, and perform the threshold expansion in the integral. Note that with this procedure, the integrands should be expanded in the $O(\mathbf{p}^4)$ remainder of p^0 . The threshold-expanded integral can be rewritten in the following manner,

$$\begin{aligned}
\hat{J}_{+-\gamma}(|\mathbf{p}|) &= \frac{e^2}{M} \int \frac{d^d \mathbf{l}}{(2\pi)^d} \frac{1}{\mathbf{l}^2} \left(\mathbf{p}^2 - \frac{(\mathbf{p}\mathbf{l})^2}{\mathbf{l}^2} \right) \frac{1}{\mathbf{l}^2 - 2\mathbf{p}\mathbf{l}} + \dots \\
&= \frac{e^2 |\mathbf{p}|}{16M} + \frac{ie^2 |\mathbf{p}|}{8\pi M} \left(L(\mu) + \ln \frac{2|\mathbf{p}|}{\mu} \right) + \dots. \tag{4.25}
\end{aligned}$$

The divergence at $d = 3$ is an infrared one. We see that power-counting is at work also here: in comparison to the exchange of a Coulomb photon, this contribution is suppressed by \mathbf{p}^2 . This particular contribution to the scattering amplitude vanishes at threshold as well.

4.5 Matching

The matching condition given in Eq. (3.12) is universal and holds in the presence of photons as well (as photons are relativistic particles, the corresponding states have the same normalization as in the relativistic theory). However, as we have explicitly seen, the singularity structure of the amplitudes near threshold is different from one given in Eq. (3.17). Further, in order to determine all couplings in the non-relativistic Lagrangian Eq. (4.2) separately (e.g. the coupling constant h_1), it is convenient to consider amplitudes with external photon legs as well.

We start with the coupling h_1 which is related to the charge radius of the scalar particle. We closely follow the method described in Ref. [173]. We consider the transition amplitude \mathbf{S}_{fi} of the charged particle in an external field A_{μ}^{ext} and define the relativistic form factor $F(t)$ through the linear term in the expansion in A_{μ}^{ext} ,

$$\mathbf{S}_{fi} = 2w(\mathbf{p}) (2\pi)^3 \delta^3(\mathbf{p} - \mathbf{q}) + ie \tilde{A}_{\mu}^{\text{ext}}(p - q) (p + q)^{\mu} F(t) + O(e^2) \quad [\text{relativistic}], \tag{4.26}$$

where $\tilde{A}_{\mu}^{\text{ext}}(p - q)$ denotes the Fourier-transform of the external field, and where $t = (p - q)^2$. At a small t ,

$$F(t) = 1 + \frac{1}{6} \langle r^2 \rangle t + O(t^2), \tag{4.27}$$

where $\langle r^2 \rangle$ stands for the mean square radius in the limit $\alpha = 0$.

The definition of the form factor in the non-relativistic case is very similar,

$$\mathbf{S}_{fi} = (2\pi)^3 \delta^3(\mathbf{p} - \mathbf{q}) + ie\tilde{A}_\mu^{\text{ext}}(p - q)F_{NR}^\mu(p, q) + O(e^2) \quad [\text{non-relativistic}]. \quad (4.28)$$

The matching condition Eq. (3.12) yields in our case

$$(p + q)^\mu F(t) = (2w(\mathbf{p})2w(\mathbf{q}))^{1/2} F_{NR}^\mu(p, q). \quad (4.29)$$

The zeroth component of the non-relativistic form factor at the lowest order in α can be directly read off from the Lagrangian Eq. (4.2), considering the coefficient of the term linear in the field A^0 ,

$$F_{NR}^0(p, q) = \left(1 - \frac{h_1}{6M^2} (\mathbf{p} - \mathbf{q})^2 + O(v^4) \right), \quad (4.30)$$

and Eq. (4.29) finally gives

$$h_1 = M^2 \langle r^2 \rangle + O(\alpha). \quad (4.31)$$

This relation is an example of matching to threshold parameters, discussed in subsection 3.6. Namely, the quantity $\langle r^2 \rangle$ is the charge radius of the relativistic scalar particle at $\alpha = 0$ and to all orders in the strong coupling constant λ_r . In order to perform matching in terms of λ_r , all what one has to do is to calculate $\langle r^2 \rangle$ in the relativistic theory at a given order in λ_r and substitute this result into Eq. (4.31). Additional calculations that would invoke non-relativistic EFT are not needed.

We now perform the matching of the coupling g_1 . For this, we consider the elastic scattering amplitude of two oppositely charged particles. Let us restrict to diagrams of order α . At this order, the relevant diagrams can be divided in two groups: those which can be made disconnected by cutting one photon line, and those which cannot,

$$T = T^{1\gamma} + \bar{T}, \quad T_{NR} = T_{NR}^{1\gamma} + \bar{T}_{NR}. \quad (4.32)$$

For the relativistic theory, this splitting is unambiguous. On the other hand, the non-relativistic Lagrangian is not unique – e.g., depending on whether one keeps the coupling h_1 in the Lagrangian or removes it using the equations of motion, the corresponding term in $T_{NR}^{1\gamma}$ will be absent. Here, we stick to \mathcal{L}_{NR} in Eq. (4.2), which generates the relativistic one-photon exchange amplitude to the relevant order in the momentum expansion. The matching condition then holds separately for the 1-photon exchange contribution, and for the remaining part of the amplitude. For this reason, we retain only the one-particle irreducible amplitudes \bar{T} and \bar{T}_{NR} in the matching condition.

We now first discuss the singularity structure of the non-relativistic scattering amplitude at threshold, and combine information about the strong sector from Eq. (3.17) with the known threshold behavior of the various diagrams with virtual photons, given in Eqs. (4.10), (4.13), (4.21), (4.23) and (4.25). It can be easily seen that at order α

- i) diagrams with transverse photons do not contribute at threshold;
- ii) each strong loop gives rise to a suppression factor $|\mathbf{p}|$, so that only diagrams with not more than one strong bubble contribute at threshold;
- iii) in the expression for \bar{T}_{NR} , one may combine the strong diagram shown in Fig. 1a together with the Coulomb correction to this diagram in Fig. 3e (there is second diagram of this type, where the Coulomb photon is exchanged after the strong vertex). One may further check that at order α the (infrared-divergent) Coulomb phase $1 + 2i\alpha\theta_c = e^{2i\alpha\theta_c} + O(\alpha^2)$ can be factorized in the whole non-relativistic amplitude.

Using Eqs. (4.10), (4.13), (4.23), (4.25), we find that the threshold behavior Eq. (3.17) is modified – at order α – by virtual photon contributions in the following manner,

$$e^{-2i\alpha\theta_c}\bar{T}_{NR} = \frac{A_1}{|\mathbf{p}|} + A_2 \ln \frac{2|\mathbf{p}|}{M} + A_3 + O(|\mathbf{p}|). \quad (4.33)$$

A straightforward calculation of the coefficients gives

$$\begin{aligned} A_1 &= \frac{\pi\alpha g_1}{2M}, & A_2 &= -\frac{\alpha g_1^2}{4\pi M^2}, \\ A_3 &= \frac{g_1}{M^2} \left\{ 1 - \frac{\alpha g_1}{8\pi} \left(\Lambda(\mu) + \ln \frac{M^2}{\mu^2} - 1 - 2\pi i \right) \right\}. \end{aligned} \quad (4.34)$$

Suppose now that one calculates the relativistic amplitude at order α , and to any order in λ_r . In order to be consistent with the non-analytic behavior predicted by the non-relativistic theory, the threshold behavior of the relativistic 1-particle irreducible amplitude must be given by

$$e^{-2i\alpha\theta_c}\bar{T} = \frac{B_1}{|\mathbf{p}|} + B_2 \ln \frac{2|\mathbf{p}|}{M} + \mathcal{T} + O(|\mathbf{p}|). \quad (4.35)$$

The infrared-finite quantity \mathcal{T} will be referred to hereafter as the “relativistic threshold amplitude.” It can be considered the $O(\alpha)$ generalization of the standard definition of the scattering amplitude, valid in the presence of real and virtual photons. [Remark: While defining the threshold amplitude, one has to discard in particular terms which diverge logarithmically at threshold. This procedure is ambiguous, and depends on the choice of the scale at which the logarithm is set to vanish. In Eqs. (4.33) and in (4.35), it was chosen to be the

reduced mass of the system. We are free, however, to choose instead a different scale, as a result of which the threshold amplitude will change accordingly. On the other hand, observable quantities, which are expressed through the threshold amplitude (e.g. bound–state energies of hadronic atoms), are independent of this scale. In the present model, this can be verified order by order in the perturbative expansion.]

Finally, we express the coupling g_1 in terms of \mathcal{T} ,

$$\mathcal{T} = 4g_1 \left\{ 1 - \frac{\alpha g_1}{8\pi} \left(\Lambda(\mu) + \ln \frac{M^2}{\mu^2} - 1 - 2\pi i \right) \right\}. \quad (4.36)$$

This completes the matching of g_1 and of h_1 .

5 Bound states

5.1 Introductory remarks

In the previous sections, we constructed a systematic non–relativistic field theory, which is equivalent to the underlying relativistic theory at small 3-momenta. The equivalence is achieved by performing a matching procedure order by order in the momentum expansion. The non–relativistic approach does not provide new information about the low–energy behavior of the scattering amplitudes, because this low–energy behavior is the information that enters the matching condition.

The non–relativistic approach becomes useful in the description of the shallow bound states in the theory. To be specific, we consider bound states in the system described by the Lagrangian Eq. (4.1). In this model, in the vicinity of the elastic threshold, there exists a tower of nearly Coulombic bound states, whose energies are approximately given by

$$E_n = 2M - \frac{M\alpha^2}{4n^2}, \quad n = 1, 2, \dots \quad (5.1)$$

Due to the combined effect of the strong and the residual electromagnetic interaction, the energy levels are displaced and acquire a finite width. Our aim is to find the pertinent corrections to the leading order formula Eq. (5.1). As already mentioned, the non–relativistic Lagrangian constructed in the previous section offers a simple, elegant and very efficient framework to solve the problem [37]. We illustrate in this section the procedure.

5.2 Coulomb problem

We start from the unperturbed solution which corresponds to a pure Coulomb potential. The unperturbed situation is described by the Lagrangian which is

obtained from the original non-relativistic Lagrangian Eq. (4.2) by discarding everything but the minimal coupling of the Coulomb photons to the non-relativistic massive particle,

$$\mathcal{L}_{NR} = -\frac{1}{2} A^0 \Delta A^0 + \sum_{\pm} \Phi_{\pm}^{\dagger} \left(iD_t - M + \frac{\Delta}{2M} \right) \Phi_{\pm}. \quad (5.2)$$

Eliminating the field A^0 through the EOM, the Hamiltonian becomes

$$\begin{aligned} \mathbf{H}_0 + \mathbf{H}_C &= \int d^3\mathbf{x} \left\{ \sum_{\pm} \Phi_{\pm}^{\dagger} \left(M - \frac{\Delta}{2M} \right) \Phi_{\pm} \right. \\ &\quad \left. - \frac{e^2}{2} (\Phi_+^{\dagger} \Phi_+ - \Phi_-^{\dagger} \Phi_-) \Delta^{-1} (\Phi_+^{\dagger} \Phi_+ - \Phi_-^{\dagger} \Phi_-) \right\}. \end{aligned} \quad (5.3)$$

We introduce creation and annihilation operators,

$$\Phi_{\pm}(0, \mathbf{x}) = \int \frac{d^3\mathbf{p}}{(2\pi)^3} e^{i\mathbf{p}\mathbf{x}} a_{\pm}(\mathbf{p}), \quad [a_{\pm}(\mathbf{p}), a_{\pm}^{\dagger}(\mathbf{k})] = (2\pi)^3 \delta^3(\mathbf{p} - \mathbf{k}), \quad (5.4)$$

and construct the bound state of two charged particles in Fock space,

$$\begin{aligned} |\Psi_{nlm}, \mathbf{P}\rangle &= \int \frac{d^3\mathbf{k}}{(2\pi)^3} \Psi_{nlm}(\mathbf{k}) |\mathbf{P}, \mathbf{k}\rangle, \\ |\mathbf{P}, \mathbf{k}\rangle &= a_+^{\dagger} \left(\frac{1}{2} \mathbf{P} + \mathbf{k} \right) a_-^{\dagger} \left(\frac{1}{2} \mathbf{P} - \mathbf{k} \right) |0\rangle, \end{aligned} \quad (5.5)$$

where $\Psi_{nlm}(\mathbf{k})$ denotes the Schrödinger wave function in momentum space, and n, l, m stand for the principal quantum number, the angular momentum and its projection in the z -direction, respectively. See appendix A for further notation, in particular, for an explicit expression of the wave functions $\Psi_{nlm}(\mathbf{k})$. The state vectors (5.5) satisfy

$$(\mathbf{H}_0 + \mathbf{H}_C) |\Psi_{nlm}, \mathbf{P}\rangle = \left(E_n + \frac{\mathbf{P}^2}{4M} \right) |\Psi_{nlm}, \mathbf{P}\rangle. \quad (5.6)$$

To proceed, we introduce the resolvent for the Coulomb problem,

$$\mathbf{G}_C(z) = \frac{1}{z - \mathbf{H}_0 - \mathbf{H}_C} = \mathbf{G}_0(z) + \mathbf{G}_0(z) \mathbf{H}_C \mathbf{G}_C(z), \quad (5.7)$$

whose matrix element between the states $|\mathbf{P}, \mathbf{k}\rangle$ develops poles at $z = E_n$. To remove the CM momentum of the matrix elements, we introduce the notation

$$\langle \mathbf{q} | \mathbf{r}(z) | \mathbf{p} \rangle = \int \frac{d^3\mathbf{P}}{(2\pi)^3} \langle \mathbf{P}, \mathbf{q} | \mathbf{R}(z) | \mathbf{0}, \mathbf{p} \rangle, \quad (5.8)$$

where $\mathbf{R}(z)$ is any operator in Fock space, and where $\mathbf{r}(z)$ denotes the pertinent operator in the CM system. The matrix element of the resolvent \mathbf{G}_C is related to Schwinger's Green function [189],

$$\begin{aligned} (\mathbf{q}|\mathbf{g}_C(z)|\mathbf{p}) &= \frac{(2\pi)^3\delta^3(\mathbf{q}-\mathbf{p})}{E-\frac{\mathbf{q}^2}{M}} - \frac{1}{E-\frac{\mathbf{q}^2}{M}} \frac{4\pi\alpha}{|\mathbf{q}-\mathbf{p}|^2} \frac{1}{E-\frac{\mathbf{p}^2}{M}} \\ &- \frac{1}{E-\frac{\mathbf{q}^2}{M}} 4\pi\alpha\eta I(E; \mathbf{q}, \mathbf{p}) \frac{1}{E-\frac{\mathbf{p}^2}{M}}, \end{aligned} \quad (5.9)$$

with

$$I(E; \mathbf{q}, \mathbf{p}) = \int_0^1 \frac{x^{-\eta} dx}{[(\mathbf{q}-\mathbf{p})^2 x + \eta^2/\alpha^2(1-x)^2(E-\frac{\mathbf{q}^2}{M})(E-\frac{\mathbf{p}^2}{M})]}, \quad (5.10)$$

where $\eta = \frac{1}{2}\alpha(-E/M)^{-1/2}$ and $E = z - 2M$. This function develops poles at $\eta = 1, 2, \dots$. The Coulomb wave functions in momentum space can be read from the residues of these poles [189].

5.3 Feshbach formalism and the Rayleigh–Schrödinger perturbation theory

We now construct a systematic perturbation theory to include the remaining strong and electromagnetic interactions which are contained in the Lagrangian Eq. (4.2). It is convenient to apply the so-called Feshbach formalism [38, 39].

The Hamiltonian of the system takes the form

$$\mathbf{H} = \mathbf{H}_0 + \mathbf{H}_C + \mathbf{V}, \quad (5.11)$$

where \mathbf{V} stands for all interactions other than the static Coulomb potential. Consider the full resolvent

$$\mathbf{G}(z) = \frac{1}{z - \mathbf{H}}. \quad (5.12)$$

It satisfies the equation

$$\mathbf{G} = \mathbf{G}_C + \mathbf{G}_C \boldsymbol{\tau} \mathbf{G}_C, \quad \boldsymbol{\tau} = \mathbf{V} + \mathbf{V} \mathbf{G}_C \boldsymbol{\tau}. \quad (5.13)$$

The spectral representation of this resolvent contains a sum over all states. In order to calculate the energy shift of the n, l level, it is convenient to remove the corresponding unperturbed pole contribution $(z - E_n)^{-1}$ (in the CM frame) from $\mathbf{G}_C(z)$ by defining

$$\bar{\mathbf{G}}_C^{nl} = \mathbf{G}_C \left\{ \mathbf{1} - \sum_m \int \frac{d^3\mathbf{P}}{(2\pi)^3} |\Psi_{nlm}, \mathbf{P}\rangle \langle \Psi_{nlm}, \mathbf{P}| \right\}. \quad (5.14)$$

We further introduce

$$\bar{\tau}^{nl} = \mathbf{V} + \mathbf{V}\bar{\mathbf{G}}_C^{nl}\bar{\tau}^{nl}, \quad (5.15)$$

and find for \mathbf{G} the representation

$$\mathbf{G} = \bar{\mathbf{G}}_C^{nl} + \bar{\mathbf{G}}_C^{nl}\bar{\tau}^{nl}\bar{\mathbf{G}}_C^{nl} + (1 + \bar{\mathbf{G}}_C^{nl}\bar{\tau}^{nl})\mathbf{\Pi}_{nl}(1 + \bar{\tau}^{nl}\bar{\mathbf{G}}_C^{nl}), \quad (5.16)$$

where

$$\mathbf{\Pi}_{nl} = \sum_m \int \frac{d^3\mathbf{P}}{(2\pi)^3} \frac{|\Psi_{nlm}, \mathbf{P}\rangle\langle\Psi_{nlm}, \mathbf{P}|}{z - \frac{\mathbf{P}^2}{4M} - E_n - (\Psi_{nl}|\bar{\tau}^{nl}(z; \mathbf{P})|\Psi_{nl})}, \quad (5.17)$$

and

$$(\Psi_{nl}|\bar{\tau}^{nl}(z; \mathbf{P})|\Psi_{nl}) = \int \frac{d^3\mathbf{P}'}{(2\pi)^3} \langle\Psi_{nlm}, \mathbf{P}'|\bar{\tau}^{nl}(z)|\Psi_{nlm}, \mathbf{P}\rangle. \quad (5.18)$$

Here we used the fact that the right-hand side does not depend on the magnetic quantum number m – here and in the following, we therefore omit the subscript m , whenever no ambiguity can occur. The singularity at $z = E_n$ is absent in the barred quantities. Therefore, the pertinent pole must occur through a zero in the denominator of the expression Eq. (5.17). In the CM frame, the relevant eigenvalue equation to be solved is

$$z_{nl} - E_n - (\Psi_{nl}|\bar{\tau}^{nl}(z)|\Psi_{nl}) = 0, \quad (5.19)$$

where the matrix element denotes the quantity on the left-hand side of Eq. (5.18), evaluated at $\mathbf{P} = 0$. To ease notation, we often will omit the indexes in z_{nl} .

The *master equation* (5.19) is a compact form of the conventional Rayleigh–Schrödinger perturbation theory, valid for unstable systems as well. It fixes the convergence domain of perturbation theory: the theory is applicable as long as the level shift does not become comparable to the distance between the ground-state and the first radial-excited Coulomb poles. Equation (5.19) is valid for a general potential – containing e.g. the interaction with the transverse photons – since in the derivation, we did not use the explicit form of the interaction Hamiltonian.

Finally, the level shifts and the widths can be obtained from the solution of the master equation,

$$z = E_n + \Delta E_{nl}, \quad (5.20)$$

where ΔE_{nl} is complex. As we shall see later, the poles of the resolvent $\mathbf{G}(z)$ occur on the second Riemann sheet in the complex z -plane, in accordance with analyticity requirements.

5.4 Energy levels

The energy shifts admit a Taylor series expansion (up to logarithms),

$$\Delta E_{nl} = a_{nl}\alpha^3 + b_{nl}\alpha^4 \ln \alpha + c_{nl}\alpha^4 + O(\alpha^5). \quad (5.21)$$

We now show how to calculate the coefficients a_{nl} , b_{nl} and c_{nl} .

We expand the matrix element in the master equation (5.19) in a Taylor series in $(z - E_n)$ and obtain

$$z - E_n = \frac{(\Psi_{nl}|\bar{\tau}^{nl}(E_n)|\Psi_{nl})}{1 - \frac{d}{dE_n}(\Psi_{nl}|\bar{\tau}^{nl}(E_n)|\Psi_{nl})} + \dots. \quad (5.22)$$

Because the numerator is a quantity of order α^3 , the second term in the denominator starts to contribute at order α^5 and can thus be dropped [42], and one finds

$$z - E_n = (\Psi_{nl}|\bar{\tau}^{nl}(E_n)|\Psi_{nl}) + O(\alpha^5). \quad (5.23)$$

It remains to evaluate the pertinent matrix elements of the operator $\bar{\tau}^{nl}(E_n)$.

We start with the determination of the perturbation \mathbf{V} from the Lagrangian Eq. (4.2). One first eliminates the non-dynamical field A^0 by using EOM. At the order of accuracy required by Eq. (5.21), it suffices to retain only following terms:

$$\begin{aligned} \mathbf{V} &= \mathbf{H}_S + \mathbf{H}_R + e\mathbf{H}_\gamma + e^2\mathbf{H}_{fin} + \dots, \\ \mathbf{H}_S &= -\frac{g_1}{M^2} \int d^3\mathbf{x} \Phi_+^\dagger \Phi_-^\dagger \Phi_+ \Phi_-, \\ \mathbf{H}_R &= -\sum_{\pm} \int d^3\mathbf{x} \Phi_{\pm}^\dagger \frac{\Delta^2}{8M^3} \Phi_{\pm}, \\ e\mathbf{H}_\gamma &= \sum_{\pm} \frac{\mp ie}{M} \int d^3\mathbf{x} \mathbf{A} \Phi_{\pm}^\dagger \nabla \Phi_{\pm}, \\ e^2\mathbf{H}_{fin} &= -\frac{e^2 h_1}{6M^2} \int d^3\mathbf{x} (\Phi_+^\dagger \Phi_+ - \Phi_-^\dagger \Phi_-)(\Phi_+^\dagger \Phi_+ - \Phi_-^\dagger \Phi_-). \end{aligned} \quad (5.24)$$

Additional terms generated by the Lagrangian Eq. (4.2) do not contribute to the energy shift at $O(\alpha^4)$, and are hence omitted. Evaluating the energy shift is now straightforward. Solving Eq. (5.15) by iterations, at the order of accuracy required we get

$$\bar{\tau}^{nl}(z) = \mathbf{H}_S + \mathbf{H}_S \bar{\mathbf{G}}_C^{nl}(z) \mathbf{H}_S + \mathbf{H}_R + e^2\mathbf{H}_{fin} + e^2\mathbf{H}_\gamma \bar{\mathbf{G}}_C^{nl}(z) \mathbf{H}_\gamma + \dots. \quad (5.25)$$

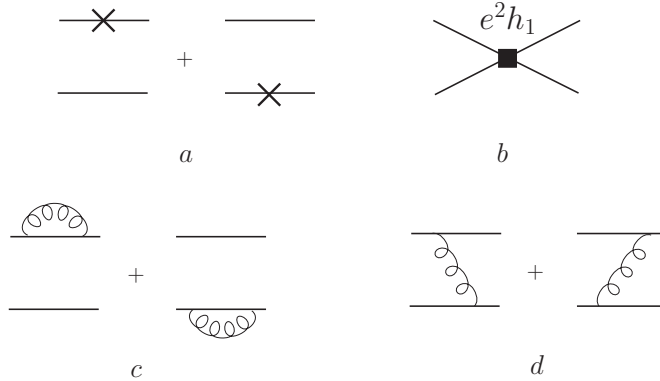


Figure 5: Diagrams contributing to the electromagnetic energy shift: a) relativistic insertions; b) finite-size effect; c) self-energy corrections due to transverse photons; d) transverse photon exchange.

Then, using Eq. (5.23), we find

$$\begin{aligned} \Delta E_{nl} = & (\Psi_{nl} | \mathbf{H}_S + \mathbf{H}_S \bar{\mathbf{G}}_C^{nl}(E_n) \mathbf{H}_S + \mathbf{H}_R + e^2 \mathbf{H}_{fin} \\ & + e^2 \mathbf{H}_\gamma \bar{\mathbf{G}}_C^{nl}(E_n) \mathbf{H}_\gamma | \Psi_{nl}) + O(\alpha^5). \end{aligned} \quad (5.26)$$

In order to evaluate this quantity, one inserts a complete set of states between the various operators – only a finite number of terms is non-zero in each sum – and calculates the integrals over the intermediate momenta. It is convenient to further split the energy shift Eq. (5.26) into so-called “strong” and “electromagnetic” parts,

$$\Delta E_{nl} = \delta_{l0} \left(\Delta E_n^{\text{str}} - \frac{i}{2} \Gamma_n \right) + \Delta E_{nl}^{\text{em}} + O(\alpha^5) \quad [\text{scalar QED}]. \quad (5.27)$$

The (real) electromagnetic shifts $\Delta E_{nl}^{\text{em}}$ are evaluated below. The above equation should be taken as a definition of the bracketed term on the right-hand side. Since the strong Hamiltonian is local, the strong corrections to the energy levels with angular momentum $l \neq 0$ are suppressed by additional powers of α . As a result of this, they vanish at the accuracy considered here, as is indicated by the Kronecker symbol in Eq. (5.27).

The naming scheme for the various corrections should not be understood literally. For example, the “electromagnetic” contribution contains the coupling h_1 which, according to Eq. (4.31), depends on the quantity $\langle r^2 \rangle$ which is a function of the “strong” coupling constant λ_r . Vice versa, there are electromagnetic corrections to the coupling g_1 which enters ΔE_n^{str} , see Eq. (4.3).

Let us first consider the electromagnetic shift. At $O(\alpha^4)$, it has contributions from the relativistic insertions, finite-size effects, and transverse photons (see

Fig. 5),

$$\begin{aligned}\Delta E_{nl}^{\text{em}} &= - \int \frac{d^3\mathbf{p}}{(2\pi)^3} |\Psi_{nl}(\mathbf{p})|^2 \frac{\mathbf{p}^4}{4M^3} + \frac{e^2 h_1}{3M^2} |\tilde{\Psi}_{n0}(0)|^2 \\ &\quad - \int \frac{d^3\mathbf{p}}{(2\pi)^3} \frac{d^3\mathbf{q}}{(2\pi)^3} \Psi_{nl}(\mathbf{p}) V_\gamma(\mathbf{p}, \mathbf{q}) \Psi_{nl}(\mathbf{q}).\end{aligned}\quad (5.28)$$

The contribution from the self-energy diagram Fig. 5c is of order α^5 and is therefore not displayed. The diagram with one transverse photon exchange (Fig. 5d) gives

$$\begin{aligned}V_\gamma(\mathbf{p}, \mathbf{q}) &= \frac{e^2}{4M^2|\mathbf{p} - \mathbf{q}|} \left((\mathbf{p} + \mathbf{q})^2 - \frac{(\mathbf{p}^2 - \mathbf{q}^2)^2}{|\mathbf{p} - \mathbf{q}|^2} \right) \frac{1}{\frac{M\alpha^2}{4n^2} + \frac{\mathbf{p}^2}{2M} + \frac{\mathbf{q}^2}{2M} + |\mathbf{p} - \mathbf{q}|} \\ &= \frac{e^2}{4M^2|\mathbf{p} - \mathbf{q}|^2} \left((\mathbf{p} + \mathbf{q})^2 - \frac{(\mathbf{p}^2 - \mathbf{q}^2)^2}{|\mathbf{p} - \mathbf{q}|^2} \right) + \dots.\end{aligned}\quad (5.29)$$

The evaluation of the pertinent integrals in Eq. (5.28) for arbitrary n, l is made easier by eliminating the terms of the type $\mathbf{p}^2 \Psi_{nl}(\mathbf{p})$ by use of the Schrödinger equation in momentum space [44]. We obtain

$$\Delta E_{nl}^{\text{em}} = \alpha^4 M \left(\frac{\delta_{l0}}{8n^3} + \frac{11}{64n^4} - \frac{1}{2n^3(2l+1)} \right) + \frac{\alpha^4 M^3 \langle r^2 \rangle}{6n^3} \delta_{l0}.\quad (5.30)$$

Note that in the calculations of the electromagnetic shift, we have replaced $\mathbf{G}_C(z)$ by $\mathbf{G}_0(z)$. It can be verified by direct calculations, that this does not affect the result at $O(\alpha^4)$. In the limit of point particles, the above result coincides with the one from Ref. [190]. Next, we turn to the calculation of the strong shift. According to Eq. (5.26), one has

$$\Delta E_n^{\text{str}} - \frac{i}{2} \Gamma_n = -\frac{\alpha^3 M g_1}{8\pi n^3} \left(1 - \frac{g_1}{M^2} \langle \bar{\mathbf{g}}_C^{n0}(E_n) \rangle \right) + O(\alpha^5),\quad (5.31)$$

where

$$\begin{aligned}\langle \bar{\mathbf{g}}_C^{n0}(E_n) \rangle &= \int \frac{d^d\mathbf{p}}{(2\pi)^d} \frac{d^d\mathbf{q}}{(2\pi)^d} (\mathbf{p} | \bar{\mathbf{g}}_C^{n0}(E_n) | \mathbf{q}) = \frac{\alpha M^2}{8\pi} \left(\Lambda(\mu) + \ln \frac{M^2}{\mu^2} - 1 + s_n(\alpha) \right), \\ s_n(\alpha) &= 2(\psi(n) - \psi(1) - \frac{1}{n} + \ln \alpha - \ln n), \quad \psi(x) = \Gamma'(x)/\Gamma(x).\end{aligned}\quad (5.32)$$

Finally, we substitute the value of the coupling constant g_1 from Eq. (4.36) into the expression for the strong energy shift Eq. (5.31). In this manner, one obtains an expression which contains only quantities defined in the relativistic theory,

$$\Delta E_n^{\text{str}} - \frac{i}{2} \Gamma_n = -\frac{\alpha^3 M}{32\pi n^3} \mathcal{T} \left(1 - \frac{\alpha(s_n(\alpha) + 2\pi i)}{32\pi} \mathcal{T} \right) + O(\alpha^5).\quad (5.33)$$

In order to calculate the strong shift of a given level, we take the real part of the this expression and obtain

$$\Delta E_n^{\text{str}} = -\frac{\alpha^3 M}{32\pi n^3} \text{Re} \mathcal{T} \left(1 - \frac{\alpha s_n(\alpha)}{32\pi} \text{Re} \mathcal{T} \right) + O(\alpha^5). \quad (5.34)$$

Equations (5.30), (5.33) and (5.34) are the main results of this section. They provide, at this order, a complete expression for the total (electromagnetic and strong) shift of the energy level with a given quantum numbers n, l . Furthermore, Eq. (5.34) is the generalization of the DGBT formula for the strong shift of the energy level of the bound state [8, 191–193] to next-to-leading order in α .

5.5 Decay into 2 photons

In the present theory, the ground state can only decay in two or more photons. This is a hard process, with a mass gap of order of the heavy particle mass M . Consequently, within the non-relativistic theory, the decay is described through the imaginary parts of the coupling constants. At leading order, this is the coupling g_1 in Eq. (5.31), with $\text{Im} g_1 = O(\alpha^2)$. According to Eq. (5.22), we may then use Eq. (5.31) to calculate this width up to and including terms of order α^5 . The result is

$$\Gamma_1^{2\gamma} = \frac{M\alpha^3}{4\pi} \text{Im} g_1 + O(\alpha^6). \quad (5.35)$$

At the order of accuracy we are working, the imaginary part of g_1 is given by (see also appendix B)

$$\text{Im} g_1 = \frac{1}{16} \sum_{2\gamma} (2\pi)^4 \delta^4(p_1 + p_2 - q_\gamma - q'_\gamma) |T^{\phi^+(p_1)\phi^-(p_2) \rightarrow 2\gamma}|^2 \Big|_{\text{threshold}} + O(\alpha^3). \quad (5.36)$$

Evaluating the matrix element at tree level, we find

$$\text{Im} g_1 = \pi\alpha^2 + O(\alpha^2\lambda_r, \alpha^3), \quad (5.37)$$

see also subsection 8.4. We finally arrive at the following result for the two-photon decay width of the ground state [54],

$$\Gamma_1^{2\gamma} = \frac{M\alpha^5}{4} + O(\alpha^5\lambda_r, \alpha^6). \quad (5.38)$$

In the real world, additional channels are open for decay (strong as well as electromagnetic). These will be treated in later sections.

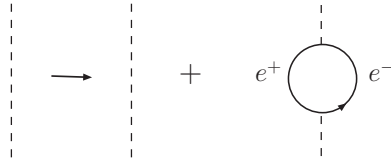


Figure 6: Modification of the static Coulomb potential by an electron loop.

5.6 Vacuum polarization due to electrons

In this subsection we separately consider a particular correction to the hadronic atom observables, which does not emerge in the model described by the Lagrangian Eq. (4.1), but is present in the case of real hadronic atoms – namely, the correction due to vacuum polarization induced by an electron loop. In order to take this effect into account, one would have to use the formulation of the low-energy effective theory of the Standard Model not in terms of photons and hadrons only [194–197], but to consider the explicit inclusion of the leptonic sector of the Standard Model as well [198]. Further, although in the treatment of the hadronic atoms weak interactions can be safely neglected, one has still to take into account the presence of electrons, which couple to photons. The reason for this is that the electron mass $m_e \approx 0.5 \text{ MeV}$ is numerically of order or smaller than αM – a scale which is “resolved” in the non-relativistic theory (M stands now for a typical reduced mass in the hadronic bound state). Examining, however, the possible contributions from the explicit electron degrees of freedom to the observables of hadronic atoms, one may easily check that these all vanish at the next-to-leading order in α with one exception. Modification of the static Coulomb potential by an electron loop (vacuum polarization) gives rise to corrections in the hadronic atom observables which are amplified by large numerical factors – powers of M/m_e , which emerge from the calculation of the matrix elements in Eq. (5.19). If one would count the quantity $\alpha M/m_e$ at $O(1)$ in order to get rid of these large factors, the vacuum polarization effect starts to contribute to the bound-state energy at $O(\alpha^3)$, i.e. at the same order as the leading-order strong shift which is calculated by using the DGBT formula. To the decay width, the contribution of the vacuum polarization effect leads to a $O(\alpha)$ correction¹².

Since the effect from the presence of electrons appears only at one place, it would be counterproductive to carry out a full-fledged inclusion of the explicit electron degrees of freedom into the framework. More easily, the same goal may be achieved, using e.g. the methods described in Ref. [200] (see also Refs. [41, 201–203]). Here one first integrates out the electron field in the generating functional.

¹²For a systematic discussion of vacuum polarization contributions within a potential model framework, see, e.g., Ref. [199].

At the order of accuracy we are working, this amounts to a modification of the kinetic Lagrangian $-\frac{1}{4}F_{\mu\nu}F^{\mu\nu}$ by the electron loop. Furthermore, at this order one may safely neglect the corrections to the transverse photon propagator, performing the static limit $k^2 \rightarrow -\mathbf{k}^2$ in the photon self-energy part. Finally, the whole effect reduces to the well-known modification of the static Coulomb potential in Eq. (5.3) through the electron loop (see Fig. 6). In momentum space, this modification reads

$$\begin{aligned} -\frac{4\pi\alpha}{\mathbf{k}^2} &\rightarrow -\frac{4\pi\alpha}{\mathbf{k}^2} - \frac{4\alpha^2}{3} \int_{4m_e^2}^{\infty} \frac{ds}{s + \mathbf{k}^2} \frac{1}{s} \left(1 + \frac{2m_e^2}{s}\right) \sqrt{1 - \frac{4m_e^2}{s}} \\ &\doteq -\frac{4\pi\alpha}{\mathbf{k}^2} + \mathbf{V}^{\text{vac}}(\mathbf{k}). \end{aligned} \quad (5.39)$$

[Here, one has removed the UV-divergence in the propagator by charge renormalization.] Considering the second term in Eq. (5.39) as a perturbation, one may calculate the corrections to the bound-state observables in a standard manner. Namely, adding \mathbf{V}^{vac} to the Hamiltonian in Eq. (5.24) and iterating, we arrive at the following correction terms to the right-hand side of Eq. (5.26),

$$(\Psi_{nl}|\mathbf{V}^{\text{vac}} + \mathbf{V}^{\text{vac}}\mathbf{G}_C^{nl}(E_n)\mathbf{H}_S + \mathbf{H}_S\mathbf{G}_C^{nl}(E_n)\mathbf{V}^{\text{vac}} + \mathbf{V}^{\text{vac}}\mathbf{G}_C^{nl}(E_n)\mathbf{V}^{\text{vac}} + \dots|\Psi_{nl}). \quad (5.40)$$

Starting with the first term, we note that the relevant matrix elements

$$\Delta E_{nl}^{\text{vac}} = (\Psi_{nl}|\mathbf{V}^{\text{vac}}|\Psi_{nl}) \quad (5.41)$$

have been evaluated analytically for any n, l in Ref. [200]. For completeness, here we reproduce the integral representation provided in Ref. [200, Eq. (B.3)] which is valid in the generic case of a bound state of two oppositely charged particles with arbitrary masses,

$$\begin{aligned} \Delta E_{nl}^{\text{vac}} &= -\frac{\mu_c\alpha^3}{3\pi n^2} \sum_{k=0}^{n-l-1} \binom{n-l-1}{k} \binom{n+l}{n-l-k-1} \xi_n^{2(n-l-k-1)} \\ &\quad \times \int_0^1 dx \frac{x^{2l+2k+1}}{(\xi_n + x)^{2n}} \sqrt{1-x^2} (2+x^2); \quad \xi_n = \frac{nm_e}{\mu_c\alpha}. \end{aligned} \quad (5.42)$$

Here μ_c denotes the reduced mass of the bound system, and m_e is the electron mass.

The second term in Eq. (5.40) contains both \mathbf{V}^{vac} and \mathbf{H}_S . Because the strong Hamiltonian \mathbf{H}_S is local, the corrections in the states with $l \neq 0$ start at higher order in α than in the S -states, see also the remark after Eq. (5.27). We therefore stick to the corrections in S -states. It is convenient to introduce the quantity

$$\delta\Psi_{n0}(\mathbf{p}) = \int \frac{d^d\mathbf{k}}{(2\pi)^d} \frac{d^d\mathbf{q}}{(2\pi)^d} (\mathbf{p}|\bar{\mathbf{g}}_C^{n0}(E_n)|\mathbf{k}) \mathbf{V}^{\text{vac}}(\mathbf{k} - \mathbf{q})\Psi_{n0}(\mathbf{q}), \quad (5.43)$$

which is called “modification of the Coulomb wave function at the origin, due to vacuum polarization.” The corrections are then most easily expressed in terms of the ratio

$$\delta_n^{\text{vac}} \doteq 2\delta\tilde{\Psi}_{n0}(0)/\tilde{\Psi}_{n0}(0). \quad (5.44)$$

The next-to-leading correction to the energy shift and width emerges through the modification of the value of the wave function at the origin (cf. with Eq. (5.31)),

$$|\tilde{\Psi}_{n0}(0)|^2 \rightarrow |\tilde{\Psi}_{n0}(0)|^2(1 + \delta_n^{\text{vac}}). \quad (5.45)$$

The quantity δ_n^{vac} is explicitly evaluated for $n = 1$ in Ref. [200]. At the present experimental accuracy, the correction δ_n^{vac} is not negligible for πH , where it amounts to approximately half a percent.

The notion of a “modified Coulomb wave function” appears here for the sake of convenience only – in this manner, one may easily parameterize the correction term and carry out a comparison with other approaches. The Feshbach formalism does not refer to the exact wave function of the bound system at all – this might even fail to be a well-defined quantity in the case of meta-stable bound states. All calculations in the Feshbach formalism are performed in terms of the resolvent $\mathbf{G}(z)$, which is a well defined quantity.

We expect that the remaining terms in Eq. (5.40) are very small, and we discard them in the following.

5.7 Energy shift and width: summary

Amazingly enough, the above results carry over nearly unchanged to the real world of hadronic atoms, described in the framework of ChPT. For this reason, we collect the results of this and the previous section for later reference.

The relevant *master equation* to be solved is

$$z - E_n - (\Psi_{nl}|\bar{\tau}^{nl}(z)|\Psi_{nl}) = 0, \quad (5.46)$$

where the matrix element on the right-hand side is the one in Eq. (5.18), evaluated at $\mathbf{P} = \mathbf{0}$. We also introduced several energy shifts,

$$z = E_n + \Delta E_{nl}, \quad (5.47)$$

$$\Delta E_{nl} = \Delta E_{nl}^{\text{em}} + \Delta E_{nl}^{\text{vac}} + \delta_{l0} \left(\Delta E_n^{\text{str}} - \frac{i}{2}\Gamma_n \right) + O(\alpha^5). \quad (5.48)$$

The understanding of these relations is as follows. i) ΔE_{nl} is a complex quantity, defined through Eq. (5.47). ii) The real shifts $\Delta E_{nl}^{\text{em}}$ and $\Delta E_{nl}^{\text{vac}}$ are defined in Eqs. (5.30) and (5.41), respectively. iii) The remainder $\Delta E_{nl} - \Delta E_{nl}^{\text{em}} - \Delta E_{nl}^{\text{vac}}$ is split into the real components ΔE_n^{str} and Γ_n , which are related to the threshold

amplitude in the underlying relativistic theory. Including vacuum polarization effects,

$$\Delta E_n^{\text{str}} - \frac{i}{2} \Gamma_n = -\frac{\alpha^3 M}{32\pi n^3} \mathcal{T} \left(1 - \frac{\alpha(s_n(\alpha) + 2\pi i)}{32\pi} \mathcal{T} + \delta_n^{\text{vac}} \right) + O(\alpha^5), \quad (5.49)$$

where \mathcal{T} is the threshold amplitude defined in Eq. (4.35).

6 On DGBT formulae in ChPT

In this section, we investigate in some detail the procedure to extract information on the hadronic scattering lengths from the energy spectrum of hadronic atoms. To start with, we perform a *Gedankenexperiment*: let us assume that the fundamental relativistic Lagrangian is given by Eq. (4.1) (the effects of vacuum polarization do not play any role here and are ignored). Assume further that one measures the energy levels of the two-body bound state and extracts the real part of the threshold amplitude $\text{Re } \mathcal{T}$ via the expressions Eqs. (5.27), (5.30) and (5.34). Can we purify $\text{Re } \mathcal{T}$ from electromagnetic interactions and determine the “purely strong” threshold amplitude? The question is tailored to quantum-mechanical models, where one considers bound states formed by the sum of Coulomb and short-range strong potentials, and where the Coulomb potential may be easily switched on or off. After this investigation, we discuss the analogous question in the framework of ChPT. We follow the ideas outlined in Ref. [204], see also Refs. [205–210].

6.1 Electromagnetic corrections in scalar QED

The amplitude \mathcal{T} defined in Eq. (4.35) depends on two coupling constants, λ_r and e . We expand \mathcal{T} in powers of the fine-structure constant,

$$\text{Re } \mathcal{T} = \bar{\mathcal{T}} + \alpha \mathcal{T}^1 + O(\alpha^2). \quad (6.1)$$

Here, $\bar{\mathcal{T}}$ denotes the “purely strong” threshold amplitude. Consider now the energy shift of the bound state, determined by Eq. (5.34). At leading order we have the standard DGBT formula [8],

$$\Delta E_n^{\text{str}} = -\frac{\alpha^3 M}{32\pi n^3} \bar{\mathcal{T}} + O(\alpha^4), \quad (6.2)$$

which may be used to measure $\bar{\mathcal{T}}$,

$$\bar{\mathcal{T}} = \mathcal{E}_n^{\text{str}} + O(\alpha), \quad \mathcal{E}_n^{\text{str}} = -\frac{32\pi n^3 \Delta E_n^{\text{str}}}{\alpha^3 M}. \quad (6.3)$$

To include higher order corrections, we rewrite Eq. (5.34) as

$$\mathcal{E}_n^{\text{str}} = \bar{\mathcal{T}} \left(1 - \frac{\alpha s_n(\alpha)}{32\pi} \bar{\mathcal{T}} \right) + \alpha \mathcal{T}^1 + O(\alpha^2). \quad (6.4)$$

This formula leads – provided that one can calculate \mathcal{T}^1 – to a refined determination of the threshold amplitude,

$$\bar{\mathcal{T}} = \mathcal{E}_n^{\text{str}} \left(1 + \frac{\alpha s_n(\alpha)}{32\pi} \mathcal{E}_n^{\text{str}} \right) - \alpha \mathcal{T}^1 + O(\alpha^2). \quad (6.5)$$

It turns out, however, that $\bar{\mathcal{T}}$ and \mathcal{T}^1 cannot be uniquely defined. Indeed, let us imagine a perturbative expansion of the amplitude, and let us retain the terms up to and including one loop. The result will have the structure

$$\text{Re } \mathcal{T} = \lambda_r + \frac{a_1}{2} \lambda_r^2 \ln \frac{M^2}{\mu_0^2} + \frac{a_2}{2} \lambda_r \alpha \ln \frac{M^2}{\mu_0^2} + b_1 \lambda_r^2 + b_2 \lambda_r \alpha + \dots, \quad (6.6)$$

where a_i, b_i are pure numbers, and where the ellipsis stands for the contributions beyond one loop. This amplitude is scale independent, because λ_r satisfies the RG equation

$$\mu_0 \frac{d}{d\mu_0} \lambda_r = a_1 \lambda_r^2 + a_2 \lambda_r \alpha + \dots. \quad (6.7)$$

What is the meaning of the splitting in Eq. (6.1)? The amplitude $\bar{\mathcal{T}}$ is given by

$$\bar{\mathcal{T}} = \bar{\lambda}_r + \frac{a_1}{2} \bar{\lambda}_r^2 \ln \frac{\bar{M}^2}{\mu_0^2} + b_1 \bar{\lambda}_r^2 + \dots, \quad (6.8)$$

where $\bar{\lambda}_r$ and \bar{M} are the couplings and masses in pure ϕ^4 theory, compare the footnote at the beginning of section 4. The coupling constant $\bar{\lambda}_r$ satisfies the RG equation with $\alpha = 0$,

$$\mu_0 \frac{d}{d\mu_0} \bar{\lambda}_r = a_1 \bar{\lambda}_r^2 + O(\bar{\lambda}_r^3). \quad (6.9)$$

The second term in the representation Eq. (6.1) is then simply the difference $\mathcal{T} - \bar{\mathcal{T}}$. In order to actually calculate it, we need to know the relation between λ_r and $\bar{\lambda}_r$ [204]. For this, we may specify the scale μ_1 at which the two couplings coincide. We denote the corresponding coupling by $\bar{\lambda}_r(\mu_0; \mu_1)$,

$$\bar{\lambda}_r(\mu_0; \mu_1) = \lambda_r(\mu_0) \left(1 - \alpha a_2 \ln \frac{\mu_0}{\mu_1} + \dots \right), \quad (6.10)$$

where the arbitrary scale μ_1 is referred to as the *matching scale*. As λ_r is independent of μ_1 , we have

$$\mu_1 \frac{d}{d\mu_1} \bar{\lambda}_r(\mu_0; \mu_1) = \alpha a_2 \bar{\lambda}_r + \dots. \quad (6.11)$$

We express the coupling λ_r through $\bar{\lambda}_r$ and arrive at the representation Eq. (6.1), with

$$\mathcal{T}^1 = \bar{\lambda}_r(\mu_0; \mu_1) \left\{ \frac{a_2}{2} \ln \frac{M^2}{\mu_1^2} + b_2 \right\} + \dots . \quad (6.12)$$

The difference between M and \bar{M} does not matter at the order of the perturbative expansion considered here.

We now come to the main point: because \mathcal{T}^1 depends on the scale μ_1 ,

$$\mu_1 \frac{d}{d\mu_1} \mathcal{T}^1 = -a_2 \bar{\lambda}_r + \dots , \quad (6.13)$$

the amplitude $\bar{\mathcal{T}}$ in Eq. (6.5) becomes convention dependent as well [whereas $\text{Re}\mathcal{T} = \bar{\mathcal{T}} + \alpha\mathcal{T}^1 + \dots$ is independent of μ_1 .] The relation between the amplitudes evaluated from Eq. (6.5) with matching scales μ_1 and μ_2 is

$$\bar{\mathcal{T}}_{\mu_2} = \bar{\mathcal{T}}_{\mu_1} \left(1 + \alpha a_2 \ln \frac{\mu_2}{\mu_1} \right) + \dots . \quad (6.14)$$

The ambiguity shows up at order α and does not affect the interpretation of the “purely strong” amplitude at leading order, which is extracted by using Eq. (6.2).

6.2 Isospin breaking effects in ChPT

In the real world, the dynamics of hadronic atoms can be analyzed with ChPT. As this is a quantum field theory, the issue of purification of the amplitude from electromagnetic contributions is affected with the same ambiguity as the toy example discussed above. Hadronic atoms are not an exception in this sense: whenever an attempt is made to split electromagnetic effects in ChPT, one is faced with this problem. We now explain how this can be handled.

We start from the observation that the Lagrangian in ChPT contains, aside from the particle fields Φ , a set of LECs, which are not determined by chiral symmetry alone. We consider ChPT in the hadronic sector, with photons included. Generically, one has

$$\mathcal{L}_{\text{ChPT}} = \mathcal{L}(\mathcal{G}; \mathcal{K}; \mathcal{M}, e; \Phi) . \quad (6.15)$$

We have classified the LECs in two groups: the ones in \mathcal{G} (*strong* LECs), which stand for those which survive at $e = 0$, like the pion decay constant in the chiral limit, the LECs L_i at order p^4 , etc. The group \mathcal{K} stands for the so called *electromagnetic* LECs that one has to introduce while incorporating electromagnetic interactions in the theory, like the pion mass difference in the chiral limit, the K_i introduced by Urech [194], etc. In addition, there are the quark masses collected in \mathcal{M} , and the electromagnetic coupling e .

Given the structure of this Lagrangian, Green functions can be evaluated in a straightforward manner. The Lagrangian is so constructed that all UV divergences cancel – the result for any quantity is independent of the renormalization scale μ_0 and can symbolically be written in the form

$$\begin{aligned} X &= X(\mathcal{G}^r; \mathcal{K}^r; \mathcal{M}, e; \mu_0; p_i), \\ \frac{dX}{d\mu_0} &= 0. \end{aligned} \tag{6.16}$$

We have indicated the dependence on the renormalized LECs $\mathcal{G}^r, \mathcal{K}^r$ and on external momenta p_i . In particular, one can determine the algebraic form of the masses $\pi^\pm, \pi^0, K^\pm, K^0, \eta, \dots$. We now define the isospin symmetry limit in the following manner.

- Set $e = 0, m_u = m_d$. The quantities \bar{X} so obtained depend on the renormalized parameters \mathcal{G}^r , on the quark masses and on the momenta.
- In the isospin symmetry limit so defined, physical masses are grouped into mass degenerate (isospin) multiplets. Assign numerical values to these. In particular, for the pion, kaon and proton mass, choose the physical values for M_{π^+}, M_{K^+}, m_p , and for the pion decay constant take $F_\pi = 92.4$ MeV.
- Isospin breaking terms are defined to be the difference $X - \bar{X}$. These depend on the full set of renormalized parameters $\mathcal{G}^r; e; \mathcal{K}^r$, and, in addition, on the physical masses, on quark mass ratios, on F_π and on the momenta.

To numerically calculate the isospin breaking corrections, one uses measurements or estimates to assign numerical values to the needed renormalized LECs, and on quark mass ratios, as a result of which the isospin breaking terms can be calculated for any quantity.

We comment the procedure.

- It is algebraically well defined and internally consistent. As far as we can judge, it agrees with calculations of isospin breaking corrections performed in recent years by many authors.
- The problem with the ambiguity in purifying quantities from electromagnetic interactions is hidden in the numerical values assigned to the LECs. Here, we assumed that all LECs are known, to within reasonable error bars. In other words, fixing the values of all LECs unambiguously defines the splitting in physical observables.
- The relation of the chiral Lagrangian to the underlying theory, QCD+QED, will not be discussed here [see Refs. [204–210] where certain aspects of the problem are considered]. It is however clear that the mentioned ambiguity will show up again once the matching of the chiral Lagrangian to

QCD+QED is performed. We take it that the uncertainties in the electromagnetic LECs are chosen in such a manner that this ambiguity is taken care of appropriately.

- Assigning, in the isospin symmetry limit, physical values to $F_\pi, M_{\pi^+}, M_{K^+}$ and to the proton mass overconstrains the available parameters in QCD ($\Lambda_{QCD}, \hat{m}, m_s$): fixing the first three quantities allows one to calculate the proton mass, and there is no reason why this mass should coincide with the physical value m_p . However, we expect the difference to be small, with a negligible effect on the quantities considered here.
- The manner in which electromagnetic corrections are treated in Ref. [206] differs from the present prescription in at least one important aspect: in that treatment, the leading-order meson mass terms that enter the strong chiral Lagrangian become scale dependent and run with α in the full theory. This is not the case in the procedure advocated here.

We add a note concerning the bookkeeping of isospin breaking corrections. Isospin breaking contributions can be evaluated as a power series in α and $m_d - m_u$ (modulo logarithms). It is useful to define a small parameter δ as a bookkeeping device,

$$\delta \sim \alpha, m_d - m_u. \quad (6.17)$$

A particular calculation is then carried out to a specific order in δ . We note that the above counting is not the only possible choice. Indeed, in the treatment of pionium [36, 40, 42, 44], the bookkeeping was performed differently: $\delta \sim \alpha, (m_d - m_u)^2$. The reason for this is that, both in the pion mass difference and in the $\pi\pi$ scattering amplitudes, the terms linear in $m_d - m_u$ are absent – isospin breaking generated by the quark mass difference start at $O((m_d - m_u)^2)$. On the other hand, if one still wants to count $(m_d - m_u)$ like α in pionium, this amounts to discarding all strong isospin breaking corrections in the final result, because the calculation was carried out at next-to-leading order in δ . We have indeed found [40, 42] that numerically, these corrections are tiny, and nothing changes in the answer if these are left out.

This concludes our review on the formulation of the general approach to hadronic atoms. We have used the lagrangian in Eq. (4.1) to illustrate the main ideas, which do depend neither on the details of the underlying interaction, nor on the choice of a particular bound state. In the remaining part of this article we consider the application of this general theory to several hadronic atoms, in the framework of chiral perturbation theory.

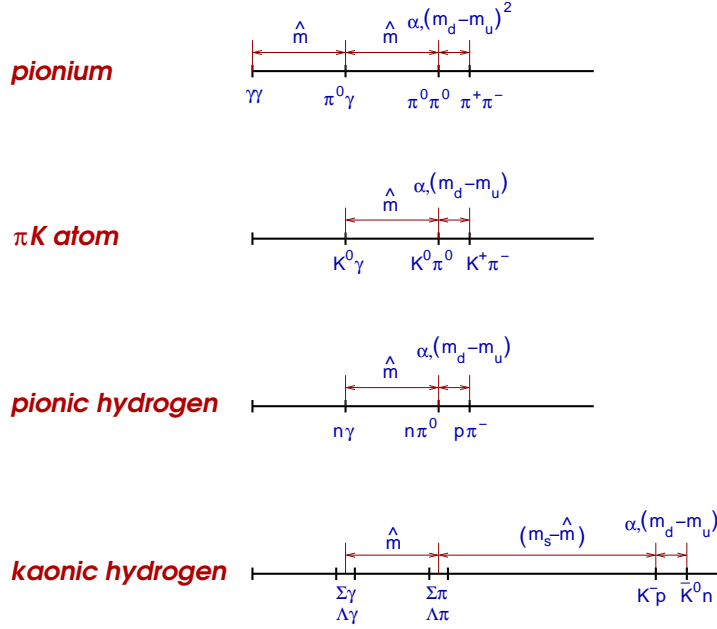


Figure 7: Decay channels of various hadronic atoms. Different thresholds are separated due to electromagnetic/strong isospin breaking [$\alpha \neq 0$, $m_u \neq m_d$], and/or $SU(3)$ breaking [$m_s \neq \hat{m}$], and/or a non-zero value of the pion mass [$\hat{m} \neq 0$]. Multi-photon states are not explicitly indicated: e.g., the decay channel of pionium into $\pi^0\pi^0$ also implies decays into states with any number of additional photons. The scales in the Figure are chosen arbitrarily.

7 Hadronic atoms and scattering lengths: General observations

Before starting the investigation of the individual atoms listed in Table 1, we find it useful to provide already here some general information on their spectra, and on the relation of these to the pertinent threshold amplitudes. We start with an investigation of the counting rules in the parameter δ introduced at the end of the last section.

7.1 Counting rules for the widths

Strong interaction energy shifts start at order δ^3 . On the other hand, the counting rules are slightly more complicated for the decay widths, because the bookkeeping of the phase space factor (in powers of δ) depends on the final state involved.

The hadronic atoms decay into states whose thresholds lie below the bound-state energy. In the cases that we consider here, the separation of the thresholds is due to (one or several of) the following mechanisms (see Fig. 7):

- i) Level splitting in the atoms, which is $O(\alpha^2)$;
- ii) Isospin breaking [$\alpha \neq 0$ and/or $m_u \neq m_d$];
- iii) $SU(3)$ breaking [$m_s \neq \hat{m}$];
- iv) Chiral symmetry breaking [$\hat{m} \neq 0$].

The phase space factor in the S -wave counts as $O(\delta^{1/2})$ for ii) and as $O(1)$ for iii) and iv). Furthermore, up to order δ^5 , only the decay width of the S -states is non-zero,

$$\text{Im } \Delta E_{nl} = -\frac{1}{2} \Gamma_n \delta_{l0} + O(\delta^5). \quad (7.1)$$

In the case of particles with spin, ΔE_{nl} denotes the averaged energy shift, see appendix A. Transition widths between different energy levels also start at $O(\delta^5)$ (see, e.g., Ref. [211]).

Taking into account the fact that the square of the Coulomb wave function at the origin counts at δ^3 , the decay widths into different final states are seen to obey the following counting rules:

Pionium

In the S -wave, pionium decays overwhelmingly into $\pi^0\pi^0$. At leading order, the decay width counts at $O(\delta^{7/2})$. Next-to-leading order isospin breaking corrections to this partial decay are of order $\delta^{9/2}$. The anomaly-induced decay into $\pi^0\gamma$ cannot proceed in the S -wave, and the decay into $\gamma\gamma$ starts at $O(\delta^5)$ [54]. At order $O(\delta^{9/2})$, the multi-photon final states (e.g. $\pi^0\pi^0\gamma$) do not contribute either, see Ref. [44] for a detailed discussion. *At order $\delta^{9/2}$, only the decay into the $\pi^0\pi^0$ final state needs to be taken into account.*

πK atom

The decay width of the πK atom into $\pi^0 K^0$ starts at order $\delta^{7/2}$, and the next-to-leading order corrections count as $O(\delta^{9/2})$. Up to $O(\delta^5)$ there are no other contributions, see Ref. [44] for a detailed discussion. *At order $\delta^{9/2}$, only the decay into the $\pi^0 K^0$ final state needs to be taken into account.*

Pionic hydrogen

In difference to pionium and to the πK atom, there are two decay channels in πH with comparable widths: the $n\pi^0$ and the $n\gamma$ states, with $\simeq 60\%$ and $\simeq 40\%$ decay probabilities, respectively. The ratio of these two quantities gives the Panofsky ratio $P \simeq 1.546$ [212, 213]. The decay width into $n\pi^0$ starts at $O(\delta^{7/2})$ and next-to-leading isospin breaking corrections to it count as $O(\delta^{9/2})$.

The decay width into $n\gamma$ starts at $O(\delta^4)$ – there are no corrections to the leading order at the accuracy we are working. The Panofsky ratio at leading order counts as $O(\delta^{-1/2})$. Again, there is no need to consider isospin breaking corrections. Further, at the accuracy we are working, the decays into final states with more than one photon can be neglected. *At order $\delta^{9/2}$, only the decays into the $n\pi^0$ and $n\gamma$ final states need to be taken into account.*

Kaonic hydrogen

Since $M_{\bar{K}^0} + m_n > M_{K^-} + m_p$, the decays of $\bar{K}H$ proceed overwhelmingly into the strong channels $\pi\Lambda$ and $\pi\Sigma$. The decay width at leading order counts as $O(\delta^3)$. The decay width into $\Sigma\gamma$, $\Lambda\gamma$, as well as next-to-leading order isospin breaking corrections to the decay into strong channels start at $O(\delta^4)$. Other decay channels are suppressed.

Remark: The couplings $\pi^+\pi^-\pi^0\gamma$ and $K^+\pi^-K^0\gamma$ in the relativistic theory are proportional to the antisymmetric tensor $\varepsilon^{\mu\nu\alpha\beta}$. For this reason, the pertinent transition amplitudes necessarily contain at least one soft momentum and are suppressed as compared to the $\pi^-p \rightarrow n\gamma$ amplitude. There is therefore no need to introduce a Panofsky ratio for these channels at the order considered here.

Pionic deuterium

Pionic hydrogen can decay e.g. into nn . Therefore, the phase space factor is of order δ^0 , and the width is of the order δ^3 .

Kaonic deuterium

Kaonic deuterium can decay e.g. into $\Sigma n\pi$, $\Lambda n\pi$. The corresponding phase space factor is of order δ^0 , and the width is of order δ^3 .

7.2 Spectrum and scattering lengths

We are concerned in this review to a large extent with the connection between the hadronic atom spectra and the underlying hadronic scattering amplitudes at threshold (scattering lengths). Four elastic reactions are involved: $\pi\pi \rightarrow \pi\pi$, $\pi K \rightarrow \pi K$, $\pi N \rightarrow \pi N$ and $\bar{K}N \rightarrow \bar{K}N$. In the isospin symmetry limit $\alpha = 0$, $m_u = m_d$, each of them is described by two independent isospin amplitudes. These are real in the first three reactions, and complex in the last reaction. The atoms considered fall into two distinct groups:

Group 1: To this group belong the first three atoms displayed in Figure 7: $A_{2\pi}$, $A_{\pi K}$, and πH . At the order considered here, these atoms can decay into states that are separated in energy from the bound state through isospin breaking effects, which are calculable in ChPT (or which can be taken into account with

the Panofsky ratio in case of πH). For each of these three atoms, there are two real threshold amplitudes in the isospin symmetry limit. Therefore, it suffices to have two experimental numbers to pin them down: the strong energy level shift and width of the ground state.

Group 2: To this group belong $\bar{K}H$, $\bar{K}D$ and πD . These atoms can decay into states that are separated in energy from the bound state also in the absence of isospin breaking, because the splitting is due to $\hat{m} \neq 0$ and(or) $\hat{m} \neq m_s$. As a result of this, the widths are enhanced. We already mentioned in subsection 2.4 that the $\bar{K}N$ scattering lengths cannot be determined from the energy level shift and width of the ground state of $\bar{K}H$ even in principle, because one has to fix two complex numbers. As we will see later, it turns out that $\bar{K}D$ provides the lacking information, see subsection 12.4. The case of πD plays a special role here. From a principle point of view, information on this compound is not needed: to measure the two real pion–nucleon scattering lengths, knowledge of the strong energy level shift and width of the ground state of πH suffices. On the other hand, due to an insufficient knowledge of one of the LECs involved, information aside from πH is presently needed. It is provided e.g. by the strong energy shift in πD , which can be related to the pion–nucleon scattering lengths. On the other hand, its width cannot be used for this purpose. The physical reason for this is the fact that πD can decay e.g. into nn final states, a reaction which cannot be related to the elastic pion–nucleon scattering amplitude. The technical reason behind this is the fact that the ratio between the strong energy level shift and the width in πD is of order δ^0 , while the imaginary part of the pion–nucleon amplitude is of order $\delta^{1/2}$: there can be no DGBT formula that relates the energy shift *and* width directly with the pion–nucleon scattering amplitude, because there would be a mismatch in counting powers of δ .

8 Pionium

8.1 DIRAC experiment at CERN

As already mentioned, the aim of the DIRAC collaboration at CERN is to measure the lifetime of the $\pi^+\pi^-$ atom in the ground state with 10% precision [72–78]. This allows one to determine the difference $|a_0 - a_2|$ of S -wave $\pi\pi$ scattering lengths at 5% accuracy. Measurements of the lifetime of $\pi^+\pi^-$ atoms have also been proposed at J-PARC and at GSI [214, 215]. For an earlier attempt to measure pionium production, see Ref. [216].

Details of the set-up of the DIRAC experiment at the CERN Proton Synchrotron can be found in Ref. [73]. The underlying idea is the following. High-energy proton–nucleus collisions produce pairs of oppositely charged pions via strong decays of intermediate hadrons. Some of these pairs form $\pi^+\pi^-$ atoms due to Coulomb final state interaction. Once produced, the $\pi^+\pi^-$ atoms prop-

agate with relativistic velocity. Before they decay into pairs of neutral pions, the atoms interact with the target atoms. This interaction excites/de-excites or breaks them up. The $\pi^+\pi^-$ pairs from the break-up exhibit specific kinematic features, which allow one to identify them experimentally. Excitation/de-excitation and break-up of the atom compete with its decay. Solving the transport equations for excitation/de-excitation and break-up leads to a target-specific relation between break-up probability and lifetime, which is believed to be known at the 1% level [77]. Measuring the break-up probability then allows one to determine the lifetime of ponium [79, 80, 217].

The first observation of $\pi^+\pi^-$ atoms [218] has set a lower limit on its lifetime, $\tau > 1.8 \times 10^{-15}$ s (90% CL). Recently [77], the DIRAC collaboration reported a measurement based on a large sample of data taken in 2001 with Ni targets, see Eq. (2.1).

As pointed out Refs. [86, 87], a measurement of the energy splitting between $2s$ - and $2p$ -states of ponium allows one to determine the combination $2a_0 + a_2$ of scattering lengths, see also section 2 of this report. Assuming $a_0 - a_2 > 0$, knowledge of the width and energy shift thus allows one to determine separately a_0 and a_2 .

8.2 Two-channel problem

In contrast to scalar QED considered in previous sections, one is concerned here with two coupled channels of non-relativistic particles, $\pi^+\pi^-$ and $\pi^0\pi^0$, which are separated by a mass gap $M_\pi - M_{\pi^0} \ll M_\pi$, see Figure 7. As a result of this, the ground state of ponium dominantly decays into $\pi^0\pi^0$, whereas its decay into $\gamma\gamma$ is suppressed by a factor $\sim 10^3$.

We investigate the decay process in the non-relativistic framework developed in previous sections. In particular, the master equation (5.46) and the decompositions Eqs. (5.47, 5.48) apply also here – we simply need to adapt the potential \mathbf{V} that occurs in the quantity $\bar{\tau}^{nl}$, see Eq. (5.15). This can be achieved by constructing the relevant Hamiltonian. We follow Refs. [36, 40, 42, 44], which use a two-channel formalism. An alternative method, based on a one-channel framework, will be invoked in the description of pionic hydrogen later in this report.

The Lagrangian of the system contains the non-relativistic charged and neutral pion fields $\pi_\pm(x), \pi_0(x)$ and the electromagnetic field $A_\mu(x)$. At the accuracy we are working, it suffices to retain only the following terms (cf. Eq. (4.2)),

$$\begin{aligned}
\mathcal{L}_{NR} = & -\frac{1}{4} F_{\mu\nu} F^{\mu\nu} + \sum_{\pm} \pi_{\pm}^{\dagger} \left(iD_t - M_{\pi} + \frac{\mathbf{D}^2}{2M_{\pi}} + \frac{\mathbf{D}^4}{8M_{\pi}^3} + \dots \right. \\
& \mp \frac{e}{6} \langle r_{\pi}^2 \rangle (\mathbf{DE} - \mathbf{ED}) + \dots \left. \right) \pi_{\pm} + \pi_0^{\dagger} \left(i\partial_t - M_{\pi^0} + \frac{\Delta^2}{2M_{\pi^0}} + \frac{\Delta^4}{8M_{\pi^0}^3} + \dots \right) \pi_0 \\
& + c_1 \pi_+^{\dagger} \pi_-^{\dagger} \pi_+ \pi_- + c_2 (\pi_+^{\dagger} \pi_-^{\dagger} \pi_0^2 + \text{h.c.}) + c_3 (\pi_0^{\dagger})^2 \pi_0^2 + \dots, \tag{8.1}
\end{aligned}$$

where c_1, c_2, c_3 denote non-relativistic four-pion couplings, and $\langle r_\pi^2 \rangle$ is the charge radius of the pion. As is shown in Ref. [44], the second-order derivative term retained in Ref. [36, 42] is in fact redundant and can be eliminated by using the equations of motion. This procedure, which merely amounts to choosing the coupling constant $c_4 = 0$ in Refs. [36, 42], does not affect any of observable quantities.

Without performing any calculation, the electromagnetic energy shift in the bound state with angular momentum l and principal quantum number n up to terms of order α^5 can be directly read off from Eq. (5.30). One finds [44]

$$\Delta E_{nl}^{\text{em}} = \alpha^4 M_\pi \left(\frac{\delta_{l0}}{8n^3} + \frac{11}{64n^4} - \frac{1}{2n^3(2l+1)} \right) + \frac{\alpha^4 M_\pi^3 \langle r_\pi^2 \rangle}{6n^3} \delta_{l0}. \quad (8.2)$$

Further, the contribution due to vacuum polarization $\Delta E_{nl}^{\text{vac}}$ is defined by Eq. (5.41) and is calculated in Ref. [200], see Eq. (5.42).

In order to evaluate the strong shift of a given level, we return to Eq. (5.46) and perform the calculations by explicitly assuming $e = 0$ everywhere, except in the static Coulomb interaction (this is a perfectly legitimate procedure up to terms of order δ^5). Suppressing everything but four-pion local interactions and the relativistic mass insertions, one has

$$\bar{\tau}^{n0}(E_n) = \bar{\mathbf{V}} + \bar{\mathbf{V}} \bar{\mathbf{G}}_C^{n0} \bar{\mathbf{V}} + \bar{\mathbf{V}} \bar{\mathbf{G}}_C^{n0} \bar{\mathbf{V}} \bar{\mathbf{G}}_C^{n0} \bar{\mathbf{V}} + \bar{\mathbf{V}} \bar{\mathbf{G}}_C^{n0} \bar{\mathbf{V}} \bar{\mathbf{G}}_C^{n0} \bar{\mathbf{V}} \bar{\mathbf{G}}_C^{n0} \bar{\mathbf{V}} + \dots, \quad (8.3)$$

where $\bar{\mathbf{V}} = \mathbf{H}_S + \mathbf{H}_R$, and

$$\begin{aligned} \mathbf{H}_S &= - \int d^3\mathbf{x} \left\{ c_1 \pi_+^\dagger \pi_-^\dagger \pi_+ \pi_- + c_2 (\pi_+^\dagger \pi_-^\dagger \pi_0^2 + \text{h.c.}) + c_3 (\pi_0^\dagger)^2 \pi_0^2 \right\}, \\ \mathbf{H}_R &= - \int d^3\mathbf{x} \left\{ \sum_{\pm} \pi_{\pm}^\dagger \frac{\Delta^4}{8M_\pi^3} \pi_{\pm} + \pi_0^\dagger \frac{\Delta^4}{8M_{\pi_0}^3} \pi_0 \right\}. \end{aligned} \quad (8.4)$$

Note that at the accuracy we are working, three interactions in Eq. (8.3) are sufficient (each iteration is suppressed by one power of δ). The general expression for the strong energy shift was already worked out in Eq. (5.19). Here, it remains to simply calculate the pertinent matrix elements.

As an illustration, let us calculate the (complex) level shift at lowest order in δ . It is clear that one should obtain the DGBT formula for the real and imaginary parts of the shift. In order to demonstrate that this is indeed the case, it suffices to consider only those contributions to the quantity $\bar{\tau}^{n0}(z)$, which are shown in Fig. 8 (the tree diagram and the neutral pion loop). We obtain

$$(z - E_n)^{\text{str}} = -|\tilde{\Psi}_{n0}(0)|^2 (c_1 + 2c_2^2 J_0(z)) + o(\delta^{7/2}), \quad (8.5)$$

where the quantity $J_0(z)$ is the loop integral defined in Eq. (3.16), with the mass M replaced by M_{π_0} . This function has a branch point at $z = 2M_{\pi_0}$ and its

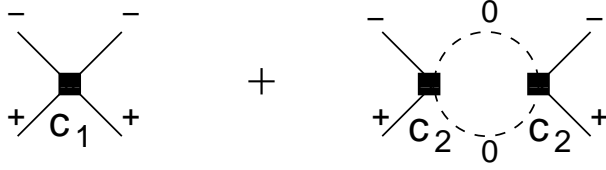


Figure 8: Lowest-order contributions to the complex energy shift of the $\pi^+\pi^-$ atom, see Eq. (8.5). The labels “+”, “-” and “0” (solid and dashed lines) denote the charged and neutral pions, respectively.

imaginary part has the same sign as the imaginary part of z throughout the cut plane. Therefore, Eq. (8.5) has no solution on the first Riemann sheet. On the other hand, if we analytically continue $J_0(z)$ from the upper rim of the cut to the second Riemann sheet, we find a zero at

$$\begin{aligned} \text{Re } z &= E_n - \frac{\alpha^3 \mu_c^3}{\pi n^3} c_1 + \dots, \\ \text{Im } z &= -\frac{\alpha^3 \mu_c^3}{\pi n^3} \frac{M_{\pi^0} \rho_n^{1/2}}{2\pi} c_2 + \dots, \end{aligned} \quad (8.6)$$

where $\rho_n = M_{\pi^0}(E_n - 2M_{\pi^0})$. Further, matching in the isospin limit yields

$$\begin{aligned} 3M_\pi^2 c_1 &= 4\pi(2a_0 + a_2) + \dots, \\ 3M_\pi^2 c_2 &= 4\pi(a_2 - a_0) + \dots, \\ 3M_\pi^2 c_3 &= 2\pi(a_0 + 2a_2) + \dots, \end{aligned} \quad (8.7)$$

where the ellipses stand for terms of order α and $(m_d - m_u)^2$. Using $|\tilde{\Psi}_{n0}(0)|^2 = \alpha^3 M_\pi^3 / (8\pi n^3)$, we finally conclude that i) Eq. (8.6) reproduces the leading order expressions Eqs. (2.2) and (2.5), and ii) the bound-state pole is indeed located on the second Riemann sheet. Note that the real and imaginary parts of the energy shift are of order δ^3 and $\delta^{7/2}$, respectively.

Calculations up to and including first non-leading order in δ are straightforward and proceed in complete analogy to the case of scalar QED, considered earlier – details may be found in Refs. [36, 40, 42, 44]. The result is

$$\Delta E_n^{\text{str}} = -\frac{\alpha^3 M_\pi}{n^3} \mathcal{A}_c(1 + K'_n) + o(\delta^4), \quad \Gamma_n = \frac{2}{9n^3} \alpha^3 p_n^* \mathcal{A}_x^2(1 + K_n) + o(\delta^{9/2}), \quad (8.8)$$

with

$$\begin{aligned}
K_n &= \frac{\Delta_\pi}{9M_\pi^2} (a_0 + 2a_2)^2 - \frac{\alpha}{3} s_n(\alpha) (2a_0 + a_2), \\
K'_n &= -\frac{\alpha}{6} s_n(\alpha) (2a_0 + a_2), \\
p_n^* &= \lambda^{1/2}(E_n^2, M_{\pi^0}^2, M_{\pi^0}^2)/(2E_n), \quad \Delta_\pi = M_\pi^2 - M_{\pi^0}^2,
\end{aligned} \tag{8.9}$$

where $s_n(\alpha)$ is given in Eq. (5.32). The quantities \mathcal{A}_x and \mathcal{A}_c coincide with the real parts of the relativistic threshold amplitudes in the channels $\pi^+\pi^- \rightarrow \pi^0\pi^0$ and $\pi^+\pi^- \rightarrow \pi^+\pi^-$, respectively, up to kinematic normalization factors. The precise relations are given in appendix A. With the normalization chosen there, one has

$$\mathcal{A}_x = a_0 - a_2 + \delta\mathcal{A}_x + o(\delta), \quad \mathcal{A}_c = \frac{1}{6} (2a_0 + a_2) + \delta\mathcal{A}_c + o(\delta), \tag{8.10}$$

where $\delta\mathcal{A}_x$ and $\delta\mathcal{A}_c$ denote isospin breaking corrections of order δ . Finally, including vacuum polarization correction in the above expressions amounts to $K_n \rightarrow K_n + \delta_n^{\text{vac}}$ and $K'_n \rightarrow K'_n + \delta_n^{\text{vac}}$, where δ_n^{vac} is defined by Eq. (5.44).

For completeness, we also display the strong shift of the P -wave states at leading order [44],

$$\Delta E_{n1}^{\text{str}} = -\frac{(n^2 - 1)}{8n^5} \alpha^5 M_\pi^3 a_1^1, \tag{8.11}$$

where a_1^1 denotes the P -wave $\pi\pi$ scattering length. The strong decay into $\pi^0\pi^0$ final states from P -wave states is forbidden by C -invariance.

The equations (8.8), (8.9), (8.10), (8.11) provide the framework for the numerical analysis of ponium observables.

8.3 DGBT formula and numerical analysis

The relations Eqs. (8.8), (8.9) and (8.10) can be rewritten as follows,

$$\begin{aligned}
\Delta E_n^{\text{str}} &= -\frac{\alpha^3 M_\pi}{6n^3} (2a_0 + a_2) (1 + \delta'_n) + o(\delta^4), \quad \delta'_n = \frac{6\delta\mathcal{A}_c}{2a_0 + a_2} + K'_n, \\
\Gamma_n &= \frac{2}{9n^3} \alpha^3 p_n^* (a_0 - a_2)^2 (1 + \delta_n) + o(\delta^{9/2}), \quad \delta_n = \frac{2\delta\mathcal{A}_x}{a_0 - a_2} + K_n.
\end{aligned} \tag{8.12}$$

At this stage one may invoke ChPT and evaluate the quantities $\delta\mathcal{A}_x$ and $\delta\mathcal{A}_c$. This procedure leads to a systematic calculation of the isospin breaking corrections.

We now demonstrate how the calculations at this concluding step are carried out. In general, the following representation for the quantities $\delta\mathcal{A}_x$ and $\delta\mathcal{A}_c$ holds in ChPT,

$$\delta\mathcal{A}_x = h_1(m_d - m_u)^2 + h_2\alpha, \quad \delta\mathcal{A}_c = h'_1(m_d - m_u)^2 + h'_2\alpha, \quad (8.13)$$

where h_i, h'_i are functions of the quark mass \hat{m} and of the RG-invariant scale of QCD. According to our definition of the isospin limit, the parameter \hat{m} is adjusted so that in this limit, the pion mass is equal to the charged pion mass M_π .

Consider, for instance, the amplitude \mathcal{A}_x at tree level in ChPT,

$$\mathcal{A}_x = \frac{3}{32\pi F^2}(4M_\pi^2 - M_{\pi^0}^2) + O(p^4, e^2 p^2). \quad (8.14)$$

In the isospin symmetry limit this expression reduces to

$$a_0 - a_2 = \frac{9M_\pi^2}{32\pi F^2} + O(p^4). \quad (8.15)$$

Comparing this with Eq. (8.14), we find

$$\mathcal{A}_x = a_0 - a_2 + \frac{3\Delta_\pi}{32\pi F^2} + O(p^4, e^2 p^2). \quad (8.16)$$

From this result, we may read off the coefficient h_2 at leading order in the chiral expansion,

$$h_2 = \frac{3(M_\pi^2 - M_{\pi^0}^2)}{32\alpha\pi F^2} + O(\hat{m}). \quad (8.17)$$

[To be precise, the first term on the right-hand side of this equation should be evaluated at $\alpha = 0$. To ease notation, we omit this request here and in the following]. On the other hand, the above calculation is not accurate enough to determine h_1 at leading order, because for this purpose, the amplitude is needed at order p^4 . This procedure may obviously be carried out order by order in the chiral expansion – all that is needed is the chiral expansion of the scattering amplitude at threshold, at $m_u \neq m_d$, $\alpha \neq 0$. As a result of this, the quantities h_i are represented as a power series in the quark mass \hat{m} (up to logarithms).

The evaluation of the amplitude for $\pi^+\pi^- \rightarrow \pi^0\pi^0$ was carried out at $O(p^4, e^2 p^2)$ in Refs. [40, 42, 195], and a detailed numerical analysis of the pionium decay width was performed in Refs. [40, 42]. This analysis results in the following value for the ground-state correction,

$$\delta\mathcal{A}_x = (0.61 \pm 0.16) \times 10^{-2}, \quad K_1 = (1.15 \pm 0.03) \times 10^{-2}. \quad (8.18)$$

	$\Delta E_{nl}^{\text{em}}$ [eV]	$\Delta E_{nl}^{\text{vac}}$ [eV]	$\Delta E_{nl}^{\text{str}}$ [eV]	$10^{15}\tau_{nl}$ [s]
$n=1, l=0$	-0.065	-0.942	-3.8 ± 0.1	2.9 ± 0.1
$n=2, l=0$	-0.012	-0.111	-0.47 ± 0.01	23.3 ± 0.7
$n=2, l=1$	-0.004	-0.004	$\simeq -1 \cdot 10^{-6}$	$\simeq 1.2 \cdot 10^4$

Table 2: Numerical values for the energy shift and the lifetime of the $\pi^+\pi^-$ atom, taken from Ref. [44]. The quantity $\Delta E_{n0}^{\text{str}}$ stands for ΔE_n^{str} , and $\tau_{n0} = (\Gamma_n)^{-1}$.

Using input scattering lengths from Refs. [13, 14], we obtain for the isospin breaking correction δ_1 in Eq. (8.12) and for the lifetime of the ground state,

$$\tau = \Gamma_1^{-1} = (2.9 \pm 0.1) \times 10^{-15} \text{ s}, \quad \delta_1 = (5.8 \pm 1.2) \times 10^{-2}. \quad (8.19)$$

We note that δ_1 amounts to a 6% correction to the leading-order DGBT formula [8]. On the other hand, the preliminary result of DIRAC, displayed in Eq. (2.1), corresponds to the following value of the difference $a_0 - a_2$,

$$a_0 - a_2 = 0.264 \begin{smallmatrix} +0.033 \\ -0.020 \end{smallmatrix} M_\pi^{-1}. \quad (8.20)$$

In Ref. [44], the energy shift of the ground state of pionium was worked out in an analogous manner (see also Ref. [219]), with the result

$$\Delta E_1^{\text{str}} = (-3.8 \pm 0.1) \text{ eV}, \quad \delta'_1 = (6.2 \pm 1.2) \times 10^{-2}. \quad (8.21)$$

As was discussed in the previous sections, the width and strong energy shift are modified by vacuum polarization effects, $\delta_n \rightarrow \delta_n + \delta_n^{\text{vac}}$, $\delta'_n \rightarrow \delta'_n + \delta_n^{\text{vac}}$, where δ_n^{vac} is defined in Eq. (5.44). For example, in the ground state, the correction amounts to $\delta_1^{\text{vac}} = 0.31 \cdot 10^{-2}$ [200]. We conclude that it is safe to neglect, in this system, the δ_n^{vac} altogether: the uncertainties in δ_n and δ'_n are larger than δ_n^{vac} itself.

Finally, in Table 2 we list different contributions to the energy shift and the lifetime for the first few levels in pionium [44], calculated by using the input scattering lengths from Refs. [13, 14]. The calculations for the S -wave states were carried out at next-to-leading order in isospin symmetry breaking. The bulk of the uncertainty in these quantities is due to the uncertainties in the pertinent scattering lengths. The lifetime of the $2p$ -state is calculated at leading order only and is determined by the $2p-1s$ radiative transition [87]. Finally, the theoretical value for the $2p-2s$ energy splitting is given by [44]

$$\Delta E^{2s-2p} = \Delta E_2^{\text{str}} + \Delta E_{20}^{\text{em}} - \Delta E_{21}^{\text{em}} + \Delta E_{20}^{\text{vac}} - \Delta E_{21}^{\text{vac}} = -0.59 \pm 0.01 \text{ eV}. \quad (8.22)$$

The uncertainty displayed is the one in ΔE_2^{str} only. To the accuracy we are working, we may neglect the strong shift in the $2p$ state, because it is of order α^5 .

8.4 Two-photon decay of ponium

The decay width of the ponium ground state in two photons is given by

$$\Gamma_1^{2\gamma} = \frac{M_\pi^5}{4} \alpha^5 |A(4M_\pi^2, -M_\pi^2, -M_\pi^2)|^2 + o(\delta^5), \quad (8.23)$$

where the invariant amplitude $A(s, t, u)$ for the process $\gamma\gamma \rightarrow \pi^+\pi^-$ is defined in Eq. (2.4) of Ref. [220]. This amplitude was evaluated at NLO in chiral $SU(3) \times SU(3)$ by Bijens and Cornet [221], and to two loops in $SU(2) \times SU(2)$ in Refs. [220, 222]. Here, we use the $SU(2) \times SU(2)$ version displayed in Eq. (5.1) of Ref. [220],

$$M_\pi^2 A(4M_\pi^2, -M_\pi^2, -M_\pi^2) = 1 + \frac{2M_\pi^2}{F_\pi^2} \left(\bar{G}_\pi(4M_\pi^2) + \frac{\bar{l}_6 - \bar{l}_5}{48\pi^2} \right) + O(M_\pi^4), \quad (8.24)$$

where

$$\begin{aligned} \bar{G}_\pi(s) &= -\frac{1}{16\pi^2} \left(1 + \frac{2M_\pi^2}{s} \int_0^1 \frac{dx}{x} \ln\left(1 - \frac{s}{M_\pi^2} x(1-x)\right) \right), \\ \bar{G}_\pi(4M_\pi^2) &= \frac{\pi^2 - 4}{64\pi^2}. \end{aligned} \quad (8.25)$$

The terms of order M_π^4 in Eq. (8.24) denote two-loop contributions, and \bar{l}_5, \bar{l}_6 are $O(p^4)$ chiral LECs [84]. These are related to the pion polarizabilities α_π and β_π ,

$$\alpha_\pi - \beta_\pi = \frac{\alpha(\bar{l}_6 - \bar{l}_5)}{24\pi^2 F_\pi^2 M_\pi} + O(M_\pi). \quad (8.26)$$

The two-photon decay width of ponium was evaluated already earlier [54, 192]. Here, we comment on the expression given by Hammer and Ng [54], who were the first to incorporate contributions from the pion polarizabilities. Their expression does not contain the contribution from \bar{G}_π , which is, in the chiral expansion, of the same order as the one from the polarizabilities. Numerically, this difference amounts to a large effect. Using $\bar{l}_6 - \bar{l}_5 = 3.0 \pm 0.3$, which corresponds to $(\alpha - \beta)_\pi = 6.0 \cdot 10^{-4} \text{ fm}^3$ [220], we obtain from Eq. (8.24)

$$M_\pi^2 A(4M_\pi^2, -M_\pi^2, -M_\pi^2) = 1 + 4.2 \cdot 10^{-2} + 2.9 \cdot 10^{-2} + O(M_\pi^4), \quad (8.27)$$

i.e., the contribution from $\bar{G}_\pi(4M_\pi^2)$ is larger than the one from the pion polarizabilities. Note also that in Ref. [54] much larger values of the polarizabilities $\alpha_\pi = -\beta_\pi = (6.8 \pm 1.4 \pm 1.2) \cdot 10^{-4} \text{ fm}^3$ have been used, tending to mask the absence of $\bar{G}_\pi(4M_\pi^2)$.

The reason why the contribution from $\bar{G}_\pi(s)$ was missed in Ref. [54] is the following. In that article, the annihilation amplitude $\gamma\gamma \rightarrow \pi^+\pi^-$ is obtained from the Compton amplitude through analytic continuation. Moreover, the authors

expand the amplitude in small photon momenta and retain only terms which are at most quadratic in this expansion. In the annihilation channel, however, the photon momenta are of the order of the pion mass. Therefore, the analytic continuation of the *truncated* Compton amplitude can be justified if and only if the expansion of this amplitude in photon momenta has a convergence radius of the order of the heavy scale in ChPT. In this case, the coefficients of such an expansion are regular in the chiral limit. However, as can be seen from Eq. (8.25), this is not what happens: at the Compton threshold, the expansion is carried out in powers of s/M_π^2 (with $s \rightarrow t$). The coefficients of the higher-order terms in the expansion of $\bar{G}(s)$ become more and more singular in the chiral limit. As a result of this, they contribute at the same order at $s = 4M_\pi^2$ and must thus be kept.

We summarize this section with the observation that the $\pi^+\pi^-$ atom is now completely understood in the framework of QCD+QED, on a conceptual as well as on a quantitative level. For bound-state observables, the theoretical predictions are made with percent accuracy. If the experiments are performed with the planned accuracy, a precise measurement of the $\pi\pi$ scattering lengths is indeed feasible.

9 πK atom

As far as the description of the bound state within the non-relativistic effective theory is concerned, the πK atom problem is completely analogous to the case of ponium considered in the previous section. For this reason, we shall display only the final results here. Details may be found in Ref. [44].

For definiteness, we consider the bound state of K^+ and π^- . The strong energy shifts and widths of the πK atom are given by expressions similar to Eq. (8.8),

$$\begin{aligned}\Delta E_n^{\text{str}} &= -\frac{2\alpha^3\mu_c^2}{n^3}\mathcal{A}_c(1+K'_n)+o(\delta^4), \\ \Gamma_n &= \frac{8\alpha^3\mu_c^2}{n^3}p_n^*\mathcal{A}_x^2(1+K_n)+o(\delta^{9/2}),\end{aligned}\tag{9.1}$$

where \mathcal{A}_x and \mathcal{A}_c are now related to the relativistic threshold amplitudes for the scattering processes $\pi^-K^+ \rightarrow \pi^0K^0$ and $\pi^-K^+ \rightarrow \pi^-K^+$, respectively, see appendix A. In particular,

$$\begin{aligned}\mathcal{A}_x &= a_0^- + \delta\mathcal{A}_x + o(\delta), & \mathcal{A}_c &= a_0^+ + a_0^- + \delta\mathcal{A}_c + o(\delta), \\ a_0^+ &= \frac{a^{1/2} + 2a^{3/2}}{3}, & a_0^- &= \frac{a^{1/2} - a^{3/2}}{3},\end{aligned}\tag{9.2}$$

where $a^{1/2}, a^{3/2}$ are the πK scattering lengths with total isospin $I = 1/2$ and $I = 3/2$, respectively, and $\delta\mathcal{A}_x, \delta\mathcal{A}_c$ denote isospin breaking terms of order δ . Furthermore,

$$\begin{aligned} K_n &= \frac{M_\pi \Delta_K + M_K \Delta_\pi}{\Sigma_+} (a_0^+)^2 - 2\alpha\mu_c (a_0^+ + a_0^-) s_n(\alpha), \\ K'_n &= -\alpha\mu_c (a_0^+ + a_0^-) s_n(\alpha), \end{aligned} \quad (9.3)$$

where $\Delta_K = M_K^2 - M_{K^0}^2$, $\Sigma_+ = M_\pi + M_K$, μ_c is the reduced mass of the $\pi^- K^+$ system, and

$$E_n = \Sigma_+ - \frac{\alpha^2 \mu_c}{2n^2}, \quad p_n^* = \lambda^{1/2} (E_n^2, M_{\pi^0}^2, M_{K^0}^2) / (2E_n). \quad (9.4)$$

The equations (9.1) can be rewritten as

$$\begin{aligned} \Delta E_n^{\text{str}} &= -\frac{2\alpha^3 \mu_c^2}{n^3} (a_0^+ + a_0^-) (1 + \delta'_n) + o(\delta^4), & \delta'_n &= \frac{\delta\mathcal{A}_c}{a_0^+ + a_0^-} + K'_n, \\ \Gamma_n &= \frac{8\alpha^3 \mu_c^2}{n^3} p_n^* (a_0^-)^2 (1 + \delta_n) + o(\delta^{9/2}), & \delta_n &= \frac{2\delta\mathcal{A}_x}{a_0^-} + K_n. \end{aligned} \quad (9.5)$$

The electromagnetic shift is given by

$$\begin{aligned} \Delta E_{nl}^{\text{em}} &= \frac{\alpha^4 \mu_c}{n^3} \left(1 - \frac{3\mu_c}{\Sigma_+}\right) \left[\frac{3}{8n} - \frac{1}{2l+1}\right] + \frac{4\alpha^4 \mu_c^3 \lambda}{n^3} \delta_{l0} \\ &+ \frac{\alpha^4 \mu_c^2}{\Sigma_+} \left[\frac{1}{n^3} \delta_{l0} + \frac{1}{n^4} - \frac{3}{n^3(2l+1)}\right], \end{aligned} \quad (9.6)$$

where $\lambda = \frac{1}{6} (\langle r_\pi^2 \rangle + \langle r_K^2 \rangle)$. Vacuum polarization introduces a small change in Eq. (9.5): $\delta_n \rightarrow \delta_n + \delta_n^{\text{vac}}$, $\delta'_n \rightarrow \delta'_n + \delta_n^{\text{vac}}$. As in ponium, this correction is very small: for example, in the ground state it amounts to $\delta_1^{\text{vac}} = 0.45 \cdot 10^{-2}$ [200]. In the numerical analysis given below this tiny contribution is neglected.

Finally, the strong shift in the P -wave state and the P -wave decay width into $\pi^0 K^0$ at leading order are given by [44]

$$\begin{aligned} \Delta E_{n1}^{\text{str}} &= -\frac{2(n^2 - 1)}{n^5} \alpha^5 \mu_c^4 (a_1^+ + a_1^-), \\ \Gamma_{n1}^{\pi^0 K^0} &= \frac{8(n^2 - 1)}{n^5} \alpha^5 \mu_c^4 (p_n^*)^3 (a_1^-)^2, \end{aligned} \quad (9.7)$$

where a_1^\pm denote P -wave πK scattering lengths.

A comprehensive numerical analysis of the πK atom observables in ChPT has been carried out in Ref. [44]. Below we give a short summary of the results

$10^2\delta_1$	$10^2\delta_2$	$10^2\delta'_1$	$10^2\delta'_2$
4.0 ± 2.2	3.8 ± 2.2	1.7 ± 2.2	1.5 ± 2.2

Table 3: Isospin breaking corrections in the DGBT-type formulae for the πK atom in ns states, taken from Ref. [44]. See Eq. (9.5) for the definition of δ_i and δ'_i .

of this analysis. The isospin breaking corrections to the πK threshold amplitudes Eq. (9.2) have been worked out by several authors [223–227] at $O(p^4, e^2p^2)$. Whereas the analytic expressions for $\delta\mathcal{A}_x$ and $\delta\mathcal{A}_c$ obtained in Refs. [223–227] are not identical, the numerical values agree within the uncertainties. In the calculations of the the πK atom observables carried out in Ref. [44], the values

$$\delta\mathcal{A}_x = (0.1 \pm 0.1) \times 10^{-2} M_\pi^{-1}, \quad \delta\mathcal{A}_c = (0.1 \pm 0.3) \times 10^{-2} M_\pi^{-1} \quad (9.8)$$

were used. Table 3 contains the final results of these calculations for the isospin breaking corrections to the strong shift and width of the ns state with $n = 1, 2$.

Next, we consider the calculation of the lifetime of the πK atom ground state, given the input for the S -wave πK scattering lengths. As discussed in section 2, different values for scattering lengths are available in the literature. In the analysis carried out in Ref. [44], the results of $O(p^4)$ calculations in ChPT [104, 228], as well as the solutions of the Roy–Steiner equations [106] have been used as an input. The prediction for the lifetime is¹³

$$\begin{aligned} \tau &= (4.8 \pm 0.2) \cdot 10^{-15} \text{ s} && \text{ChPT } O(p^4), \\ \tau &= (3.7 \pm 0.4) \cdot 10^{-15} \text{ s} && \text{Roy-Steiner equations [106]}. \end{aligned} \quad (9.9)$$

Finally, in Table 4 we display various contributions to the energy shift and width of the low-lying levels of the πK atom, taken from Schweizer [44]. Moreover, because the strong shift in the P -wave is small, one obtains for the $2s - 2p$ level splitting [44]

$$\Delta E^{2s-2p} = \Delta E_2^{\text{str}} + \Delta E_{20}^{\text{em}} - \Delta E_{21}^{\text{em}} + \Delta E_{20}^{\text{vac}} - \Delta E_{21}^{\text{vac}} = -1.4 \pm 0.1 \text{ eV}. \quad (9.10)$$

We summarize that, as a result of the investigation carried out in Ref. [44], the next-to-leading order isospin breaking corrections to the observables of the πK atom in the ground state are now known with a precision that is comparable to the one in pionium. In our opinion, this is a completely satisfactory situation from the point of view of the data analysis of possible future experiment. We refer the reader back to subsection 2.2 for comments concerning the relevance of measuring πK scattering lengths.

¹³Schweizer [44] does not quote an uncertainty for the lifetime which result from ChPT at order p^4 . For completeness, we re-evaluated the first line of Eq. (9.9), using the value $a_0^- = 0.079 \pm 0.001 M_\pi^{-1}$, given in Ref. [44].

	$\Delta E_{nl}^{\text{em}}$ [eV]	$\Delta E_{nl}^{\text{vac}}$ [eV]	$\Delta E_{nl}^{\text{str}}$ [eV]	$10^{15}\tau_{nl}$ [s]
$n=1, l=0$	-0.095	-2.56	-9.0 ± 1.1	3.7 ± 0.4
$n=2, l=0$	-0.019	-0.29	-1.1 ± 0.1	29.4 ± 3.3
$n=2, l=1$	-0.006	-0.02	$\simeq -3 \times 10^{-6}$	$\simeq 0.7 \times 10^4$

Table 4: Numerical values for the energy shift and the lifetime of the πK atom, taken from Ref. [44]. The quantity $\Delta E_{n0}^{\text{str}}$ stands for ΔE_n^{str} , and $\tau_{n0} = (\Gamma_n)^{-1}$.

10 Pionic hydrogen

10.1 Pionic hydrogen experiments at PSI

During the last decade, the Pionic Hydrogen Collaboration at PSI performed high-precision measurements of strong interaction parameters of both, pionic hydrogen (πH) and pionic deuterium (πD) [1, 109–118] in order to extract independent information about the S -wave πN scattering lengths. In this section, we mainly discuss pionic hydrogen.

This exotic atom is formed, when the kinetic energy of a negative pion is of the order of a few eV. The incoming pion is captured by the Coulomb field in highly excited states and a de-excitation cascade starts, which proceeds through X -ray emission as well as through other (non-radiative) mechanisms. The atomic cascade ends in the ground state, which then decays, mainly in $n\gamma$ and $n\pi^0$ states. The experimental setup uses the high-intensity low-energy pion beam $\pi E5$ at PSI. The energy shifts are extracted from the measured X -ray lines, see Fig. 9. In particular, the strong interaction shift in the ground state is obtained from the measured mean transition energy E_{3p-1s} .

The theoretical framework is analogous to the one summarized in subsection 5.7, see also below. The quantity E_{3p-1s} is related to the energy levels by $E_{3p-1s} = \text{Re}(z_{31} - z_{10})$, where

$$z_{nl} = E_n + \Delta E_{nl}, \quad X_{nl} = \frac{1}{2(2l+1)} \sum_{j=|l-\frac{1}{2}|}^{l+\frac{1}{2}} (2j+1)X_{nlj}; \quad X = z, \Delta E. \quad (10.1)$$

Here, E_n stands for the pure Coulomb energy, $j = l \pm \frac{1}{2}$ denotes the total angular momentum of a given eigenstate, and ΔE_{nlj} is the energy shift of a generic energy level z_{nlj} of πH , labeled by the quantum numbers n, l, j . Further, in analogy with Eqs. (5.46), (5.47) and (5.48), this energy shift is further split into an electromagnetic piece, a contribution from vacuum polarization and from the strong shift,

$$\Delta E_{nlj} = \Delta E_{nlj}^{\text{em}} + \Delta E_{nlj}^{\text{vac}} + \delta_{l0}(\Delta E_n^{\text{str}} - \frac{i}{2}\Gamma_n) + o(\delta^4). \quad (10.2)$$

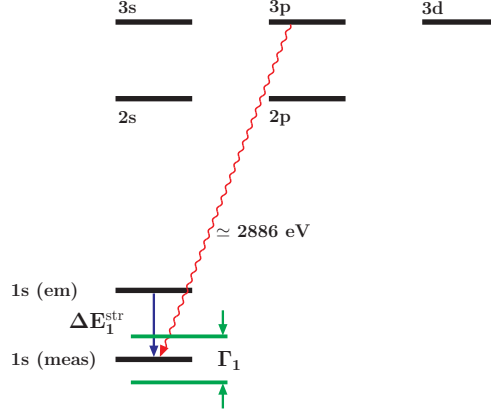


Figure 9: The scheme of energy levels of πH with the $3p - 1s$ X -ray transition. The displacement and the finite width of the ground state are explicitly shown.

The strong shift of the ground state is determined from

$$\Delta E_1^{\text{str}} = E_{3p-1s}^{\text{em}} + E_{3p-1s}^{\text{vac}} - E_{3p-1s}, \quad (10.3)$$

where E_{3p-1s}^{em} and E_{3p-1s}^{vac} are the (theoretical values for) the electromagnetic transition energy and the vacuum polarization contribution,

$$E_{3p-1s}^{\text{em}} = E_3 - E_1 + \Delta E_{31}^{\text{em}} - \Delta E_{10}^{\text{em}}, \quad E_{3p-1s}^{\text{vac}} = \Delta E_{31}^{\text{vac}} - \Delta E_{10}^{\text{vac}}. \quad (10.4)$$

Here, $\Delta E_{nl}^{\text{em}}$ is defined through $\Delta E_{nlj}^{\text{em}}$ according to Eq. (10.1). In addition, one makes use of the fact that the strong–interaction shift of the $3p$ state is suppressed by additional powers of α and is therefore negligible (see, e.g., Ref. [229]).

The following values for the strong energy shift and width of the ground state have been reported back in 2001 [114],

$$\begin{aligned} \Delta E_1^{\text{str}} &= -7.108 \pm 0.013 \text{ (stat)} \pm 0.034 \text{ (syst)} \text{ eV}, \\ \Gamma_1 &= 0.868 \pm 0.040 \text{ (stat)} \pm 0.038 \text{ (syst)} \text{ eV}. \end{aligned} \quad (10.5)$$

One determines the S -wave πN scattering lengths a_{0+}^+ and a_{0+}^- from

$$\begin{aligned} \Delta E_1^{\text{str}} &= -2\alpha^3 \mu_c^2 (a_{0+}^+ + a_{0+}^-) (1 + \delta_1') + o(\delta^4), \\ \Gamma_1 &= 8\alpha^3 \mu_c^2 p_1^* \left(1 + \frac{1}{P}\right) [a_{0+}^- (1 + \delta_1)]^2 + o(\delta^{9/2}), \end{aligned} \quad (10.6)$$

where P denotes the Panofsky ratio, and μ_c is the reduced mass of the $\pi^- p$ system. Further, $p_1^* = \lambda^{1/2}(E_1^2, m_n^2, M_{\pi^0}^2)/(2E_1)$ is the CM momentum of the $\pi^0 n$ pair after decay.

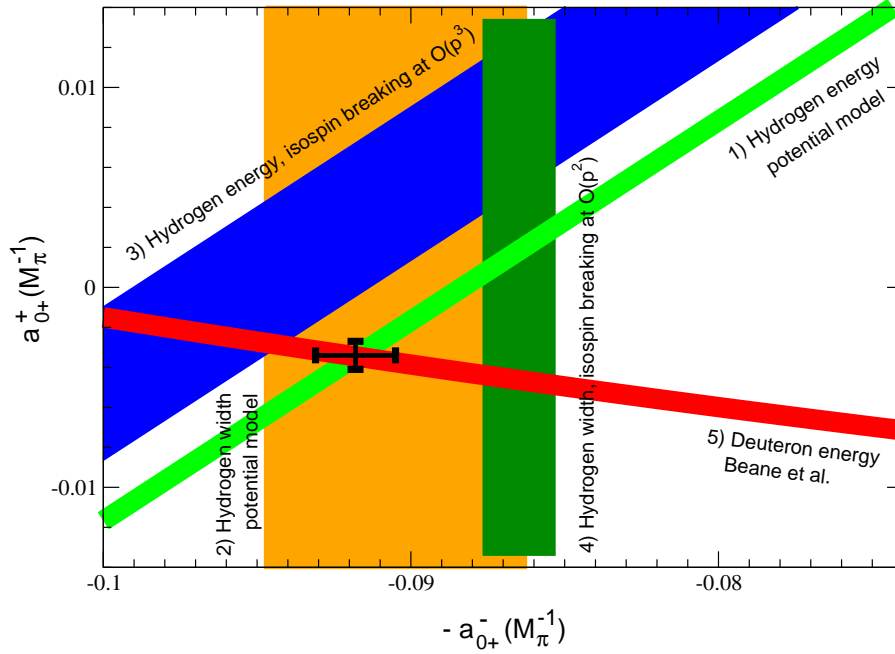


Figure 10: Determination of the πN S -wave scattering lengths from the energy shift and width of πH : i) Old analysis (bands 1 and 2), which is using the data of Ref. [114] given in Eq. (10.5) and applying the isospin breaking corrections, calculated in the potential model [230], see Eq. (10.7); ii) New analysis (bands 3 and 4), which is using preliminary data of Ref. [118] given in Eq. (2.8), together with the isospin breaking corrections calculated in ChPT, see Eqs. (10.42) and (10.44). The scattering lengths evaluated [132] from the πD energy shift Eq. (2.9) are shown in band 5. The cross indicates the solution Eq. (10.8) for the scattering lengths in the old analysis.

The quantities δ'_1 and δ_1 stand for the isospin breaking corrections, which in ChPT are of order α or $m_d - m_u$. The lowest-order DGBT formula has $\delta'_1 = \delta_1 = 0$. In the analysis of the data given in Ref. [114], one has used the values obtained in a potential scattering model [230],

$$\delta'_1 = (-2.1 \pm 0.5) \cdot 10^{-2}, \quad \delta_1 = (-1.3 \pm 0.5) \cdot 10^{-2}. \quad (10.7)$$

Recently, a new calculation of the isospin breaking corrections within a potential model has been performed in Ref. [231]. The pertinent scattering lengths still contain residual electromagnetic effects that cannot be removed with the potential model used in Ref. [231] (of course, the same is true for the analysis of Ref. [230]). We refer the reader to Ref. [231] for more details.

The analysis of the experimental data proceeds as follows. Equations (10.5)

and (10.6) generate two constraints on the possible values of the scattering lengths a_{0+}^+ and a_{0+}^- . They are displayed with the two linear bands 1,2 in Fig. 10 (here, one assumes that a_{0+}^- is positive). The widths of the bands are determined by both, the experimental error in ΔE_1^{str} and in Γ_1 , and by the theoretical uncertainty in Eq. (10.7)¹⁴. In addition, in the same Figure we also plot the band which emerges [132] from the measurement of the strong energy shift Eq. (2.9) of πD , see comments in subsection 2.3.

In the analysis carried out in Ref. [132], all three bands happen to intersect in a very small domain, suggesting a coherent overall picture. The S -wave πN scattering lengths can then be determined very well from the intersection domain of these three bands:

$$a_{0+}^+ = (-0.0034 \pm 0.0007)M_\pi^{-1}, \quad a_{0+}^- = (0.0918 \pm 0.0013)M_\pi^{-1} \quad \text{Ref. [132].} \quad (10.8)$$

This picture, however, has undergone substantial changes in the last few years, on the experimental as well as on the theory side. First, upgrading of the experiment has resulted in an increased accuracy of the measured πH width, as well as in substantially decreasing its central value, compare Eqs. (10.5) and (2.8). Second, as already stated in the introduction, results like those given in Eq. (10.7) cannot be trusted *ab initio*: the potential model, which was used to derive these results, does not include the full content of isospin breaking in QCD+QED (see also Ref. [231]). We will discuss this in a quantitative manner later in this section. Here, we simply note that, if one applies the isospin breaking corrections calculated in ChPT [41, 43, 45] to the πH energy and width given in Ref. [118] and Eq. (2.8), the central values of the scattering lengths are shifted, see the bands 3 and 4 in the Figure. There is now no more a common intersection area between the πH and the πD bands, hinting at an internal inconsistency of the theoretical methods which were used to analyze the data. The most radical proposal for circumventing the problem is to exclude the πD data from the global analysis, thus avoiding the potentially largest source of the systematic error which stems from a poor control of the multiple-scattering series for the πd scattering length. It was argued that, if the planned 2% accuracy for the width is achieved, it must be possible to determine the πN scattering lengths from πH alone [119]. We will investigate this possibility later in this section.

10.2 Effective theory and counting rules

The case of πH which is considered here, differs in two aspect from ponium and from the πK atom: first and most importantly, it decays with a $\simeq 40\%$ probability into the channel $n\gamma$, where the CM momentum of the decay products is

¹⁴We treat the uncertainties in the isospin breaking corrections Eq. (10.7) as systematic ones, combine them quadratically with the systematic uncertainty in the energy shift and width in Eq. (10.5), and add to the result the statistical uncertainties in Eq. (10.5) linearly.

of order of the pion mass. It is clear that, if one tries to include $n\gamma$ intermediate states explicitly, this will upset the whole power-counting scheme of the non-relativistic approach, where M_π plays the role of a hard scale [45]. For this reason, we apply a method already used in section 5 for the calculation of the two-photon decay width: we construct a non-relativistic theory in which the $n\gamma$ channel is “integrated out”, and where its contribution appears only through the low-energy effective couplings. One could then study πH in the non-relativistic theory with two channels $\pi^- p$ and $\pi^0 n$ [45], which closely resembles the ponium case. However, we choose a different strategy here. Namely, in order to demonstrate the flexibility of the approach, we find it instructive to consider the inclusion of the $n\pi^0$ channel into the list of “shielded” channels as well and work with a one-channel theory. The final result must of course agree with the one obtained in the two-channel setting [45].

The second generalization is related to the fact that the nucleons are fermions. However, the inclusion of particles with spin into the non-relativistic framework is nearly trivial and proceeds straightforwardly.

In order to establish the Lagrangian of the system, one has to merely write down all possible operators with a minimal number of derivatives, which are consistent with all symmetries (see also Refs. [37, 173, 174]). The result is

$$\begin{aligned}
\mathcal{L}_{NR} = & -\frac{1}{4} F_{\mu\nu} F^{\mu\nu} + \psi^\dagger \left\{ i\mathcal{D}_t - m_p + \frac{\mathcal{D}^2}{2m_p} + \frac{\mathcal{D}^4}{8m_p^3} + \dots \right. \\
& - c_p^F \frac{e\boldsymbol{\sigma}\mathbf{B}}{2m_p} - c_p^D \frac{e(\mathcal{D}\mathbf{E} - \mathbf{E}\mathcal{D})}{8m_p^2} - c_p^S \frac{ie\boldsymbol{\sigma}(\mathcal{D} \times \mathbf{E} - \mathbf{E} \times \mathcal{D})}{8m_p^2} + \dots \left. \right\} \psi \\
& + \sum_{\pm} \pi_{\pm}^\dagger \left\{ iD_t - M_\pi + \frac{\mathbf{D}^2}{2M_\pi} + \frac{\mathbf{D}^4}{8M_\pi^3} + \dots \mp c^R \frac{e(\mathbf{D}\mathbf{E} - \mathbf{E}\mathbf{D})}{6M_\pi^2} + \dots \right\} \pi_{\pm} \\
& + g_1(\psi^\dagger \psi)(\pi_-^\dagger \pi_-) + e_1 \left\{ (\psi^\dagger \overleftrightarrow{\mathcal{D}}^2 \psi)(\pi_-^\dagger \pi_-) + (\psi^\dagger \psi)(\pi_-^\dagger \overleftrightarrow{\mathbf{D}}^2 \pi_-) \right\} + \dots,
\end{aligned} \tag{10.9}$$

where ψ stands for the non-relativistic proton field, \mathcal{D} and \mathbf{D} denote the covariant derivatives acting on the proton and the charged pion, with $\psi^\dagger \overleftrightarrow{\mathcal{D}}^2 \psi = \psi^\dagger (\mathcal{D}^2 \psi) + (\mathcal{D}^2 \psi^\dagger) \psi$ (similar for the pions) and $c_p^F, c_p^D, c_p^S, c^R, g_1, e_1$ are various non-relativistic couplings. In the 4-particle sector, we discard the vertices that correspond to the P -wave interactions, as well as spin-flip terms, since these do not contribute at the accuracy we are working.

The effective theory based on the Lagrangian Eq. (10.9) enables one to evaluate the energy shift and the decay width of pionic hydrogen perturbatively in the isospin breaking parameter $\delta \sim \alpha \sim (m_d - m_u)$. The power counting rules in this parameter are as follows (see also subsection 7). The leading-order strong

energy shift in Eq. (10.6) is of order δ^3 , and the correction term δ'_1 counts at $O(\delta)$. In the formula for the decay width, the CM momentum p_1^* corresponding to the decay into the $\pi^0 n$ final state, counts at $O(\delta^{1/2})$. Further, since the cross section for $\pi^- p \rightarrow n \gamma$ starts at $O(\alpha)$, one gets $1/P = O(\delta^{1/2})$. The correction term δ_1 in Eq. (10.6) counts again at $O(\delta)$. Our final aim is to evaluate the energy shift up to and including terms of order δ^4 , and the decay width up to and including terms of order $\delta^{9/2}$. It can be checked that at this accuracy no other terms than already displayed in Eq. (10.9) are needed.

Next we note that Eq. (10.9) now includes the effective-range term with the coupling e_1 . This term has been discarded previously for scalar QED, as well as for pionium and the πK atom. The reason for this is that, if the coupling e_1 stays finite in the limit $\delta \rightarrow 0$, the effective-range term does not contribute at the accuracy we are working. It can be however shown that in our case e_1 is singular as $\delta \rightarrow 0$. In general, the counting of the effective couplings g_1, e_1, \dots in the parameter δ changes, when one integrates out the $\pi^0 n$ state. To illustrate this, we compare the threshold momenta for the γn and $\pi^0 n$ intermediate states in the CM frame, denoted by $p_\gamma^*(0)$ and $p^*(0)$ respectively (see appendix C):

$$\begin{aligned} \pi^- p \rightarrow n \gamma & : \quad p_\gamma^*(0) = \frac{\lambda^{1/2}((m_p + M_\pi)^2, m_n^2, 0)}{2(m_p + M_\pi)} = O(\delta^0), \\ \pi^- p \rightarrow \pi^0 n & : \quad p^*(0) = \frac{\lambda^{1/2}((m_p + M_\pi)^2, m_n^2, M_{\pi^0}^2)}{2(m_p + M_\pi)} = O(\delta^{1/2}). \end{aligned} \quad (10.10)$$

As it will be demonstrated below, in the presence of a shielded $\pi^0 n$ intermediate state, the dependence of the constants g_1 and e_1 on the parameter δ becomes non-analytic. For example, unlike the previous cases, unitarity now gives $\text{Im } g_1 = O(\delta^{1/2})$ (see appendix C). Moreover, we shall see that $\text{Im } e_1 = O(\delta^{-1/2})$ and, due to this fact, the effective-range contribution survives at next-to-leading order in the decay width of pionic hydrogen. To summarize, more complicated power counting rules in the parameter δ is the price one pays for using a one-channel formalism.

10.3 Matching

Let us next consider matching of the parameters of the effective non-relativistic Lagrangian Eq. (10.9) to ChPT. The matching in the one-particle sector, which determines the couplings c_p^F , c_p^D , c_p^S and c^R , is completely analogous to one carried out in subsection 4.5. The matrix elements of the electromagnetic current between two proton / two charged pion states at leading order in the coupling

constant e are given by the standard expressions

$$\begin{aligned}\langle p' s' | J_\mu^{\text{em}}(0) | p s \rangle &= e \bar{u}(p', s') \left\{ \gamma_\mu F_1(Q^2) + \frac{i}{2m_p} \sigma_{\mu\nu} Q^\nu F_2(Q^2) \right\} u(p, s), \\ \langle \pi^\pm(p') | J_\mu^{\text{em}}(0) | \pi^\pm(p) \rangle &= \pm e (p' + p)_\mu F_\pi(Q^2),\end{aligned}\quad (10.11)$$

where $Q_\mu = (p' - p)_\mu$. At a small momenta, the form factors can be expanded, yielding

$$\begin{aligned}F_1(Q^2) &= 1 + \frac{Q^2}{6} \langle r_p^2 \rangle + O(Q^4), & F_2(Q^2) &= \kappa_p + O(Q^2), \\ F_\pi(Q^2) &= 1 + \frac{Q^2}{6} \langle r_\pi^2 \rangle + O(Q^4).\end{aligned}\quad (10.12)$$

Here $F_1(Q^2), F_2(Q^2)$ and $F_\pi(Q^2)$ are the Dirac and Pauli form factors of the proton and the electromagnetic form factor of the pion, respectively (see appendix A). Further, $\langle r_p^2 \rangle$ and κ_p denote the charge radius squared and the anomalous magnetic moment of the proton. Expanding the form factors in powers of 3-momenta and performing the matching enables one to read off the values of the low-energy constants at leading order in the parameter δ [41],

$$\begin{aligned}c_p^F &= 1 + \kappa_p, & c_p^D &= 1 + 2\kappa_p + \frac{4}{3} m_p^2 \langle r_p^2 \rangle, \\ c_p^S &= 1 + 2\kappa_p, & c^R &= M_\pi^2 \langle r_\pi^2 \rangle.\end{aligned}\quad (10.13)$$

The four-particle couplings g_1, e_1 are determined through matching to the $\pi^- p$ elastic amplitude in the vicinity of threshold, calculated in ChPT. The procedure is described in detail in the appendices A and C. Below, we merely recall the notation. In total, we shall need the pion-nucleon amplitudes in 4 different physical channels labeled “c/x/0/n”, respectively:

$$p\pi^- \rightarrow p\pi^- \text{ (c)} / p\pi^- \rightarrow n\pi^0 \text{ (x)} / n\pi^0 \rightarrow n\pi^0 \text{ (0)} / n\pi^- \rightarrow n\pi^- \text{ (n)} .$$

Channel n shows up only in the πD case. One calculates these amplitudes at $O(\alpha, (m_d - m_u))$ in ChPT and obtains the threshold amplitudes $\mathcal{T}_{c,x,0,n}$. It is convenient to define the real threshold amplitudes $\mathcal{A}_{c,x,0,n}$, which are proportional to $\text{Re } \mathcal{T}_{c,x,0,n}$, see Eq. (A.29). The normalization is chosen so that, approaching the isospin limit, one has

$$\begin{aligned}\mathcal{A}_c &= a_{0+}^+ + a_{0+}^- + \delta\mathcal{A}_c + \dots, & \mathcal{A}_x &= -a_{0+}^- + \delta\mathcal{A}_x + \dots, \\ \mathcal{A}_0 &= a_{0+}^+ + \delta\mathcal{A}_0 + \dots, & \mathcal{A}_n &= a_{0+}^+ - a_{0+}^- + \delta\mathcal{A}_n + \dots,\end{aligned}\quad (10.14)$$

where $\delta\mathcal{A}_c, \delta\mathcal{A}_x, \delta\mathcal{A}_n = O(\delta)$, $\delta\mathcal{A}_0 = O(\delta^{1/2})$ are leading isospin breaking corrections and the ellipses stand for higher-order terms. The corrections at order $\delta^{1/2}$ emerge due to the unitary cusp. At the order of accuracy we are working, the couplings g_1 and e_1 are finally expressed in terms of $\mathcal{A}_c, \mathcal{A}_x$ and \mathcal{A}_0 .

10.4 Bound state – electromagnetic shift

A generic solution of the unperturbed Schrödinger equation with pure Coulomb potential, which describes the bound state of spin 0 (charged pion) and spin $\frac{1}{2}$ (proton) particles is characterized by the following set of quantum numbers: the principal quantum number $n = 1, 2, \dots$, the angular momentum $l = 0, 1, 2, \dots$, the total angular momentum $j = |l - \frac{1}{2}|, l + \frac{1}{2}$, and its z -component $m = -j, \dots, j$. The explicit expression for the wave function is given by

$$|\Psi_{nljm}(\mathbf{P})\rangle = \sum_{\sigma} \int \frac{d^3\mathbf{q}}{(2\pi)^3} \langle jm|l(m-\sigma)\frac{1}{2}\sigma\rangle \Psi_{nl(m-\sigma)}(\mathbf{q})|\mathbf{P}, \mathbf{q}, \sigma\rangle, \quad (10.15)$$

$$|\mathbf{P}, \mathbf{q}, \sigma\rangle = b^{\dagger}(\eta_1\mathbf{P} + \mathbf{q}, \sigma)a^{\dagger}(\eta_2\mathbf{P} - \mathbf{q})|0\rangle.$$

Here, $\eta_1 = m_p/\Sigma_+$, $\eta_2 = M_{\pi}/\Sigma_+$, $\Sigma_+ = (m_p + M_{\pi})$, $\mu_c = m_p M_{\pi}/\Sigma_+$, a^{\dagger}, b^{\dagger} stand for the creation operators of the non-relativistic pion and proton, $\langle jm|l(m-\sigma)\frac{1}{2}\sigma\rangle$ are the pertinent Clebsch-Gordan coefficients, and $\Psi_{nlm}(\mathbf{q})$ denotes the Coulomb wave function in the momentum space.

The energy shift is given by the counterpart of Eqs. (5.46, 5.47),

$$\Delta E_{nlj} = (\Psi_{nlj}|\bar{\tau}^{nlj}(E_n)|\Psi_{nlj}) + o(\delta^4), \quad (10.16)$$

where $E_n = \Sigma_+ - \frac{1}{2n^2}\mu_c\alpha^2$ is the Coulomb energy for this state, and where we have again used the fact that the matrix element on the right-hand side does not depend on m . The quantity $\bar{\tau}^{nlj}(E_n)$ is defined through the equation

$$\bar{\tau}^{nlj}(z) = \mathbf{V} + \mathbf{V}\bar{\mathbf{G}}_C^{nlj}(z)\bar{\tau}^{nlj}(z), \quad (10.17)$$

where, as before, \mathbf{V} denotes the perturbation Hamiltonian (everything except the static Coulomb interaction) and the pole-subtracted Coulomb resolvent is now given by

$$\bar{\mathbf{G}}_C^{nlj}(z) = \mathbf{G}_C(z) - \sum_m \int \frac{d^3\mathbf{P}}{(2\pi)^3} \frac{|\Psi_{nljm}(\mathbf{P})\rangle\langle\Psi_{nljm}(\mathbf{P})|}{z - E_n - \frac{\mathbf{P}^2}{2\Sigma_+}}. \quad (10.18)$$

According to Eq. (10.2), the total energy shift ΔE_{nlj} is given by a sum of several terms. The *electromagnetic shift* is [41, 46]

$$\begin{aligned} \Delta E_{nlj}^{\text{em}} &= -\frac{m_p^3 + M_{\pi}^3}{8m_p^3 M_{\pi}^3} \left(\frac{\alpha\mu_c}{n}\right)^4 \left\{ \frac{4n}{l + \frac{1}{2}} - 3 \right\} - \frac{\alpha^4 \mu_c^3}{4m_p M_{\pi} n^4} \left\{ -4n\delta_{l0} - 4 + \frac{6n}{l + \frac{1}{2}} \right\} \\ &+ \frac{2\alpha^4 \mu_c^3}{n^4} \left(\frac{c_p^F}{m_p M_{\pi}} + \frac{c_p^S}{2m_p^2} \right) \left\{ \frac{n}{2l+1} - \frac{n}{2j+1} - \frac{n}{2} \delta_{l0} \right\} \\ &+ \frac{4\alpha^4 \mu_c^3}{n^3} \delta_{l0} \left(\frac{c_p^D}{8m_p^2} + \frac{c^R}{6M_{\pi}^2} \right). \end{aligned} \quad (10.19)$$

Corrections	Notation	Ref. [230]	Ref. [41]
Point Coulomb, KG equation	E_{10}^{KG}	-3235.156	-3235.156
Finite size effect (proton, pion)	E_{10}^{fin}	0.102	0.100
Vacuum polarization, order α^2	E_{10}^{vac}	-3.246	-3.241
Relativistic recoil, proton spin and anomalous magnetic moment	E_{10}^{rel}	0.047	0.047
Vacuum polarization, order α^3		-0.018	
Vertex correction		0.007	

Table 5: Contributions to the electromagnetic binding energy of the π^-p atom ground state and the correction due to vacuum polarization, in eV. Vacuum polarization at order α^3 and the vertex correction have not yet been calculated within the non-relativistic approach.

The above analytic calculation neatly reproduces the numerical results of Ref. [230] for the ground-state energy. In order to facilitate the comparison, we split the electromagnetic shift by introducing the same naming scheme as in Ref. [230] (see Table 5),

$$-\frac{1}{2}\mu_c\alpha^2 + \Delta E_{10}^{\text{em}} = E_{10}^{\text{KG}} + E_{10}^{\text{fin}} + E_{10}^{\text{rel}}, \quad (10.20)$$

where

$$\begin{aligned} E_{10}^{\text{KG}} &= -\frac{1}{2}\mu_c\alpha^2\left(1 + \frac{5}{4}\alpha^2\right), \\ E_{10}^{\text{fin}} &= \frac{2}{3}\alpha^4\mu_c^3\left(\langle r_p^2 \rangle + \langle r_\pi^2 \rangle\right), \\ E_{10}^{\text{rel}} &= -\frac{1}{2}\mu_c\alpha^4\left(\frac{\mu_c}{4\Sigma_+} + \frac{m_p^2}{\Sigma_+^2} - 1 - \frac{2\kappa_p M_\pi^2}{\Sigma_+^2}\right). \end{aligned} \quad (10.21)$$

The comparison is displayed¹⁵ in Table 5. As is seen, the agreement is very good up to some higher-order contributions, which have not been yet calculated in

¹⁵We used $M_\pi = 139.56995$ MeV, $m_p = 938.27231$ MeV, $m_e = 0.51099907$ MeV, $\langle r_p^2 \rangle = (0.849 \text{ fm})^2$, $\langle r_\pi^2 \rangle = (0.657 \text{ fm})^2$, $\kappa_p = 1.79284739$, $\alpha^{-1} = 137.035989561$, see also Ref. [230]. The above value for $\langle r_p^2 \rangle$ somewhat differs from the recent update that can be found in the literature [232]. To make the comparison easy, we however do not change this value.

the effective field theory framework. Further, we have checked that the analytic expressions for E_{10}^{KG} and for E_{10}^{rel} agree with the analytic result given out in Ref. [233]. [These authors did not determine E_{10}^{fin}].

We conclude this subsection with a few remarks.

1. Eq. (10.19) provides a compact analytic expression for the electromagnetic shifts at order α^4 , for any n, l, j .
2. To include the contribution $\Delta E_{nl}^{\text{vac}}$ from vacuum polarization at order α^2 , one may use the integral representation worked out in Ref. [200]. It is reproduced for convenience in Eq. (5.42).
3. One may wish to include still vacuum polarization contributions from order α^3 , and vertex corrections, as displayed in Table 5. Note, however, that the uncertainty generated by the LEC f_1 that occurs in the strong energy shift is an order of magnitude larger than vacuum polarization at order α^3 . Indeed, one has [see Eq. (10.31) below]

$$\Delta E_1^{\text{str}}|_{f_1} = \frac{4\alpha^4\mu_c^3}{M_\pi} f_1. \quad (10.22)$$

For $f_1 = -1 \text{ GeV}^{-1}$, this amounts to a shift of -0.15 eV . An uncertainty in f_1 of the order of -100 MeV^{-1} induces therefore a shift in ΔE_1^{str} which is of the same size as the contribution from vacuum polarization at order α^3 . We see no way to pin down f_1 to this precision in the foreseeable future.

4. For these reasons, the electromagnetic shifts Eqs. (10.19) and (5.42) provide a convenient representation, of sufficient accuracy, that allows one to easily incorporate changes in the values of the pertinent parameters $\langle r^2 \rangle_\pi, \dots$, whenever needed. Together with Eqs. (10.2), (10.3) and (10.4), they allow one to translate measured energy shifts into strong shifts in an easy manner.

10.5 DBGT formula for πH

Finally, at the accuracy we are working, the strong shifts and widths are (cf. with Eq. (5.31))

$$\Delta E_n^{\text{str}} - \frac{i}{2} \Gamma_n = -\frac{\alpha^3\mu_c^3}{\pi n^3} (g_1 + 4\gamma_n^2 e_1 - g_1^2 \langle \bar{\mathbf{g}}_C^{n0}(E_n) \rangle) + \dots, \quad (10.23)$$

where $\gamma_n = \gamma/n$, and

$$\langle \bar{\mathbf{g}}_C^{n0}(E_n) \rangle = \frac{\alpha\mu_c^2}{2\pi} \left(\Lambda(\mu) + \ln \frac{4\mu_c^2}{\mu^2} - 1 + s_n(\alpha) \right). \quad (10.24)$$

Moreover, in order to arrive at Eq. (10.23), we have used that

$$\int \frac{d^d \mathbf{p}}{(2\pi)^d} \mathbf{p}^2 \Psi_{n0}(\mathbf{p}) = -\gamma_n^2 \tilde{\Psi}_{n0}(0). \quad (10.25)$$

To arrive at this result, we used the Schrödinger equation in momentum space for the Coulomb wave function $\Psi_{n0}(\mathbf{p})$, and took into account that no-scale integrals vanish in dimensional regularization.

Expressing now the couplings g_1 and e_1 through the threshold scattering amplitudes (see appendix C for details), we arrive at our final result

$$\begin{aligned} \Delta E_n^{\text{str}} &= -\frac{2\alpha^3 \mu_c^2}{n^3} \mathcal{A}_c (1 + K'_n) + o(\delta^4), \\ \Gamma_n &= \frac{8\alpha^3 \mu_c^2 p_n^*}{n^3} \left(1 + \frac{1}{P}\right) \mathcal{A}_x^2 (1 + K_n) + o(\delta^{9/2}), \end{aligned} \quad (10.26)$$

where p_n^* stands for the relative 3-momentum of the $n\pi^0$ pair after the decay of the Coulombic bound state,

$$p_n^* = \frac{\lambda^{1/2}(E_n^2, m_n^2, M_{\pi^0}^2)}{2E_n}. \quad (10.27)$$

Finally, the correction terms at this order are given by

$$\begin{aligned} K'_n &= -\alpha \mu_c (a_{0+}^+ + a_{0+}^-) s_n(\alpha) + \delta_n^{\text{vac}}, \\ K_n &= -2\alpha \mu_c (a_{0+}^+ + a_{0+}^-) s_n(\alpha) + 2\mu_c \Delta m (a_{0+}^+)^2 + \delta_n^{\text{vac}}, \end{aligned} \quad (10.28)$$

where $s_n(\alpha)$ is given in Eq. (5.32). For $n = 1$, this result coincides with the one given in Ref. [45].

10.6 Isospin breaking corrections and data analysis

Chiral expansion of the threshold amplitude

The threshold amplitudes which enter Eq. (10.26) contain itself isospin breaking corrections, that we identify in the manner displayed in Eq. (10.14). The correction to the bound state energy shift in the notation Eq. (10.6) is then given by

$$\delta'_n = \frac{\delta \mathcal{A}_c}{a_{0+}^+ + a_{0+}^-} + K'_n. \quad (10.29)$$

The correction $\delta \mathcal{A}_c$ can be calculated systematically, order by order in ChPT. Further, K'_n can be evaluated by using the values of the scattering lengths from e.g. Ref. [114] and the vacuum polarization correction from Ref. [200]. For

example, for the ground state, this gives $K'_1 = 0.66 \cdot 10^{-2} + 0.48 \cdot 10^{-2} = 1.14 \cdot 10^{-2}$, where $\delta_1^{\text{vac}} = 0.48 \cdot 10^{-2}$. For the chiral expansion of the isospin breaking part in the threshold amplitudes, we write

$$\delta\mathcal{A}_c = \delta\mathcal{A}_{c,2} + \delta\mathcal{A}_{c,3} + O(p^4). \quad (10.30)$$

The first two terms have been evaluated by Refs. [41, 43, 234, 235] (Ref. [235] does not provide a complete analytic expression of the scattering amplitude). At order p^2 , the result is

$$\delta\mathcal{A}_{c,2} = \frac{1}{4\pi(1 + M_\pi/m_p)} \left(\frac{4\Delta_\pi}{F_\pi^2} c_1 - \frac{e^2}{2} (4f_1 + f_2) \right). \quad (10.31)$$

For $\delta\mathcal{A}_{c,3}$, see Ref. [43]. Unlike in the case of pionium, this correction contains nontrivial strong and electromagnetic LECs c_1, f_1, f_2 [236, 237] already at lowest order. This introduces a sizable systematic error in the theoretical prediction of the corresponding contributions to δ'_n . In order to proceed further, we have first to specify the values of these LECs.

Strong LECs: c_i

There are different options for fixing the values of the LECs in the strong sector. In the context of the present problem, it is consistent to determine these constants from the threshold data on πN scattering, similar to Refs. [43, 238, 239]. Below, we closely follow the method of Ref. [238], using the same conventions and notations. We denote the isospin symmetric spin-nonflip πN amplitude by $D^+(q^2, t)$, where $q^2 = \lambda(s, m_p^2, M_\pi^2)/4s$ is the square of the CM momentum and s, t, u are the usual Mandelstam variables. In the vicinity of threshold the quantity $\text{Re } D^+(q^2, t)$ can be expanded in Taylor series,

$$\text{Re } D^+(q^2, t) = D_{00}^+ + D_{10}^+ q^2 + D_{01}^+ t + \dots \quad (10.32)$$

The amplitudes D_{ij}^+ contain the LECs c_1, c_2, c_3 [out of which we need c_1]. On the other hand, these amplitudes can be expressed in terms of the threshold parameters (see, e.g., Ref. [238]),

$$\begin{aligned} D_{00}^+ &= 4\pi(1 + \eta) a_{0+}^+, \\ D_{10}^+ &= 4\pi(1 + \eta) \left\{ \frac{a_{0+}^+}{2\eta m_p^2} + b_{0+}^+ + a_{1-}^+ + 2a_{1+}^+ \right\}, \\ D_{01}^+ &= 2\pi \left\{ \frac{a_{0+}^+}{4m_p^2} + a_{1-}^+ + a_{1+}^+(2 + 3\eta) \right\}, \end{aligned} \quad (10.33)$$

where $\eta = M_\pi/m_p$ and $a_{l\pm}^+, b_{l\pm}^+$ stand for the scattering lengths and for the effective ranges. Consequently, given an algebraic expression for the amplitude

LECs	$O(p^2)$	$O(p^3)$	$O(p^4)$
c_1	-0.9	-1.2	-1.2
c_2	2.6	4.0	2.6
c_3	-4.4	-6.1	-6.1

Table 6: The central values of the LECs c_1, c_2, c_3 , extracted from the experimental data at different chiral orders (in units of GeV^{-1}).

$D^+(q^2, t)$, one may solve for the constants c_1, c_2, c_3 in terms of the experimentally measured threshold parameters and other strong LECs, whose contribution enters $D^+(q^2, t)$ first at order p^4 and is small. Moreover, using $D^+(q^2, t)$ calculated at $O(p^2), O(p^3), O(p^4), \dots$, one may extract the couplings c_i from data at the same order – the differences between the numerical values corresponds to the residual quark mass dependence in these constants¹⁶ (note that, while doing this, we treat D_{00}^+, D_{10}^+ and D_{01}^+ as a fixed input and do not expand in the variable η).

In Table 6 we summarize the central values of c_1, c_2, c_3 at different chiral orders. As an experimental input, we have used Koch’s values for the threshold parameters [5]. Other LECs which contribute to $D^+(q^2, t)$ at order p^4 are: $O(p^4)$ LEC \bar{l}_3 from the pion sector and the fourth-order pion–nucleon LECs $e_1 \dots e_6$ [238]. In the calculations we use $\bar{l}_3 = 2.9$ and set the finite part of the constants e_i to 0 at the scale $\mu = m_p$. We have checked that the dependence of c_1, c_2, c_3 on these LECs is rather weak, so even a large uncertainty here does not affect the final result. From this Table one readily sees that, going from $O(p^2)$ to $O(p^3)$ leads to substantial quark mass effects in all c_i , see also Ref. [146]. On the other hand, c_1 and c_3 become stable already at $O(p^3)$, suggesting that the procedure is convergent.

Table 6 contains only central values. The estimate of the uncertainties is more subtle. The quoted experimental uncertainties on the threshold parameters are rather small. However, since in actual calculations one is truncating amplitudes at a given order in ChPT, the uncertainty in the LECs is set to reflect the uncertainty due to the higher orders as well. Bearing this in mind, we assign the following error estimate to our central value of c_1 :

$$c_1 = -1.2 \pm 0.3 \text{ GeV}^{-1} \quad [\text{order } p^4]. \quad (10.34)$$

At order $O(p^2)$ we assign an asymmetric error:

$$c_1 = -0.9_{-0.5}^{+0.2} \text{ GeV}^{-1} \quad [\text{order } p^2]. \quad (10.35)$$

Here we take the same uncertainty as in the recent analysis of LECs of the $O(p^2)$ Lagrangian [240]. In this paper, the author compiles various determinations of

¹⁶We thank T. Becher and H. Leutwyler for providing us with the explicit analytic expression for the amplitude $D^+(q^2, t)$ up to and including the fourth order terms.

the couplings known in the literature, including the information about the sub-threshold πN amplitudes and the NN potential [146, 236, 241–245]. The resulting values of c_1 range from -0.7 GeV^{-1} to -1.4 GeV^{-1} , which is in reasonable agreement with our finding (the sign of the uncertainty for c_1 in Ref. [240] must be reversed). On the other hand, our error bars are generous enough to include the shift of the central value when going from $O(p^2)$ to $O(p^3)$. We therefore expect that the result remains stable with respect to higher-order quark mass effects.

Finally, we note that our former result $c_1 = -(0.93 \pm 0.07) \text{ GeV}^{-1}$ at $O(p^2)$ [43] includes the uncertainty of the scattering lengths only. Even though that result is compatible with the above one within the error bars, we prefer to use a more conservative error estimate here.

Electromagnetic LECs: f_1 and f_2

Next, we turn to the electromagnetic constants f_1, f_2 . The quantity f_1 occurs in the chiral expansion of the nucleon mass and in elastic pion–nucleon scattering $\pi^\pm p(n) \rightarrow \pi^\pm p(n)$. The electromagnetic part of the proton–neutron mass difference is given by the constant f_2 at leading order in the chiral expansion,

$$-e^2 F^2 f_2 = (m_p - m_n)^{\text{em}}. \quad (10.36)$$

Here we disagree with Ref. [246, Eq. (12)] by a factor of 2. Numerically, we use $(m_p - m_n)^{\text{em}} = (0.76 \pm 0.3) \text{ MeV}$ [247], or

$$f_2 = -(0.97 \pm 0.38) \text{ GeV}^{-1}. \quad (10.37)$$

We are left with the determination of f_1 . The sum $m_p + m_n$ contains the combination $e^2(f_1 + f_3)$ - the constants f_1 and f_3 can thus not be disentangled from information on the nucleon masses. We may consider $m_p + m_n$ as a quantity that fixes f_3 , once f_1 is known. Therefore, elastic pion–nucleon scattering is the only realistically accessible source of information on f_1 . In principle, one may consider combinations of amplitudes that vanish in the isospin symmetry limit, and determine f_1 from those. The combination

$$X = T^{\pi^+ p \rightarrow \pi^+ p} + T^{\pi^- p \rightarrow \pi^- p} - 2T^{\pi^0 p \rightarrow \pi^0 p} \quad (10.38)$$

has this property. The tree graphs of X start at order p^2 and contain f_1 - that one may try to determine hence from here. Of course, one is faced with a problem of accuracy: in order to determine X , one needs to consider the difference of two large numbers, quite aside from the fact that the cross section $\pi^0 p \rightarrow \pi^0 p$ is not known experimentally¹⁷. It remains also to be seen whether a combination of experimental data and lattice calculations can provide a reliable estimate of f_1 .

¹⁷For a proposal to measure the elastic scattering of neutral pions, see, e.g., Ref. [248].

In the absence of precise experimental information, we can i) rely on order-of-magnitude estimates, or ii) consider model calculations. As to order-of-magnitude estimates, we follow Fettes and Meißner [249] and write

$$F^2 e^2 |f_1| \simeq \frac{\alpha}{2\pi} m_p,$$

or

$$|f_1| \simeq 1.4 \text{ GeV}^{-1}, \quad (10.39)$$

because f_1 is due to a genuine photon loop at the quark level (we divide by 2π rather than by 4π [249] to be on the conservative side). This estimate also confirms the expectation [41] that $|f_1|$ has the same size as $|f_2|$, see Eq. (10.37).

In Refs. [250, 251], $O(p^2)$ LECs have been estimated in the framework of a quark model, with the result (in our notation)

$$\begin{aligned} c_1 &= -1.2 \text{ GeV}^{-1}, \\ (f_1, f_2, f_3) &= (-2.3 \pm 0.2, -1.0 \pm 0.1, 2.1 \pm 0.2) \text{ GeV}^{-1}. \end{aligned} \quad (10.40)$$

For a recent attempt to calculate f_1 by using a method related to resonance saturation, see Ref. [252].

Isospin breaking correction δ_1, δ'_1 and data analysis

Using the values of LECs at $O(p^2)$, which are given in Eqs. (10.35), (10.37) and (10.39), we find that

$$\delta'_1 = (-4_{-4}^{+3}) \cdot 10^{-2} \quad [\text{order } p^2], \quad (10.41)$$

where the central value corresponds to $f_1 = 0$. We add the uncertainties quadratically. The bulk of the uncertainty is due to the one in f_1 and c_1 .

As mentioned above, the calculation of the isospin breaking correction at $O(p^3)$ in ChPT has been carried out in Ref. [43], see also Ref. [235]. Using the estimate Eq. (10.34) for c_1 , these calculations lead to

$$\delta'_1 = (-9.0 \pm 3.5) \cdot 10^{-2} \quad [\text{order } p^3]. \quad (10.42)$$

It turns out that, albeit the loop contributions at $O(p^3)$ are sizable due to the presence of chiral logarithms, the contribution of LECs at this order is quite small. The uncertainty is dominated by the uncertainty in f_1 and, to a certain extent, by the one in c_1 . We expect that the contributions of the higher-order LECs, which are multiplied by additional powers of M_π , will be even more suppressed and do not alter significantly the uncertainty displayed. At this order, isospin breaking in the π^-p elastic scattering amplitude is still of purely electromagnetic origin: the terms with $(m_d - m_u)$ appear first at $O(p^4)$.

The isospin breaking corrections in the charge-exchange and to the $\pi^- n \rightarrow \pi^- n$ elastic threshold amplitudes at $O(p^2)$ are [45, 48]

$$\begin{aligned}\delta\mathcal{A}_x &= \frac{1}{16\pi(1 + M_\pi/m_p)} \left(\frac{g_A^2 \Delta_\pi}{m_p F_\pi^2} + 2e^2 f_2 \right) + O(p^3), \\ \delta\mathcal{A}_n &= \frac{1}{4\pi(1 + M_\pi/m_p)} \left(\frac{4\Delta_\pi}{F_\pi^2} c_1 - \frac{e^2}{2} (4f_1 - f_2) \right) + O(p^3).\end{aligned}\quad (10.43)$$

One may use the above expression to evaluate the correction term to the decay width in Eq. (10.6). At this order, one has [45]¹⁸

$$\delta_1 = (0.6 \pm 0.2) \cdot 10^{-2} \quad [\text{order } p^2], \quad (10.44)$$

where we take $g_A = 1.27$, and where the error comes from the uncertainty in f_2 . Note that, unlike the amplitude \mathcal{A}_c , the isospin breaking part of the charge-exchange amplitude at $O(p^2)$ does not contain the quantities f_1 and c_1 . In this channel, one is, therefore, able to determine the isospin breaking corrections to a much better accuracy. Still, achieving an accuracy that is comparable to the present experimental precision is not possible without the evaluation of the corrections of order $O(p^3)$ (at least). This task should urgently be addressed.

The results given in Eqs. (10.42) and (10.44) should be contrasted with the ones obtained in the framework of potential models, see Eq. (10.7). As anticipated, these two sets are rather different, because potential model do not, in general, fully reflect QCD+QED.

We now come back to the discussion of Fig. 10, which was presented in the beginning of this section. It is seen that presently, the theoretical uncertainty in the scattering length a_{0+}^+ is much larger than assumed in the potential model approach. For this reason, a precise determination of a_{0+}^+ from hydrogen data alone is not possible, unless one finds a way to pin down f_1 more precisely. On the other hand, as we will show later in this article, a simultaneous analysis of πH and πD data may allow one to pin down the scattering lengths in a more reliable manner.

11 Kaonic hydrogen

11.1 The kaonic hydrogen and kaonic deuterium experiments at DAΦNE

An unique source of negative kaons, which provides important conditions for the study of the low-energy kaon-nucleon interaction, has been made available

¹⁸Note that in Ref. [45], $O(p^2)$ expressions for the scattering lengths were used in numerical calculations, instead of their experimental values. If we use the a_{0+}^+ and a_{0+}^- from e.g. Ref. [114], the result changes insignificantly to $\delta_1 = (0.7 \pm 0.2) \cdot 10^{-2}$ [at order p^2].

by the DAΦNE electron–positron collider in Frascati. The DEAR experiment at DAΦNE and its successor SIDDHARTA aim at a precision measurement of the strong interaction shifts and widths of $\bar{K}H$ and $\bar{K}D$. The final aim is to extract the antikaon–nucleon scattering lengths from the measured characteristics of these atoms [149–152, 154, 155].

In the DEAR experiment the low–momentum negative kaons, produced in the decay of the ϕ -mesons at DAΦNE, leave the thin–wall beam pipe, are degraded in energy to a few MeV, enter a gaseous target through a thin window and are finally stopped in the gas. The stopped kaons are captured in an outer orbit of the gaseous atoms, thus forming the exotic kaonic atoms. The kaons cascade down and some of them will reach the ground state emitting X -rays.

As mentioned before, recent results of the DEAR collaboration [154] for the shift and the width of the kaon hydrogen in its $1s$ ground state (see Eq. (2.14)) considerably improve the accuracy of the earlier KpX experiment at KEK [153] and confirm the repulsive character of the K^-p scattering at threshold. It should be also pointed out that the DEAR central result deviates from all earlier experiments [153, 253–255], see also Fig. 12 below. Below we shall discuss the implications of these beautiful new measurements for establishing the precise values of the $\bar{K}N$ scattering lengths a_0 and a_1 . The discussion is based on Ref. [46].

11.2 DGBT–type formulae for kaonic hydrogen

The non–relativistic theory of $\bar{K}H$ [46] is almost a carbon copy of the πH case. It is, on the other hand, amusing that the existing small differences at the end result in a strikingly different picture (this, in our opinion, is another demonstration of the power and flexibility of the NRQFT approach). We do not present many explicit formulae, because they often look identical in the πH and $\bar{K}H$ case – we rather concentrate on those properties of these two systems which are not the same. For example, there is no need to carry out again the calculation of the electromagnetic shift – it is given by the corresponding expression derived in the pionic hydrogen case Eq. (10.19) after obvious replacements $M_\pi \rightarrow M_K$ and $\langle r_\pi^2 \rangle \rightarrow \langle r_K^2 \rangle$.

We start to list those characteristic features of the $\bar{K}N$ system which cause a difference to the case of pionic hydrogen.

- i) The only states that are degenerate in mass with the K^-p state in the isospin limit $\delta \rightarrow 0$, are the states $K^-p + m\gamma$, $\bar{K}^0n + m'\gamma$, with $m, m' = 0, 1, \dots$. It is convenient to use a framework which explicitly “resolves” all these states in the non–relativistic theory. On the contrary, the effect of other intermediate states, whose mass is not degenerate with that of the K^-p state in the isospin limit, could be included in the couplings of the non–relativistic effective Lagrangian.

- ii) Breaking of $SU(3)$ symmetry, which is proportional to the quark mass difference $m_s - \hat{m}$, is much larger than isospin breaking effects. For this reason, we count $m_s - \hat{m}$ as $O(1)$ in δ . Because there are open strong channels below K^-p threshold – e.g. $\pi\Sigma$, $\pi^0\Lambda$, the real and imaginary parts of strong kaon–nucleon couplings count as $O(1)$. This leads to a completely different power counting as compared to the πH case (see also subsection 7): the strong shift and width are quantities of order δ^3 .

In the non-relativistic theory, where the neutral ($\bar{K}^0 n$) channel is explicitly resolved, the couplings are analytic in δ (there are no corrections that go like $\sqrt{\delta}$, cf. with the discussion in section 10 and in appendix C). The expansion of a typical 4-particle coupling constant (similar as in Eq. (10.9)) is given by

$$g_i = g_i^{(0)} + \alpha g_i^{(1)} + (m_d - m_u) g_i^{(2)} + O(\delta^2), \quad (11.1)$$

where $g_i^{(0)}, g_i^{(1)}, g_i^{(2)}, \dots$ are functions of the strange quark mass m_s , along with $\hat{m} = \frac{1}{2}(m_u + m_d)$.

- iii) The Panofsky ratio Eq. (A.34) in πH is of order $\delta^{-1/2}$. Numerically, the branching ratio into the $n\gamma$ channel amounts to a contribution of $\simeq 40\%$ in the total decay width. In contrast to this, in the case of $\bar{K}H$, this branching ratio counts as $O(\delta^{-1})$. The measured branching ratios into the leading $\Lambda\gamma$, $\Sigma\gamma$ channels are of the order of a per mille [256] (the theoretical description of this quantity by using chiral Lagrangians [57, 257] gives a result which is consistent with the experiment by order of magnitude). Consequently, the perturbative treatment of the effects due to these channels is justified. At the numerical precision one is working, and bearing in mind present experimental and theoretical uncertainties, they may even be neglected altogether.
- iv) The $\bar{K}^0 n$ intermediate state lies in the vicinity the K^-p threshold. Due to this fact, the well-known unitary cusp emerges in the K^-p elastic scattering amplitude (see, e.g., Refs. [258–260] and appendix C) which is the source of huge isospin breaking corrections (note that the cusp effect is also the dominant isospin breaking effect in some other low-energy processes, e.g. in neutral pion photo-production off nucleons [261, 262] as well as $K \rightarrow 3\pi$ decays [88–93].).
- v) The $\Lambda(1405)$ never appears explicitly in this approach, that is correlated with counting $(m_s - m_u)$ as a hard scale. The influence of the resonance is only indirect and results in a large $\bar{K}N$ threshold scattering amplitude, which then leads to a significant increase of the isospin breaking corrections.

Due to the presence of the $\bar{K}^0 n$ states, the relative weight of the isospin breaking correction in the K^-p threshold amplitude is dramatically increased.

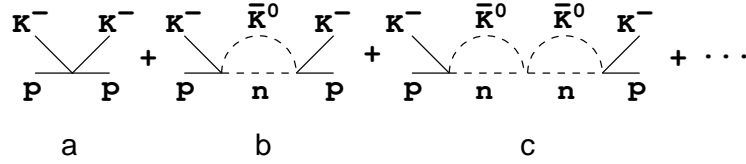


Figure 11: $\bar{K}^0 n$ bubbles in the threshold amplitude of elastic $K^- p$ scattering. Note that the bubbles with $K^- p$ in the intermediate state vanish at threshold.

Consider, for instance, the real part of this amplitude, which contains any number of the s -channel bubbles with $K^- p$ and $\bar{K}^0 n$ intermediate states. Further, the contribution of the former vanishes at threshold, and only the neutral loops contribute to the threshold amplitude (see Fig. 11).

Consider now the series of the bubble diagrams shown in this Figure. Since the $\bar{K}^0 n$ state lies higher than $K^- p$ state, the contribution from a single $\bar{K}^0 n$ bubble, which is shown in Fig. 11b, at threshold is real and proportional to $q_0 = (2\mu_0(m_n + M_{\bar{K}^0} - m_p - M_K))^{1/2} = O(\sqrt{\delta})$, where μ_0 is the reduced mass of the $\bar{K}^0 n$ pair. Thus, the isospin breaking correction to the threshold amplitude, which stems from the diagram Fig. 11b, starts at $O(\sqrt{\delta})$ (note that $q_0 = 0$ in the isospin limit). Moreover, since both real and imaginary parts of the $\bar{K}N$ couplings g_i , which appear in the vertices, count as $O(1)$, the contribution of the diagram in Fig. 11b to the real part of the threshold amplitude counts always as $O(\sqrt{\delta})$, irrespective of the fact whether the neutral loop is real or imaginary (in the latter case, the unitary cusp is below threshold and influences the real part of the amplitude through coupling to the inelastic channels).

For comparison, let us consider the counterpart of the diagram Fig. 11b in the πN case, in the non-relativistic theory where the $\pi^0 n$ state is explicitly resolved. It is purely imaginary at threshold, since $m_n + M_{\pi^0} < m_p + M_\pi$. Furthermore, the imaginary part of the non-derivative πN couplings counts as $O(\delta)$ since there are no open strong inelastic channels in this case (the channel γn contributes at $O(\delta)$). For this reason, there is no contribution from this diagram to the real part of the threshold amplitude at $O(\sqrt{\delta})$. Only the product of two neutral bubbles, which is shown in Fig. 11c can contribute to the real part, but this contribution starts at $O(\delta)$. To summarize, the isospin breaking corrections in the $\bar{K}N$ and πN amplitudes emerge at $O(\sqrt{\delta})$ and $O(\delta)$, respectively – no wonder that the former are much larger in magnitude than the latter.

The crucial observation which enables one to find the way out is the following: albeit the isospin breaking corrections which are non-analytic in the parameter δ are large, these can be expressed solely in terms of those scattering lengths which one tries to extract from the experiment. Consequently, the presence of these large corrections does not affect the accuracy of the extraction procedure. On the other hand, the isospin breaking corrections at $O(\delta)$ cannot be expressed it

terms of the scattering lengths alone – these in particular contain the LECs from the isospin breaking sector of the ChPT Lagrangian. One expects, however, that this error, introduced by the $O(\delta)$ terms, should be of the order of magnitude of a few percent, as in the pionic hydrogen.

To illustrate the above statement, let us consider the bubble sum shown in Fig. 11 in the non-relativistic effective theory, using only non-derivative 4-particle vertices. The corresponding approximate non-relativistic $K^-p \rightarrow K^-p$ scattering amplitude, which we denote as $\mathcal{T}_{c,NR}^{(0)}$, is given by the following expression,

$$\mathcal{T}_{c,NR}^{(0)} = \frac{2\pi}{\mu_c} \frac{\frac{1}{2}(a_0 + a_1) + q_0 a_0 a_1}{1 + \frac{q_0}{2}(a_0 + a_1)} \doteq \frac{2\pi}{\mu_c} a_c, \quad (11.2)$$

where μ_c is the reduced mass of the K^-p system, and where we have used the matching in the absence of isospin breaking to relate various non-derivative $\bar{K}N$ couplings to the pertinent combinations of two scattering lengths a_0 and a_1 (the error introduced is of order δ). Note also that for our purposes, it would be enough to include the contributions from the first two diagrams only. We shall however sum up the whole series shown in Fig. 11 – the difference which we introduce is again of order δ . The crucial observation is that, albeit the isospin breaking corrections in $\mathcal{T}_{c,NR}^{(0)}$ are of order $\sqrt{\delta}$, the difference $\mathcal{T}_{c,NR} - \mathcal{T}_{c,NR}^{(0)} = O(\delta)$, where $\mathcal{T}_{c,NR}$ denotes the full non-relativistic amplitude. In other words, the leading-order isospin breaking effect due to the neutral loop has been explicitly included in the quantity $\mathcal{T}_{c,NR}^{(0)}$.

Finally, using the matching condition, one may define the relativistic amplitude, corresponding to the relativistic bubble sum given by Eq. (11.2),

$$\mathcal{T}_c^{(0)} = 2m_p 2M_K \mathcal{T}_{c,NR}^{(0)} = 8\pi (m_p + M_K) a_c, \quad (11.3)$$

which has the same property as its non-relativistic counterpart, namely, the difference $\mathcal{T}_c - \mathcal{T}_c^{(0)} = O(\delta)$, where \mathcal{T}_c is the relativistic elastic amplitude for $K^-p \rightarrow K^-p$. In general, one has

$$\mathcal{T}_c = \mathcal{T}_c^{(0)} + \frac{i\alpha\mu_c^2}{4M_K m_p} (\mathcal{T}_c^{(0)})^2 + \delta\mathcal{T}_c + o(\delta), \quad (11.4)$$

which is nothing but the definition of the correction term $\delta\mathcal{T}_c$ (the second term in the above definition with the imaginary coefficient has been added for convenience. It starts at order δ). Note also, that Eq. (11.4) is the generalization of the relation

$$\mathcal{T}_c = 8\pi (m_p + M_K) \frac{1}{2} (a_0 + a_1) + O(\sqrt{\delta}). \quad (11.5)$$

The main message here is: in contrast to Eq. (11.5), the quantity $\delta\mathcal{T}_c$ in Eq. (11.4) is of order δ and therefore can be assumed to be not too large. Note also that

Eq. (11.2) exactly coincides with the amplitude introduced in Refs. [258, 259]. In our approach we however in addition demonstrate that this modification accounts for *all* potentially large $O(\sqrt{\delta})$ corrections to the threshold amplitude.

The results of our findings can be finally summarized as a modified DGBT-type formula for generic ns energy levels of $\bar{K}H$,

$$\Delta E_n^{\text{str}} - \frac{i}{2} \Gamma_n = -\frac{\alpha^3 \mu_c^3}{4\pi m_p M_K n^3} (\mathcal{T}_c^{(0)} + \delta \mathcal{T}_c) \left\{ 1 - \frac{\alpha \mu_c^2 s_n(\alpha)}{8\pi m_p M_K} \mathcal{T}_c^{(0)} + \dots \right\} + o(\delta^4), \quad (11.6)$$

where $\delta \mathcal{T}_c = O(\delta)$ and ellipses stand for (tiny) vacuum polarization contribution, which we do not display explicitly.

One expects that the equation (11.6) is much better suited for the analysis of the DEAR experimental data than the original DGBT formula. In this equation, potentially large (parametrically enhanced) isospin breaking corrections at $O(\sqrt{\delta})$ and¹⁹ $O(\delta \ln \delta)$ are explicitly separated from the rest, which is analytic in δ and is assumed to be small. Indeed, in Ref. [46] an estimate of this $O(\delta)$ term has been carried out at tree level in the $SU(3)$ version of ChPT. The calculations result in the effect at a percent level that supports the above conjecture. In the numerical analysis of the DEAR data that follow, we shall always set $\delta \mathcal{T}_c = 0$.

Finally, it is interesting to note that Eq. (11.2) enables one to independently test the limits of applicability of the method for a given values of the scattering lengths *a posteriori*. Namely, in order to be consistent, the term of order of δ in the expansion of the above amplitude should not exceed a few percent, and the following terms must be negligible (see Table 7). This is, however, not the case for all input values of scattering lengths available in the literature, see Refs. [46, 49] for a detailed discussion.

11.3 Analysis of the DEAR data

The Figure 12 summarizes the analysis of the DEAR data with the help of Eq. (11.6). Here we display the predicted value of the energy shift and width in the ground state, using different scattering lengths as an input, see Table 8. These predictions are compared with the DEAR measurement, as well as earlier experimental data. The comparison enables one to immediately conclude that the scattering data, to which the parameters of Refs. [159, 161, 163, 166] are fitted, are, in general, not consistent with the DEAR data [46]. This conclusion is valid for all input scattering lengths shown in Fig. 12, except those from Ref. [163]. For a further discussion on this issue, we refer to Refs. [162, 164].

The comparison allows one to conclude that:

¹⁹The corrections at $O(\delta \ln \delta)$, which are referred to as ‘‘Coulomb corrections’’ hereafter, emerge from the second term in curly brackets in Eq. (11.6).

	Ref. [159] $a_0 = -1.31 + 1.24i$ $a_1 = 0.26 + 0.66i$	Ref. [263] $a_0 = -1.70 + 0.68i$ $a_1 = 0.37 + 0.60i$
$a_{c,0}$	$-0.52 + 0.95i$	$-0.66 + 0.64i$
$a_{c,1}$	$-0.68 + 1.09i$	$-0.98 + 0.66i$
$a_{c,2}$	$-0.67 + 1.15i$	$-1.04 + 0.73i$
$a_{c,3}$	$-0.65 + 1.16i$	$-1.04 + 0.75i$
$a_{c,\infty} \doteq a_c$	$-0.65 + 1.15i$	$-1.03 + 0.76i$

Table 7: Expansion of the $K^-p \rightarrow K^-p$ scattering length a_c in powers of q_0 (bubble approximation, see Eq. (11.2)). The index n in $a_{c,n}$ corresponds to the n -th iteration. The results are given in fm.

Source	a_0	a_1
Meißner and Oller [159]	$-1.31 + i1.24$	$0.26 + i0.66$
Borasoy, Nißler and Weise, fit “ u ” [161]	$-1.48 + i0.86$	$0.57 + i0.83$
Oller, Prades and Verbeni, fit “ A_4^+ ” [163]	$-1.23 + i0.45$	$0.98 + i0.35$
Martin [263]	$-1.70 + i0.68$	$0.37 + i0.60$
Borasoy, Meißner and Nißler, fit “full” [166]	$-1.64 + i0.75$	$-0.06 + i0.57$

Table 8: $\bar{K}N$ scattering lengths a_0 and a_1 (in fm) from the literature. These scattering lengths are used as an input in the calculations of the kaon-deuteron scattering length.

- i) The corrections due to the unitary cusp, which start at $O(\sqrt{\delta})$, are indeed huge. Even at the present accuracy level, it is absolutely necessary to take them into account.
- ii) The Coulomb corrections that are amplified by $\ln \alpha$, are also quite sizable. For example, choosing scattering lengths from Refs. [159, 263], we obtain that the real part of the correction term in the ground state amounts up to 9% and 15%, respectively.
- iii) The key point here is that one does not indeed need to know the numerical values of these large corrections very accurately. Since both the unitary and Coulomb corrections depend on the scattering lengths a_0, a_1 only, in the numerical analysis, which aims to extract exactly these scattering lengths from the data, it suffices to know the algebraic form of this dependence.

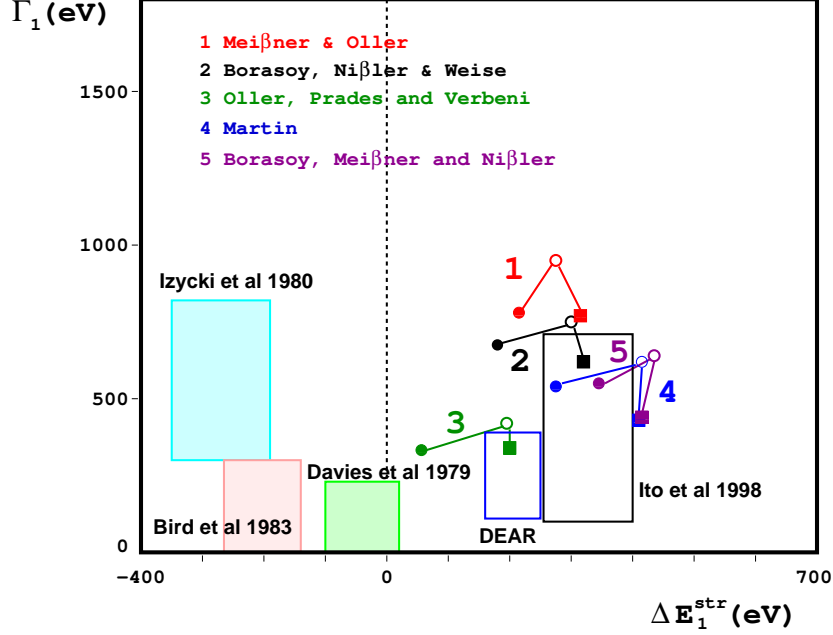


Figure 12: Isospin breaking corrections in the energy shift and width of kaonic hydrogen: different input for scattering lengths a_0 and a_1 from Refs. [159, 161, 163, 166, 263], see Table 8. Filled dots correspond to the DGBT formula (no isospin breaking), empty dots include the effect of the unitary cusp and filled squares, in addition, take the Coulomb corrections into account.

One may further refine the analysis of $\bar{K}H$ data, fully including the restrictions from unitarity [49]. We first rewrite Eq. (11.2),

$$a_0 + a_1 + \frac{2q_0}{1 - q_0 a_c} a_0 a_1 - \frac{2a_c}{1 - q_0 a_c} = 0. \quad (11.7)$$

The quantity a_c is fixed from experiment, by using Eqs. (11.2), (11.6), and neglecting corrections of order δ . We decompose the scattering lengths into their real and imaginary parts,

$$a_I = x_I + iy_I, \quad I = 0, 1; \quad a_c = u + iv. \quad (11.8)$$

Solving Eq. (11.7) for a_0 and requiring that its imaginary part is positive leads to a quadratic constraints on x_1, y_1 : in the (x_1, y_1) - plane, a_1 is expelled from a circle determined by u, v and q_0 , and similarly for $1 \leftrightarrow 2$. Explicitly,

$$\begin{aligned} (x_I + \frac{1}{q_0})^2 + (y_I - r)^2 &\geq r^2; \quad I = 0, 1, \\ r &= [(1 + q_0 u)^2 + q_0^2 v^2] (4vq_0^2)^{-1}. \end{aligned} \quad (11.9)$$

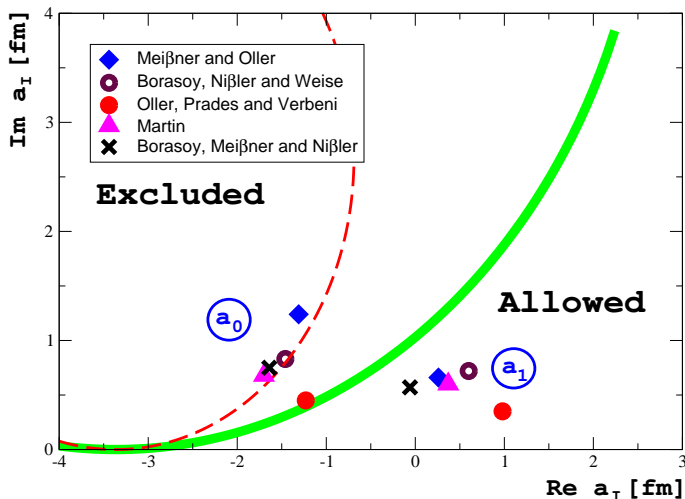


Figure 13: Restrictions set by the DEAR data on the values of the scattering lengths a_0 and a_1 (thick solid line). For comparison, we give the scattering lengths from Table 8. The dashed line corresponds to the restrictions obtained by using KpX data instead of DEAR data.

Part of this circle is shown in Fig. 13 (note that, bearing in mind the preliminary character of the DEAR data [154], we use only central values in order to illustrate the construction of the plot. We do not provide a full error analysis). In order to be consistent with the DEAR data, both a_0 and a_1 should be on the outside of this universal DEAR circle²⁰. For comparison, on the same Figure we also indicate (much milder) restrictions, which arise, when KpX data are used instead of DEAR data. The values of a_0 and a_1 , plotted in this Figure, are again taken from Table 8. As before, we see that in most of the approaches it is rather problematic to get a value for a_0 which is compatible with DEAR (the price to pay for this is the presence of a very narrow $I = 1$ pole in the scattering amplitudes close to K^-p threshold for the solutions from Ref. [163]). This kind of analysis may prove useful in the near future, when the accuracy of the DEAR is increased that might stir efforts on the theoretical side, aimed at a systematic quantitative description of the $\bar{K}N$ interactions within unitarized ChPT.

In conclusion we note that, in our opinion, the present experimental data are still not precise enough to clearly distinguish between different low-energy approaches to $\bar{K}N$ interactions which are based on the unitarization of ChPT.

²⁰Note that an analysis of the $\bar{K}H$ data alone does not allow one to determine both scattering lengths a_0 and a_1 separately, even at leading order in δ . The reason for this lies in the fact that both real and imaginary parts of a_I , $I = 0, 1$ count at $O(1)$, due to the presence of the open channels below threshold.

In the future, however, DEAR/SIDDHARTA can pose very stringent constraints on theoretical models, provided the measurements are carried out with the announced accuracy.

12 Pionic and kaonic deuterium

12.1 Introductory remarks and DGBT formulae

Pionic (kaonic) deuterium is a hadronic atom, made up from π^- (K^-) and the deuteron, which in turn is a shallow bound state of the proton and the neutron, held together by strong interactions. Constructing a theory of these bound states constitutes one step further in the sophistication of the NRQFT approach.

The characteristic momentum for the deuteron is $\bar{\gamma} = \sqrt{m_N \varepsilon_d} \simeq 46$ MeV, with $\varepsilon_d = 2.22$ MeV its binding energy. This quantity is still three times smaller than the pion mass, but much larger than the typical momenta in hadronic atoms $\simeq 1$ MeV. Consequently, in a very good approximation one may consider the pionic deuterium as a 2-body bound state and apply the machinery that has been developed in sections 3, 4 and 5. This program has been carried out in Refs. [47, 61] for πD . It can be generalized to the case of $\bar{K}D$ without any change – the interested reader may consult these article for details. The analysis of pionic (kaonic) deuterium data directly determines the pion–deuteron (kaon–deuteron) threshold amplitude. For illustration, we give the expression for the πD energy shift at next–to–leading order in isospin breaking [47],

$$\Delta E_1^{\text{str,d}} - \frac{i}{2} \Gamma_1^{\text{d}} = -2\alpha^3 \mu_d^2 \mathcal{A}_{\pi d} \left\{ 1 - 2\alpha \mu_d \mathcal{A}_{\pi d} (\ln \alpha - 1) + \dots \right\}, \quad (12.1)$$

where μ_d denotes the reduced mass of the π^-d system and (cf. with Eq. (11.4)), and

$$\mathcal{A}_{\pi d} = \mathcal{A}_c - 2\pi i \alpha \mu_d (\mathcal{A}_c)^2 = a_{\pi d} + \Delta \mathcal{A}_{\pi d}. \quad (12.2)$$

Here, \mathcal{A}_c denotes the pion–deuteron threshold amplitude, defined in Eq. (A.31), $a_{\pi d}$ is the pion–deuteron scattering length in the isospin limit and $\Delta \mathcal{A}_{\pi d}$ stands for the isospin breaking correction. The energy shift of $\bar{K}D$ at next–to–leading order is also given by Eq. (12.1), after an obvious replacement $\mathcal{A}_{\pi d} \rightarrow \mathcal{A}_{\bar{K}d}$ and using an appropriate reduced mass. However, the case of $\bar{K}D$ inherently differs from πD in one important aspect. Namely, the estimated ratio of the binding energy to the decay width in the ground state of $\bar{K}D$ amounts up only to $\simeq 8.6$ (see Ref. [49]) and is much larger in the pionic deuterium. This value can be still considered as large enough [49] to justify using the machinery based on the Rayleigh–Schrödinger perturbation theory (see section 5), but the corrections at next–to–next–to–leading order might be not completely negligible, when the

accuracy of SIDDHARTA data is close to the planned one [154, 155]. We therefore conclude that it could be interesting to perform – at some point in the future – an estimate of these corrections within the non-relativistic EFT in a manner described in section 5.

At the next step of the investigation one has to “resolve” the scattering length (threshold amplitude) on the composite object (deuteron) in terms of the underlying hadron dynamics, since for us this scattering length is primarily interesting as an additional source of information about the pion–nucleon (kaon–nucleon) scattering lengths. This is the most difficult part of the problem.

Let us first ignore the isospin breaking corrections altogether and start with πD . In lowest order in $\bar{\gamma}/M_\pi$ there exists an universal relation, which relates the pion–deuteron threshold amplitude to the threshold parameters of the pion–nucleon interactions,

$$a_{\pi d} = \frac{1 + \eta}{1 + \eta/2} (a_{\pi p} + a_{\pi n}) + O(\bar{\gamma}/M_\pi), \quad \eta = M_\pi/m_N, \quad (12.3)$$

where $a_{\pi p}$ and $a_{\pi n}$ denote pertinent linear combinations of the S -wave πN scattering lengths, see, e.g., Ref. [124]. The relation for the $\bar{K}d$ scattering length is completely similar. However the correction term in Eq. (12.3), albeit down by the small factor $\bar{\gamma}/M_\pi \simeq 1/3$, turns out to be even larger numerically than the first term. The reason for this in the case of πD is that the first term is chirally suppressed. A similar situation emerges also in the case of $\bar{K}D$, however for a different reason. Here, the kaon–nucleon scattering lengths are so large that the multiple scattering expansion seems not to converge anymore (see, e.g., Ref. [264] for a nice discussion of this issue). We conclude that, in order to extract useful information from experiments on pionic (kaonic) deuterium, an accurate evaluation of the correction term in Eq. (12.3) is necessary.

Existing calculations of pion–deuteron and kaon–deuteron scattering lengths have been carried out in different settings. The description of low-energy meson scattering on the deuteron is one of the central topics of the potential scattering theory and has been thoroughly investigated during decades. It would be absolutely impossible to cover all this very interesting work here, or even to provide a fairly complete bibliography. We cite here only few sources [22, 66, 68, 122–130, 265–269], which we have consulted on the subject.

In recent years, calculations based on low-energy effective theories of QCD in the two-nucleon sector have started to appear. These calculations enable one to extract (in principle) the pion–nucleon and kaon–nucleon scattering lengths in QCD directly from the experimental data, without any additional model-dependent input. Below, we give a very condensed review of these calculations.

12.2 Pion–deuteron scattering

Recently, there has been a considerable activity [131–138] in the study of πd scattering on the basis of the low–energy effective field theory of QCD with non–perturbative pions, where multi–pion exchanges are included into the NN potential that is later iterated to all orders. The approach was first formulated in Weinberg’s seminal paper [139] and has recently reached a level of sophistication that allows one to perform systematic precision calculations in two–nucleon as well as in many–nucleon systems. For a recent review of this approach, see Ref. [141]. Alternatively, the calculations of the πd scattering length have been also performed in the EFT with heavy/perturbative pions [47, 142, 143].

It is instructive to briefly compare calculations carried out in the two different settings. The couplings of the EFT with heavy pions include the threshold parameters of the πN scattering (scattering length, effective range, etc). Thus, the perturbative expansion in this EFT, which is carried in powers of $\bar{\gamma}/M_\pi$, produces the multiple–scattering expansion exactly in a form one is looking for. Unfortunately, individual terms in the multiple–scattering series get strongly scale–dependent after the renormalization. The scale dependence can be only canceled by a (large) three–body contribution, coming from the 6–particle LECs. And, since the value of these LECs is completely unknown, this leads to a large uncertainty in the multiple–scattering series [47, 142, 143].

On the other hand, it has been shown [131, 132, 135, 136, 270] that the scale dependence in the EFT with perturbative pions is rather mild and therefore the pertinent three–body LECs need not be large. This conjecture is independently supported by using dimensional estimate and resonance saturation for these LECs [47, 132]. Physically, the strong scale dependence in the heavy pion EFT (large LECs) reflects the increased uncertainty caused by working with a smaller energy cutoff, than for the EFT with non–perturbative pions. The price to pay for suppressing the size of the three–body force is however that the expansion parameters in the latter approach are initially quark masses and not the πN scattering lengths.

The conversion of the chiral expansion for the πd scattering length into the form of the multiple–scattering series can be achieved on the basis of the following heuristic observation (see Ref. [132]): it turns out that those contributions in the chiral expansion, which do not have a counterpart in multiple–scattering series (these are the diagrams that correspond to virtual annihilation and creation of pions, see e.g. Fig. 14b,c), are numerically suppressed with respect to the diagrams with no mass gap (Fig. 14a), although both emerge at the same chiral order. In Ref. [132] this property was formalized by introducing the so–called “modified power–counting.” Now, re–grouping the contributions in accordance to this new counting, in Ref. [132] it has been shown that up–to–and–including fourth order the pion–deuteron scattering length can be expressed in terms of the pion–nucleon scattering lengths (calculated at $O(p^3)$ in ChPT) and a remain–

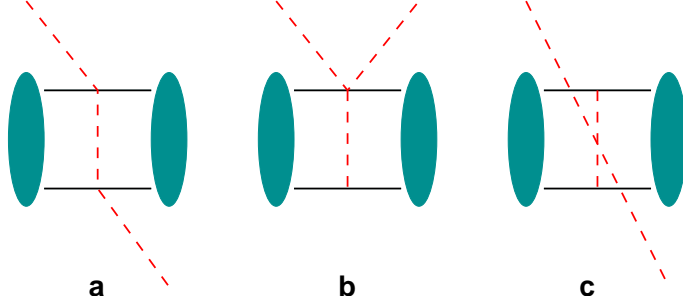


Figure 14: Illustration of the modified power counting in the theory with non-perturbative pions. The shaded blobs denote the wave function of the deuteron, and the solid and dashed lines correspond to the nucleons and pions, respectively. Diagrams b) and c), albeit being of the same order in ChPT, are strongly suppressed as compared to the diagram a), see Ref. [132].

der (the boost, or Fermi-motion correction), which turns out to be numerically not very large [132] albeit strongly scale-dependent. Moreover, unknown LECs emerge first at fifth order in modified counting and are expected to give a small contribution.

If one neglects the nucleon recoil (static approximation), the final expression for the pion-deuteron scattering length can be rewritten in a remarkably simple form [132],

$$\begin{aligned} \text{Re } a_{\pi d} = & 2 \frac{1 + \eta}{1 + \eta/2} a_{0+}^+ + 2 \frac{(1 + \eta)^2}{1 + \eta/2} ((a_{0+}^+)^2 - 2(a_{0+}^-)^2) \frac{1}{2\pi^2} \left\langle \frac{1}{\mathbf{q}^2} \right\rangle_{\text{wf}} \\ & + 2 \frac{(1 + \eta)^3}{1 + \eta/2} ((a_{0+}^+)^3 - 2(a_{0+}^-)^2(a_{0+}^+ - a_{0+}^-)) \frac{1}{4\pi} \left\langle \frac{1}{|\mathbf{q}|} \right\rangle_{\text{wf}} + a_{\text{boost}} + \dots, \quad (12.4) \end{aligned}$$

where $\langle \dots \rangle_{\text{wf}}$ stands for various wave function averages (we remind the reader that the above expression is obtained under the assumption of exact isospin symmetry). Note that Eq. (12.4) has indeed the form of usual multiple-scattering series, known from EFT with heavy pions [47, 143] (or the potential scattering theory). The difference however is that the wave functions, which are used to calculate the averages, are the wave functions in the EFT with non-perturbative pions. In the calculations in Ref. [132] the NLO wave functions with the cut-off mass in the interval $\Lambda = (500 \dots 600)$ MeV [271] have been used, yielding $\langle 1/\mathbf{q}^2 \rangle_{\text{wf}} = (12.3 \pm 0.3)M_\pi$ and $\langle 1/|\mathbf{q}| \rangle_{\text{wf}} = (7.2 \pm 1.0)M_\pi^2$. The boost correction in Eq. (12.4) is $a_{\text{boost}} = (0.00369 \dots 0.00511)M_\pi^{-1}$ (the strong scale dependence of the boost correction is related to neglecting Δ -resonance contribution, see below).

Further, the first term in the series is chirally suppressed and is anomalously small. The contribution of the second term (which is quadratic in the scattering

lengths) is large, but higher-order contributions become again smaller, so that the series are likely to converge. The measured value of the pion–deuteron scattering length is [112]

$$\text{Re } \mathcal{A}_{\pi d}^{\text{exp}} = -(0.0261 \pm 0.0005) M_{\pi}^{-1}. \quad (12.5)$$

From Eqs. (12.2) and (12.4) one obtains a relation between a_{0+}^+ and a_{0+}^- , provided that the isospin-breaking part $\Delta\mathcal{A}_{\pi d}$ in Eq. (12.2) is dropped. This relation is shown in Fig. 10, see the band named “Deuteron, Beane et al.” In the same Figure we plot the bands which correspond to the a_{0+}^+ and a_{0+}^- , determined from the πH energy shift and width [118]. The combined analysis of the πH and the πD data finally yields the result displayed in Eq. (10.8), see Ref. [132].

We would like to mention that there were additional approximations made in Eq. (12.4). In particular, as already stated, the static approximation for the pion propagator was used, resulting in averages $\langle 1/|\mathbf{q}|^n \rangle_{\text{wf}}$. The possibility of lifting this approximation has been considered in Refs. [47, 137, 272], where it has been demonstrated that different corrections to the static limit largely cancel each other, so that Eq. (12.4) indeed describes the exact result quite accurately. What is important, corrections to the static limit can be calculated perturbatively, because the multiple-scattering series converges in the pion–deuteron case. Further, higher-order contributions (most notably, the so-called dispersive contribution) have been calculated recently and shown to be rather small [133] (for another estimate of the size of this correction in a different setting, see, e.g., Ref. [140]). The boost corrections were recently re-calculated taking into account the explicit Δ -resonance [138]. It has been in particular shown that the inclusion of the Δ -resonance removes the large scale-dependence of the boost correction. However, since our main aim here was to demonstrate the general framework for the numerical analysis of the πD data, we have refrained from including the results of the ongoing work into our final plot shown in Fig. 10. Note also that the error bars in Fig. 10 reflect the uncertainty in the coefficients of Eq. (12.4), but not these additional approximations or the higher-order terms. In other words, we believe that there is still some room left for systematically improving the numerical precision in Eq. (12.4) in the framework with non-perturbative pions.

12.3 Isospin breaking in the πd scattering length

As already mentioned in section 10, the pion–deuteron scattering length, given by Eq. (12.4), is not consistent with new data on pionic hydrogen. Namely, from Fig. 10 one immediately observes that the intersection area for new πH bands moves far away from the πD band. However, the correction terms, which were mentioned in the previous subsection, are too small to be responsible for the large shift of the πD band, which is needed to reconcile the new πH and πD data. Consequently, new mechanisms should be sought that could be a possible source

of large contributions to Eq. (12.4). It should be also understood that the only loophole left in the multiple-scattering series Eq. (12.4) is assuming isospin symmetry. It is therefore interesting to check whether isospin breaking corrections to Eq. (12.4) can bridge the gap with the new hydrogen data [48].

Already in 1977, Weinberg has pointed out [273] that the isospin breaking corrections to certain pion-nucleon scattering amplitudes could become large, if the leading isospin-symmetric contributions to these amplitudes are chirally suppressed. Unfortunately, Weinberg's statement refers to the scattering processes with neutral pions that makes it difficult to verify with present experimental techniques [see, however, footnote 17].

It turns out, however, that this large isospin breaking correction emerges in the quantity $\mathcal{A}_{\pi d}$ as well, since the leading-order term is proportional to the isospin even pion-nucleon scattering length a_{0+}^+ and is thus very small (see Eq. (12.4)). Quite surprisingly, such (a rather obvious) phenomenon has not been explored so far until very recently [48]. Studies of isospin breaking in the πd system (see, e.g., Refs. [126, 134, 140, 274]) include effects coming from the virtual photons at low energy and/or the particle mass differences in the loops. Numerically these effects, which emerge at higher orders in ChPT, indeed turn out to be moderate. However, as it is well known (see section 10), isospin breaking in ChPT at leading order emerges through the direct quark-photon coupling encoded in the LECs f_1, f_2 as well as due to the explicit quark mass dependence of the pion-nucleon amplitudes, which have not been taken into account in these investigations.

Quite obviously, the leading-order isospin breaking correction to the pion-deuteron scattering length is given by (cf. with Eq. (12.3))

$$\text{Re } \Delta \mathcal{A}_{\pi d} = \frac{1 + \eta}{1 + \eta/2} (\delta \mathcal{A}_c + \delta \mathcal{A}_n) + O(p^3), \quad (12.6)$$

where the quantities $\delta \mathcal{A}_c$ and $\delta \mathcal{A}_n$ are defined by Eqs. (10.31) and (10.43), respectively.

In the numerical calculations the same parameters as in section 10 are used. Namely, since the isospin breaking correction for $\mathcal{A}_{\pi d}$ is evaluated at $O(p^2)$ only, for consistency we use the value $c_1 = -0.9_{-0.5}^{+0.2} \text{ GeV}^{-1}$ at order p^2 , see Eq. (10.35). For the same reason, here we have applied $O(p^2)$ isospin breaking corrections everywhere, although for the energy shift $O(p^3)$ result is also known (see section 10).

At the leading order, the isospin breaking correction to the πd scattering length is independent on the deuteron structure and is extremely large

$$\text{Re } \Delta \mathcal{A}_{\pi d} = -(0.0110_{-0.0081}^{+0.0058}) M_\pi^{-1}, \quad (12.7)$$

or, $\text{Re } \Delta \mathcal{A}_{\pi d} / \text{Re } a_{\pi d}^{\text{exp}} = 0.42$ (central values). Plotting again the bands in the (a_{0+}^+, a_{0+}^-) -plane (see Fig. 15), it is seen that the correction in Eq. (12.7) moves the deuteron band in the right direction: the isospin breaking corrections amount for the bulk of the apparent discrepancy between the experimental data on πH and πD in Figure 10.

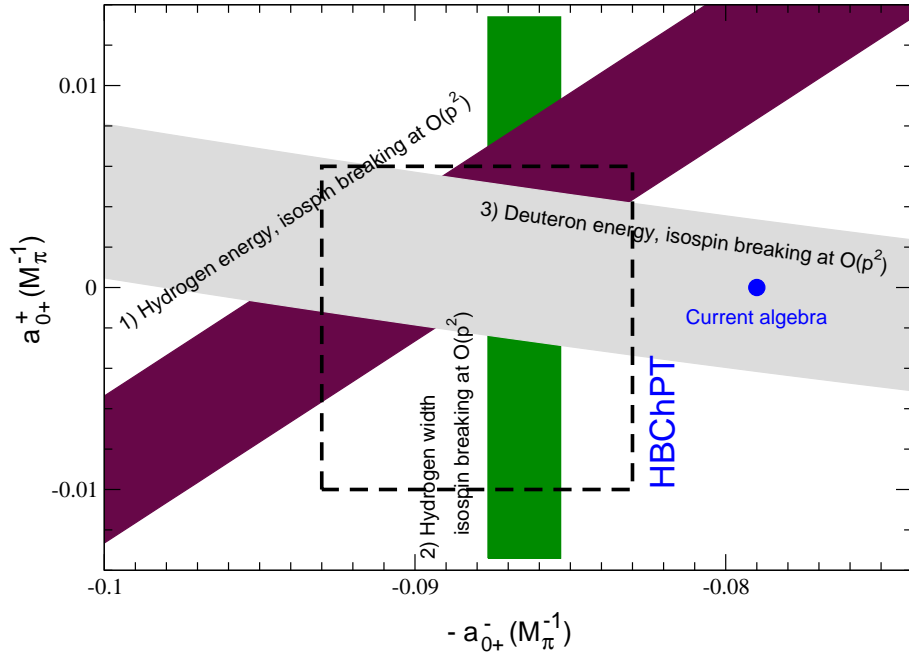


Figure 15: Determination of the πN S -wave scattering lengths a_{0+}^+ and a_{0+}^- from the combined analysis of the experimental data on the πH energy shift and width, as well as the πD energy shift. Isospin breaking corrections have been evaluated in the EFT framework: see Eqs. (10.41), (10.44) and (12.6) for bands 1), 2) and 3), respectively. The filled circle denotes the current algebra prediction [275], and the dashed box corresponds to the $O(p^3)$ calculation in Heavy Baryon ChPT [236]. See main text for more comments.

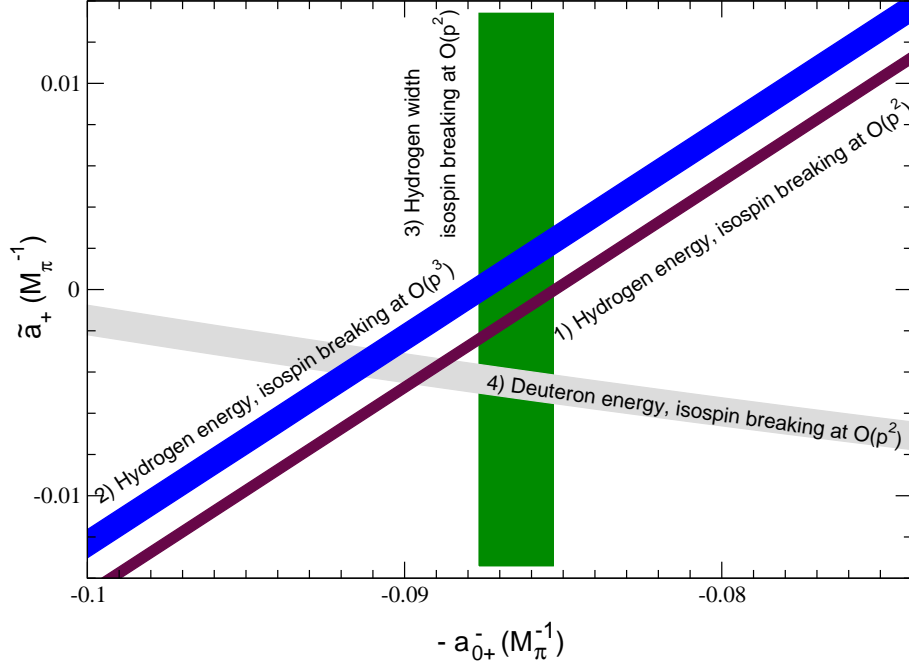


Figure 16: The quantity \tilde{a}_+ defined in Eq. (12.8), plotted against a_{0+}^- , see Ref. [276]. It is seen that, with the isospin breaking corrections evaluated at $O(p^2)$, the three bands 1), 3) and 4) have no common intercept [276]. However, one also concludes that the corrections from higher orders are larger than the uncertainty at $O(p^2)$ coming from the LECs alone. The distance between the bands 1) and 2), corresponding to the same πH energy shift and to the isospin-breaking corrections evaluated at $O(p^2)$ and at $O(p^3)$, respectively, may serve as a rough estimate of the higher-order terms.

It is useful to comment here on the peculiar algebraic structure of these isospin breaking terms, which allows one set up a more convenient framework for the analysis of πH and πD data. First, we note that the widths of the two bands 1) and 3) in Figure 15 are mainly due to the uncertainties in the LECs c_1, f_1 that occur in $\delta\mathcal{A}_{c,n}$. On the other hand, as pointed out in Refs. [48, 276, 277], these two LECs occur in the same combination in the energy shifts of πH and πD at order p^2 in isospin breaking. Introducing the quantity [276]

$$\tilde{a}_+ = a_{0+}^+ + \frac{1}{4\pi(1+\eta)} \left(\frac{4\Delta_\pi}{F_\pi^2} c_1 - 2e^2 f_1 \right), \quad (12.8)$$

the expressions for the energy shifts in πH and πD then contain only \tilde{a}_+ and a_{0+}^- (up to small contributions from the scattering length a_{0+}^+). One may then display the available information in the (\tilde{a}_+, a_{0+}^-) -plane [276], see Figure 16, from where it is seen that the data on πH and πD do not lead to a common intersection²¹.

Taking into account higher order terms in the multiple scattering theory of πD improves the situation [276]. On the other hand, up to now, isospin breaking effects have been taken into account only at $O(p^2)$ in πD , albeit certain contributions are already calculated [133, 274]. We illustrate in Figure 16 that these higher order terms do indeed matter: the blue band displays the band from the energy shift in πH , provided that terms at order p^3 in isospin breaking are taken into account (that band corresponds to the blue band in Figure 10, translated here to the variable \tilde{a}_+). We conclude that a similar investigation for πD is urgently needed. A more complete analysis may then lead to an improved determination of the scattering length a_{0+}^- and of the quantity \tilde{a}_+ , because there is an additional consistency constraint between πH and πD data. On the other hand, the problem with the measurement of a_{0+}^+ persists: unless one finds means to pin down f_1 more reliably, the uncertainty in a_{0+}^+ , which must ultimately be determined from \tilde{a}_+ , is of the order of a_{0+}^+ itself.

For completeness, we now display results of independent analyses of the πH data performed by other groups.

- In Ref. [23] an analysis of the πH data has been performed and the GMO sum rule has been used for a precise determination of the πNN coupling constant. The energy shift and width of πH were taken from Ref. [116] and Ref. [114], respectively, and the isospin breaking corrections

$$\delta'_1 = (-7.2 \pm 2.9) \cdot 10^{-2} \quad [43], \quad \delta_1 = (0.6 \pm 0.2) \cdot 10^{-2} \quad [45] \quad (12.9)$$

have been applied. The final results for the scattering lengths are

$$a_{0+}^+ + a_{0+}^- = 0.0933 \pm 0.0029 M_\pi^{-1}, \quad a_{0+}^- = 0.0888 \pm 0.0040 M_\pi^{-1}. \quad (12.10)$$

²¹This seems to be in contradiction to the common intersection of the bands 1) and 3) in Fig. 15. However, that intersection corresponds to a different choice of the LECs in the πH and πD energy shifts, and signals an apparent consistency only [278].

- In the second work of Ref. [118], the isospin breaking corrections from Eq. (12.9) have been applied to the recently measured values of the energy shift and width given in Eq. (2.8). The result is

$$a_{0+}^+ = 0.0069 \pm 0.0031 M_\pi^{-1}, \quad a_{0+}^- = 0.0864 \pm 0.0012 M_\pi^{-1}. \quad (12.11)$$

12.4 Kaon-deuteron scattering

It is expected that the forthcoming measurement of the (complex) energy shift of $\bar{K}D$ by the SIDDHARTA collaboration at DAΦNE [154, 155] enables one to extract – in combination with $\bar{K}H$ data – independently both S -wave $\bar{K}N$ scattering lengths a_0 and a_1 . We show in this subsection that this indeed appears to be a feasible task.

We start with the kaon–deuteron threshold amplitude $\mathcal{A}_{\bar{K}d}$, which is extracted from the analysis of $\bar{K}D$ data. This amplitude must be “unfolded” in terms of elementary $\bar{K}N$ scattering lengths, via multiple–scattering theory. Because the multiple–scattering series for the kaon–deuteron scattering length is likely not to converge at all, a re–summation is needed. A detailed investigation of the problem within an EFT framework has been carried out recently in Refs. [49, 279], see also Ref. [280] for a treatment of the same problem in potential scattering theory. The multiple–scattering series has been re–summed in Refs. [49, 279] to all orders, assuming that the nucleons are static (this is also referred to as Fixed Centers Approximation (FCA)), and neglecting derivative $\bar{K}N$ interactions. The resulting expression is given by

$$\left(1 + \frac{M_K}{M_d}\right) \mathcal{A}_{\bar{K}d} = \int_0^\infty dr (u^2(r) + w^2(r)) \hat{\mathcal{A}}_{\bar{K}d}(r), \quad (12.12)$$

where $u(r)$ and $w(r)$ denote the usual S - and D -wave components of the deuteron wave function, which are normalized via the condition $\int_0^\infty dr (u^2(r) + w^2(r)) = 1$. The NLO wave functions in the theory with non–perturbative pions [141, 281] have been used in the calculations [49]. Furthermore,

$$\hat{\mathcal{A}}_{\bar{K}d}(r) = \frac{\tilde{\mathcal{A}}_c + \tilde{\mathcal{A}}_n + (2\tilde{\mathcal{A}}_c\tilde{\mathcal{A}}_n - \mathcal{B}_x^2)/r - 2\mathcal{B}_x^2\tilde{\mathcal{A}}_n/r^2}{1 - \tilde{\mathcal{A}}_c\tilde{\mathcal{A}}_n/r^2 + \mathcal{B}_x^2\tilde{\mathcal{A}}_n/r^3} + \delta\hat{\mathcal{A}}_{\bar{K}d}, \quad (12.13)$$

with $\mathcal{B}_x^2 = \tilde{\mathcal{A}}_x^2/(1 + \tilde{\mathcal{A}}_0/r)$, and

$$\left(1 + \frac{M_K}{m_p}\right) \mathcal{A}_{c,n,x,0} = \tilde{\mathcal{A}}_{c,n,x,0}, \quad (12.14)$$

where $\mathcal{A}_{c,n,x,0}$ denote the threshold scattering amplitudes for $K^-p \rightarrow K^-p$, $K^-n \rightarrow K^-n$, $K^-p \rightarrow \bar{K}^0n$ and $\bar{K}^0n \rightarrow \bar{K}^0n$, respectively, see appendix A. Retaining only the leading isospin breaking effects which are due to the unitary

cusps, these amplitudes can be expressed through the scattering lengths a_0 and a_1 (cf. with Eq. (11.2)),

$$\begin{aligned}\mathcal{A}_c &= \frac{\frac{1}{2}(a_0 + a_1) + q_0 a_0 a_1}{1 + \frac{q_0}{2}(a_0 + a_1)} + \dots, & \mathcal{A}_n &= a_1 + \dots, \\ \mathcal{A}_x &= \frac{\frac{1}{2}(a_0 - a_1)}{1 - \frac{iq_c}{2}(a_0 + a_1)} + \dots, & \mathcal{A}_0 &= \frac{\frac{1}{2}(a_0 + a_1) - iq_c a_0 a_1}{1 - \frac{iq_c}{2}(a_0 + a_1)} + \dots,\end{aligned}\tag{12.15}$$

where

$$\begin{aligned}q_c &= \sqrt{2\mu_c \Delta}, & q_0 &= \sqrt{2\mu_0 \Delta}, & \Delta &= m_n + M_{\bar{K}^0} - m_p - M_K, \\ \mu_c &= \frac{m_p M_K}{m_p + M_K}, & \mu_0 &= \frac{m_n M_{\bar{K}^0}}{m_n + M_{\bar{K}^0}}.\end{aligned}\tag{12.16}$$

The isospin limit corresponds to $q_c = q_0 = 0$ ²². Finally, the quantity $\delta\hat{\mathcal{A}}_{\bar{K}d}$ contains the 6-particle non-derivative LEC, which describes interaction of the kaon with two nucleons. A dimensional estimate yields a few percent systematic uncertainty due to the presence of this LEC [49]. In the numerical results, which are displayed below, this term is neglected completely.

Remark: We comment on an important difference between the kaon-deuteron and pion-deuteron scattering in this respect. In the case of pion-deuteron scattering, a formula similar to Eq. (12.13) can be derived, see, e.g., Ref. [126]. The πN threshold amplitudes that enter the expression are real, up to small isospin breaking effects. On the other hand, due e.g. to the process $\pi d \rightarrow nn$, the imaginary part of the corresponding correction $\delta\hat{\mathcal{A}}_{\pi d}$ does not vanish in the isospin symmetry limit. It is, therefore, expected to dominate the contributions from the first part, as a result of which the imaginary part of the pion-deuteron scattering amplitude at threshold cannot provide information on the πN scattering lengths. In contrast to this, the imaginary parts of the $\bar{K}N$ amplitudes in Eq. (12.13) are of order one. As just mentioned, it is expected that $\delta\hat{\mathcal{A}}_{\bar{K}d}$ is small as compared to the first term, and is neglected here. This explains why kaonic deuterium does provide information on the imaginary part of the scattering lengths, while pionic deuterium does not. For an investigation of this issue in the framework of a potential model, see Ref. [269].) End of remark

²²Here, we identify $\mathcal{A}_{c,n,x,0}$ in Eqs. (12.13) and (12.14) with the $\bar{K}N$ amplitudes evaluated at the pertinent physical thresholds. In the language of non-relativistic EFT, this amounts to neglecting diagrams which describe rescattering of \bar{K} on the same nucleon. Including the rescattering contributions leads to the replacement of $\mathcal{A}_{x,0}$ by the amplitudes evaluated at $s = (M_K + m_p)^2$ instead of $s = (M_{\bar{K}^0} + m_n)^2$. In addition, in the static approximation the mass difference Δ is neglected in the neutral kaon propagator (for comparison, see also Refs. [269, 280], where the problem has been addressed within the framework of a potential model). Numerically, the effect may not be negligible. However, following Ref. [49], we do not take it into account at this point.

We would like to emphasize that, in order to reduce the systematic error on the calculated kaon–deuteron scattering length, it would be very important to extend the calculations beyond the lowest–order formula Eq. (12.12) by using the non–relativistic Lagrangian method of Ref. [49]. In particular, it would be interesting to estimate the effect of lifting FCA, as well as to evaluate the contribution of the D -waves (derivative interactions). The comparison with the Faddeev approach indicates that these corrections may not be negligible (see, e.g., Ref. [264, 269]).

The main goal of the DEAR/SIDDHARTA experiment is to determine individual $\bar{K}N$ scattering lengths a_0 and a_1 from the analysis of combined $\bar{K}H$ and $\bar{K}D$ data. Since the experimental results on the $\bar{K}D$ are still absent, in Ref. [49] such an analysis has been carried out, using synthetic input $\bar{K}D$ data. The procedure can be schematically described as follows. From Eq. (11.7) one determines one of the scattering lengths, say a_1 . Substituting this expression into Eqs. (12.12), (12.13) and (12.15), one arrives at a non–linear equation for determining a_0 with a given input value of $\mathcal{A}_{\bar{K}d}$.

The numerical solution of the above equation, carried out in Ref. [49], leads to an interesting conclusion. It turns out that unitarity and input DEAR data for $\bar{K}H$ impose severe constraints on the possible input values of $\mathcal{A}_{\bar{K}d}$, for which the solutions for the $\bar{K}N$ scattering lengths with $\text{Im } a_I \geq 0$ do exist. The allowed region in the $(\text{Re } \mathcal{A}_{\bar{K}d}, \text{Im } \mathcal{A}_{\bar{K}d})$ -plane is shown Fig. 17. It also turns out that the allowed values for $\mathcal{A}_{\bar{K}d}$ qualitatively agree with the value of the \bar{K}^0d scattering length extracted from the $pp \rightarrow d\bar{K}^0K^+$ reaction [282]. Finally, we note that the region where solutions do exist is much larger in the case of the KpX input [153], than for the DEAR input of kaonic hydrogen [49].

The message of the investigation carried out in Ref. [49] is very clear: the combined analysis of DEAR/SIDDHARTA data on $\bar{K}H$ and $\bar{K}D$ is more restrictive than one would *a priori* expect. Moreover, if the corrections to the lowest–order approximate result (going beyond FCA and including derivative couplings) are moderate, they will not change the qualitative picture shown in Fig. 17. On the other hand, they constitute the largest potential source of theoretical uncertainty at present.

We conclude with the expectation that the combined analysis of the forthcoming high–precision data from DEAR/SIDDHARTA collaboration on $\bar{K}H$ and deuterium will enable one to perform a stringent test of the framework used to describe low–energy kaon–deuteron scattering, as well as to extract the values of a_0 and a_1 with reasonable accuracy. On the other hand, a considerable amount of theoretical work – related to a systematic calculation of higher–order corrections – is still to be carried out before this goal is reached.

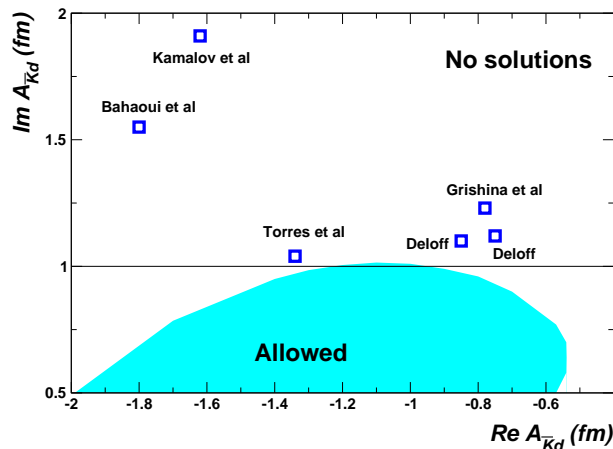


Figure 17: The region in the $(\text{Re } \mathcal{A}_{\bar{K}d}, \text{Im } \mathcal{A}_{\bar{K}d})$ -plane where solutions for a_0 and a_1 do exist. NLO wave functions [141, 281] with the cutoff parameter $\Lambda = 600$ MeV have been used in the calculations (for $\Lambda = 450$ MeV, the result changes insignificantly). For comparison, we also show the results of various calculations of $\mathcal{A}_{\bar{K}d}$ [266, 267, 269, 283] (squares). As we see, none of the calculated scattering lengths is located in the shaded area. The figure is the same as in Ref. [49].

13 Potential scattering theory

In this section, we provide a condensed version of our view of the relation between EFT and potential model calculations.

Many calculations of various hadronic atom properties were carried out within the framework of potential scattering theory since the seminal work of Deser et al. [8]. Potential model calculations (see, e.g., Refs. [22, 66–68, 122–124, 126, 127, 191, 229–231, 265–269, 284–300]) were basically the only theoretical setting to address the issue until rather recently, when methods of (effective) QFT came in use to tackle the problem. Already the very first example investigated in this new framework – the lifetime of the ground state of ponium – revealed a qualitative difference of the two approaches: A major contribution of the so-called isospin breaking corrections to the energy-level shift turned out to be of opposite sign in the two approaches (cf. Ref. [290] and Refs. [25, 30]). As mentioned in section 10, similar discrepancies were later found in the calculation of the energy shift in πH (Ref. [230] and Refs. [41, 43]), see also the recent work Ref. [231]. These isospin breaking corrections are of the order of the envisaged experimental accuracy, and it is therefore important to reveal the reason for the difference. This section is devoted to a clarification of this point.

We find it most instructive to illustrate the two approaches in the case of the strong energy shift of πH . We display three expressions for the energy shift in

the ground state, in chronological order:

$$\Delta E_1^{\text{str}} = \begin{cases} N \operatorname{Re} \mathcal{T} & (a) \\ N \operatorname{Re} \hat{\mathcal{T}} \left\{ 1 + \beta_1 \frac{\operatorname{Re} \hat{\mathcal{T}}}{r_B} + O(r_B^{-2}) \right\} & (b) \\ N \operatorname{Re} \mathcal{T}_c \left\{ 1 - \frac{\mu_c^2 \alpha}{4\pi m_p M_\pi} (\ln \alpha - 1) \operatorname{Re} \mathcal{T}_c \right\} + o(\delta^4) & (c) \end{cases}$$

$$N = -\frac{\alpha^3 \mu_c^3}{4\pi m_p M_\pi}.$$

The amplitudes \mathcal{T} , $\hat{\mathcal{T}}$ and \mathcal{T}_c stand for the elastic $\pi^- p \rightarrow \pi^- p$ amplitude at threshold, in specific settings. The formulae (a), (b) and (c) were derived by Deser et al. [8], by Trueman [191] (properly adapted here), and by Lyubovitskij and Rusetsky [41], respectively. The first two are potential model ones, whereas the last one uses the EFT framework advocated in this report²³. We now discuss these expressions in turn, and start with (a). Here, \mathcal{T} is the elastic scattering amplitude in the absence of Coulomb interaction. Additional terms on the right hand side of this relation were not considered in Ref. [8]. The second relation corresponds to an expansion in powers of $\hat{\mathcal{T}}/r_B$, where $\hat{\mathcal{T}}$ is evaluated in the presence of the Coulomb interaction. The coefficient β_1 depends on the dimensionless ratio r_0/r_B , where $r_0(r_B)$ stands for the effective range (Bohr radius). In order to compare these two formulae, one needs to know the relation between the amplitudes \mathcal{T} and $\hat{\mathcal{T}}$. In Ref. [191], the relation [301]

$$\operatorname{Re} \hat{\mathcal{T}} = \operatorname{Re} \mathcal{T} \left\{ 1 - \frac{\mu_c^2 \alpha \ln \alpha}{4\pi m_p M_\pi} \operatorname{Re} \mathcal{T} + O(\alpha) \right\} \quad (13.1)$$

was invoked, which indicates that (a) is a first order approximation of (b), in the sense of the expansion performed in (b).

We now come to the relation displayed in (c), worked out in Ref. [41], see also section 10. Optically, the relation is similar to (a), (b). However, as is worked out at length in this report, (c) is based on a very general framework: quantum field theory. This framework allows one to include in a systematic manner strong and electromagnetic interactions. The amplitude \mathcal{T}_c is of the form

$$\operatorname{Re} \mathcal{T}_c = 8\pi(m_p + M_\pi) (a_{0+}^+ + a_{0+}^-) + \alpha F_1 + (m_d - m_u) F_2 + o(\delta), \quad (13.2)$$

where the first term on the right hand side is a particular combination of πN scattering lengths, and where the coefficients $F_{1,2}$ depend on the underlying theory. In this report, this is taken to be QCD+QED, and the corrections encoded

²³As mentioned, there were very many potential model calculations over the last four decades, improving (b) in several respects. However, the basic difference between these approaches and EFT remained untouched. For this reason, we stick to the evaluation by Trueman for simplicity.

by $F_{1,2}$ stand for the so-called short-distance electromagnetic contributions to the scattering amplitude. The quantities $F_{1,2}$ can be calculated in ChPT, in an expansion in the quark masses $m_u = m_d$, in terms of a well-defined set of LECs.

It is at this stage that the EFT framework and the potential model calculations differ: EFT allow one to provide a direct contact between the measured energy shifts and the calculated scattering lengths in QCD. For more details on the relation between the EFT and potential model framework, we refer the interested reader to Ref. [302]. In this reference, it is proved that the relation between the strong energy shift in the form (c) also holds in potential scattering, a property that goes under the name *universality*. Universality clearly shows that it is not the use of the potential framework that causes discrepancies with the EFT approach, but the choice of the short-range potential, which must include isospin breaking effects properly.

In our opinion, for the reasons just outlined, potential model calculations are superseded by EFT methods in the case of simple systems like $A_{2\pi}$, $A_{\pi K}$, πH and $\bar{K}H$. On the other hand, in more complicated systems like πD and $\bar{K}D$, the results of calculations performed within potential models may still be useful as a hint about the expected magnitude of different contributions. However, in order to avoid an uncontrollable systematic error, one would have to address the same calculations within the framework of low-energy effective theories of QCD as well.

14 Summary and outlook

In recent years, a general theory of hadronic atoms has been developed, as is outlined in this review. It relies in an essential manner on effective field theories: ChPT, which describes the interactions of hadrons and photons at low energy, and non-relativistic effective QFT, that are used to describe hadronic bound states. It turns out that the treatment of any hadronic bound system is pretty universal within this theory (i.e., independent of any details characterizing the constituents) and can be carried out with a surprising ease. The approach is *systematic*: the terms that are neglected count at higher orders in a power-counting scheme as compared to the ones that are retained. Another important feature of the present approach is the fact that the needed effective field theories are built on top of QCD+QED by successively integrating out various high-energy scales. Consequently, calculating observables of a hadronic bound state within this approach, one ends up with a quantity that is evaluated in the fundamental theory of strong and electromagnetic interactions.

The theory of hadronic atoms presented here merges several fields of theoretical physics. As already pointed out, it heavily relies on ChPT and on non-relativistic effective field theories. Presently, the attention is shifted to hadronic atoms containing the deuteron or other (light as well as heavy) nuclei. As a result of this, methods of few-body physics and in-medium properties of hadrons are

needed in addition.

We believe that the conceptual problems of a theory of hadronic atoms have now been clarified to a large extent. In this review, we have described several specific applications. There is, however, still room left for future investigations on the subject. We have collected in Table 9 our view of the status of the *theoretical description* of the various hadronic compounds. The first column in the Table displays the system under consideration, and the second one contains the status of the relation between the energy spectra and the pertinent scattering amplitudes. The third column displays information about the relation between the hadronic amplitudes and the various scattering lengths, whereas the last one refers to keywords related to the underlying physics.

The main points displayed in the Table are the following.

- i) A precise calculation of isospin breaking corrections in pionic hydrogen energy shift and width should be performed. This implies calculations done solely in ChPT, in analogy with Ref. [43]. In particular, it would be useful to evaluate the charge-exchange amplitude at $O(p^3)$ (for the width) and, possibly, at $O(p^4)$ for both π^-p elastic and charge-exchange amplitudes (energy shift and width).
- ii) Using the results of these calculations, the analysis of the πH data should be done anew. In particular, it would be very interesting to update the value of a_{0+}^+ and of the pion-nucleon σ -term.
- iii) In πK scattering, the structure of higher order ChPT contributions [105] remains to be understood in view of the low-energy theorem Eq. (2.7). An issue still to be investigated is the relation between the large/small $SU(3)$ quark condensate scenario, and the pertinent scattering lengths.
- iv) A substantial progress in the precise quantitative description of pion-deuteron scattering in the chiral EFT would be extremely desirable. This implies systematic calculations of various higher-order correction terms, including both, isospin conserving [Eq. (12.4)] and isospin breaking [Eq. (12.6)] contributions, see e.g. Ref. [133].
- v) We believe that $\bar{K}H$ and $\bar{K}D$, which will be investigated by the SIDDHARTA experiment at DAΦNE [154, 155], represent the most challenging theoretical task at present. Many issues should be addressed in this context. For example, one has to gain a deeper insight into the incompatibility of the DEAR and scattering data. Is it possible to fit all data by using unitarized ChPT? What kind of additional experimental input could help to critically constrain the parameters of a fit?
- vi) Still in connection with the SIDDHARTA experiment, it would be a major breakthrough to present a systematic EFT calculation of the kaon-deuteron

	$(\Delta E, \Gamma) \rightarrow \mathcal{T}$	$\mathcal{T} \rightarrow a$	Underlying physics
$A_{2\pi}$	perfect	perfect	<ul style="list-style-type: none"> · $\pi\pi$ scatt. lengths · large/small quark condensate
$A_{\pi K}$	perfect	perfect	<ul style="list-style-type: none"> · πK scatt. lengths · large/small $SU(3)$ quark condensate
πH	perfect	<ul style="list-style-type: none"> · large uncertainty (LECs) · to be done: $O(p^4)$ in energy shift $O(p^3), O(p^4)$ in the width 	<ul style="list-style-type: none"> · πN scatt. lengths · πN σ-term · pion–nucleon coupling constant
$\bar{K}H$	reasonably good	<ul style="list-style-type: none"> · $O(\sqrt{\delta}), O(\delta \ln \delta)$: done · $O(\delta)$ (tree level): done · $O(\delta)$ (loops): unrealistic 	<ul style="list-style-type: none"> · $\bar{K}N$ scatt. lengths · unitarized ChPT
πD	good	<p><i>isospin conserving sector:</i> in good shape [still in progress]</p> <p><i>isospin breaking sector:</i> leading order: done (huge) higher orders: partly done/ in progress</p>	<ul style="list-style-type: none"> · πN scatt. lengths · EFT in $2N$ sector · 3-body calculations in EFT · fixing LECs
$\bar{K}D$	satisfactory	<p><i>isospin conserving sector:</i> nonder. coupling, stat. approx.: done deriv. coupling: to be done</p> <p><i>isospin breaking sector:</i> lead. order: to be completed higher orders: unrealistic</p>	<ul style="list-style-type: none"> · $\bar{K}N$ scatt. lengths · unitarized ChPT · EFT in the $2N$ sector · 3-body calculations in EFT

Table 9: Status of the theoretical description of various hadronic compounds, ordered according to increasing complexity. The first column displays the system, the second the relation between the spectrum and the scattering amplitude \mathcal{T} , the third column concerns the relation between the scattering amplitude \mathcal{T} and the scattering lengths, and the last column displays issues of the underlying physics.

scattering length in terms of the threshold parameters of the $\bar{K}N$ interaction beyond the approximations used in Refs. [49, 279].

On the *experimental side*, very precise data on πH are underway [118]. The DIRAC collaboration has improved on the uncertainty of the lifetime measurement of pionium, see Ref. [81], and an update of the central value of $a_0 - a_2$ is anxiously awaited. A successful measurement of individual scattering lengths via excited states, and πK scattering lengths, would be extremely welcome. We are looking forward to precise data on $\bar{K}H$ and $\bar{K}D$ from SIDDHARTA. In conclusion, there are exciting times ahead on the experimental side.

Acknowledgments: We thank W. Weise for inviting us to write this report. We are grateful for discussions and/or comments on the manuscript to V. Baru, B. Borasoy, C. Curceanu-Petrascu, E. Epelbaum, T. Ericson, A. Gal, D. Gotta, C. Guaraldo, H.-W. Hammer, Ch. Hanhart, A.N. Ivanov, M.A. Ivanov, S. Karshenboim, A. Kudryavtsev, H. Leutwyler, V. E. Markushin, J. Marton, E. Matisinos, Ulf-G. Meißner, L. Nemenov, G. Rasche, J. Schacher, L. Simons, D. Trautmann. Partial financial support from the EU Integrated Infrastructure Initiative Hadron Physics Project (contract number RII3-CT-2004-506078) and DFG (SFB/TR 16, “Subnuclear Structure of Matter”) and from the Swiss National Science Foundation is gratefully acknowledged. This research is also part of the project supported by the DFG under contracts FA67/31-1, GRK683, President grant of Russia “Scientific Schools” No. 5103.2006.2, and by the EU Contract No. MRTN-CT-2006-035482 “FLAVIANet”. One of us (J.G.) is grateful to the Alexander von Humboldt-Stiftung and to the Helmholtz-Gemeinschaft for the award of a prize that allowed him to stay at the HISKP at the University of Bonn, where part of this work was performed. He also thanks the HISKP for the warm hospitality during these stays.

A Notation

In this appendix, we collect some of the notation used.

A.1 General

The following Coulombic bound states are considered:

$$\text{Scalar QED} / \pi^+\pi^- / \pi^\mp K^\pm / \pi^-p / K^-p / \pi^-d / K^-d .$$

In all these cases, at least one of the particles has spin zero. We always attach the label 1 to the particle with non-zero spin (if present). The masses of the particles are denoted by m_1 and m_2 . We further define

$$\Sigma_+ = m_1 + m_2, \quad \mu_c = \frac{m_1 m_2}{\Sigma_+}, \quad \eta_{1,2} = \frac{m_{1,2}}{\Sigma_+}, \quad (\text{A.1})$$

where Σ_+ and μ_c denote the full mass and the reduced mass of a system of two particles, respectively.

A.2 Coulombic bound states

For Coulomb bound states, we use

$$\begin{aligned} E_n &= \Sigma_+ - \frac{\mu_c \alpha^2}{2n^2}, & \gamma_n &= \frac{\gamma}{n}, & \gamma &= \alpha \mu_c, & r_B &= \gamma^{-1}, \\ \alpha^{-1} &= 137.036, \end{aligned} \quad (\text{A.2})$$

where E_n stand for the unperturbed Coulomb energies and r_B is the Bohr radius for a given state. Further, in the case of the two spin-0 particles, the bound-state obeys the Schrödinger equation

$$(\mathbf{H}_0 + \mathbf{H}_C)|\Psi_{nlm}(\mathbf{P})\rangle = \left(E_n + \frac{\mathbf{P}^2}{2\Sigma_+} \right) |\Psi_{nlm}(\mathbf{P})\rangle, \quad (\text{A.3})$$

with the wave function given by

$$\begin{aligned} |\Psi_{nlm}(\mathbf{P})\rangle &= \int \frac{d^3\mathbf{q}}{(2\pi)^3} \Psi_{nlm}(\mathbf{q}) |\mathbf{P}, \mathbf{q}\rangle, \\ |\mathbf{P}, \mathbf{q}\rangle &= a_1^\dagger(\eta_1\mathbf{P} + \mathbf{q}) a_2^\dagger(\eta_2\mathbf{P} - \mathbf{q}) |0\rangle. \end{aligned} \quad (\text{A.4})$$

The same formulae in case of a particle with spin is

$$(\mathbf{H}_0 + \mathbf{H}_C)|\Psi_{nljm}(\mathbf{P})\rangle = \left(E_n + \frac{\mathbf{P}^2}{2\Sigma_+} \right) |\Psi_{nljm}(\mathbf{P})\rangle, \quad (\text{A.5})$$

and

$$|\Psi_{nljm}(\mathbf{P})\rangle = \sum_{\sigma} \int \frac{d^3\mathbf{q}}{(2\pi)^3} \langle jm|l(m-\sigma)s\sigma\rangle \Psi_{nl(m-\sigma)}(\mathbf{q}) |\mathbf{P}, \mathbf{q}, \sigma\rangle, \\ |\mathbf{P}, \mathbf{q}, \sigma\rangle = b_1^{\dagger}(\eta_1\mathbf{P} + \mathbf{q}, \sigma) a_2^{\dagger}(\eta_2\mathbf{P} - \mathbf{q}) |0\rangle. \quad (\text{A.6})$$

In the above formulae, $a_{1,2}^{\dagger}$ and b_1^{\dagger} denote creation operators of particles without and with spin.

The wave functions $\Psi_{nlm}(\mathbf{q})$ are the Fourier transform of standard Coulomb wave functions $\tilde{\Psi}_{nlm}(\mathbf{x})$ in coordinate space,

$$\Psi_{nlm}(\mathbf{q}) = \int d^3\mathbf{x} e^{-i\mathbf{q}\mathbf{x}} \tilde{\Psi}_{nlm}(\mathbf{x}). \quad (\text{A.7})$$

The normalization is

$$\int d^3\mathbf{x} |\tilde{\Psi}_{nlm}(\mathbf{x})|^2 = 1, \quad \int \frac{d^3\mathbf{q}}{(2\pi)^3} |\Psi_{nlm}(\mathbf{q})|^2 = 1. \quad (\text{A.8})$$

Explicitly [303],

$$\Psi_{nlm}(\mathbf{q}) = \frac{N_{nlm} |\mathbf{q}|^l}{[\mathbf{q}^2 + \gamma_n^2]^{l+2}} C_{n-l-1}^{l+1} \left(\frac{\mathbf{q}^2 - \gamma_n^2}{\mathbf{q}^2 + \gamma_n^2} \right) Y_l^m(\theta, \varphi), \quad (\text{A.9})$$

where $C_n^m(x)$ are Gegenbauer polynomials, with generating function

$$(1 - 2xs + s^2)^{-m} = \sum_{n=0}^{\infty} C_n^m(x) s^n, \quad (\text{A.10})$$

and N_{nlm} are normalization constants, chosen in conformity with Eq. (A.8). From this representation,

$$\Psi_{nlm}(\mathbf{q}) \sim \begin{cases} |\mathbf{q}|^l, & |\mathbf{q}| \rightarrow 0 \\ |\mathbf{q}|^{-4-l}, & |\mathbf{q}| \rightarrow \infty \end{cases}. \quad (\text{A.11})$$

The ground-state wave function is

$$\Psi_{100}(\mathbf{q}) = \frac{(64\pi\gamma^5)^{1/2}}{(\mathbf{q}^2 + \gamma^2)^2}. \quad (\text{A.12})$$

Due to rotational symmetry, the corrections to the energy levels, which are calculated with the use of the above wave functions, do not depend on the index m . Therefore, we use everywhere $m = 0$ and introduce the shorthand notation

$$\Psi_{nl}(\mathbf{q}) = \Psi_{nl0}(\mathbf{q}), \quad \tilde{\Psi}_{nl}(\mathbf{x}) = \tilde{\Psi}_{nl0}(\mathbf{x}). \quad (\text{A.13})$$

We often need the wave function at the origin,

$$|\tilde{\Psi}_{n0}(0)|^2 = \frac{\alpha^3 \mu_c^3}{\pi n^3}. \quad (\text{A.14})$$

In the bound-state calculations we use the notation

$$s_n(\alpha) = 2(\psi(n) - \psi(1) - \frac{1}{n} + \ln \alpha - \ln n), \quad \psi(x) = \Gamma'(x)/\Gamma(x). \quad (\text{A.15})$$

A.3 Master equation

When only the Coulomb interactions are present, the resolvent $(z - \mathbf{H})^{-1}$ is meromorphic in the complex z -plane, cut along the positive real axis above the elastic threshold. The poles are located at $z = E_n$. If other interactions are turned on, the bound-state poles are shifted from their pure Coulomb values into the complex plane. The degeneracy of the energy eigenvalues is lifted as well. The (complex) energy shift is given by

$$\Delta E_{nlj} = z_{nlj} - E_n = (\Psi_{nlj} | \bar{\tau}^{nlj}(E_n) | \Psi_{nlj}) + o(\delta^4), \quad (\text{A.16})$$

where the matrix element is calculated between unperturbed Coulomb wave functions and does not depend on the quantum number m . Further, z_{nlj} denotes the new position of the pole, which was shifted from its original position at E_n and the pole-subtracted amplitude $\bar{\tau}^{nlj}(z)$ is defined by Eq. (10.17). In order to simplify notations, we often do not attach explicit indexes nlj to the pole position in the text. In the case of two spin-0 particles, the index j must be suppressed. In the main text, we refer to equation (A.16) as *master equation*.

A.4 Energy shift of the atom

The energy shift is further split into the electromagnetic and strong pieces, as well as the term corresponding to the vacuum polarization (whenever electrons are present)

$$\Delta E_{nlj} = \Delta E_{nlj}^{\text{em}} + \Delta E_{nl}^{\text{vac}} + \delta_{l0} \left(\Delta E_n^{\text{str}} - \frac{i}{2} \Gamma_n \right) + o(\delta^4). \quad (\text{A.17})$$

(If both particles have spin 0, the above formulae are modified by merely discarding the index j). The first term in this expression is given by Eq. (8.2), Eq. (9.6) or Eq. (10.19), for the case of $\pi^+ \pi^-$, $\pi^\mp K^\pm$ and $\pi^- p$ atoms, respectively. The second term, which corresponds to the vacuum polarization contribution, in the case of the spin-0 particles is given by Eq. (5.41) and its generalization to the case of particles with spin is straightforward. Namely, this contribution does not depend on the total momentum j . Further, at the order in isospin breaking parameter δ we are working, only the S -wave strong shift should be taken into account. The

strong shift in higher partial waves is suppressed by additional powers of δ and does not contribute at this order.

Further, note that if the splitting between the energy levels with the same orbital momentum l is tiny, it is convenient to define the averaged level energies

$$\Delta E_{nl} = \mathcal{N}_\ell^{-1} \sum_{j=|l-s|}^{l+s} (2j+1) \Delta E_{nlj}, \quad \mathcal{N}_\ell = \sum_{j=|l-s|}^{l+s} (2j+1). \quad (\text{A.18})$$

When one speaks, e.g., about the energy of $1s$ or $3p$ levels in πH , this average is meant.

A.5 Threshold amplitude

Let us now consider the definition of the threshold amplitude. The scattering amplitude for the process $1 + 2 \rightarrow 3 + 4$ is given by (the trivial term without interaction is omitted)

$$\langle p_1 \sigma', p_2; out | q_1 \sigma, q_2; in \rangle = i(2\pi)^4 \delta^4(p_1 + p_2 - q_1 - q_2) T_{\sigma' \sigma}(p_1, p_2; q_1, q_2). \quad (\text{A.19})$$

The above amplitude describes the scattering in the channel with oppositely charged particles, as well as in other channels (e.g. in the “neutral” channel). The Condon–Shortley–de Swart phase convention is used. If there are no particles with spin, the indexes σ', σ should be dropped.

At the order we are working, it suffices to evaluate the scattering amplitude Eq. (A.19) at order α . Starting from Eq. (A.19), one arrives at the threshold amplitude as a result of the following procedure. In a first step, the one–photon exchange piece is subtracted in the elastic scattering amplitude of two oppositely charged particles,

$$\bar{T}_{\sigma' \sigma}(p_1, p_2; q_1, q_2) = T_{\sigma' \sigma}(p_1, p_2; q_1, q_2) + \Gamma_{\sigma' \sigma}^\mu(p_1, q_1) \frac{e^2 g_{\mu\nu}}{t} \Gamma^\nu(p_2, q_2), \quad (\text{A.20})$$

where $t = (p_1 - q_1)^2 = (p_2 - q_2)^2$, and $\Gamma_{\sigma' \sigma}^\mu(p_1, q_1)$ and $\Gamma^\nu(p_2, q_2)$ denote the electromagnetic current matrix elements of particles 1 and 2, respectively (if the particle 1 has no spin, the $\Gamma_{\sigma' \sigma}^\mu(p_1, q_1)$ is replaced by $\Gamma^\mu(p_1, q_1)$). This procedure is demonstrated in Fig. A.1. In the inelastic channels, there is no one–photon exchange diagram and $\bar{T}_{\sigma' \sigma} = T_{\sigma' \sigma}$. Moreover, it is not needed to remove the one–photon piece in the elastic scattering amplitude with at least one neutral particle as well, because the pertinent contribution to the spin–nonflip amplitude is not singular at threshold.

We now list the decomposition of the matrix elements $\Gamma_{\sigma' \sigma}^\mu(p_1, q_1)$.

i) Spin 0 (pion, kaon)

$$\Gamma^\mu(p, q) = (p + q)^\mu F(Q^2), \quad Q = p - q; \quad F(0) = 1. \quad (\text{A.21})$$

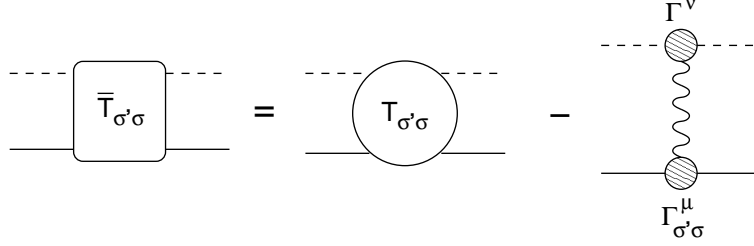


Figure A.1: Subtraction of the one–photon exchange diagram, see Eq. (A.20).

ii) Spin $\frac{1}{2}$ (proton)

$$\Gamma_{\sigma'\sigma}^{\mu}(p, q) = \bar{u}(p, \sigma') \left(\gamma^{\mu} F_1(Q^2) + i\sigma^{\mu\nu} Q_{\nu} \frac{F_2(Q^2)}{2m_p} \right) u(q, \sigma), \quad (\text{A.22})$$

$$F_1(0) = 1, \quad F_2(0) = \kappa_p, \quad (\text{A.23})$$

where F_1 and F_2 denote the Dirac and Pauli form factors, respectively, and κ_p is the anomalous magnetic moment

iii) Spin–1 (deuteron)

The decomposition is given, e.g., in Refs. [304, 305].

In the next step, we define the spin–nonflip amplitude by averaging over spins

$$\bar{T}(p_1, p_2; q_1, q_2) = \frac{1}{2s+1} \sum_{\sigma} \bar{T}_{\sigma\sigma}(p_1, p_2; q_1, q_2). \quad (\text{A.24})$$

At the final step, we go to the two particle CM frame, defined by $\mathbf{p}_1 = -\mathbf{p}_2 = \mathbf{p}$ and $\mathbf{q}_1 = -\mathbf{q}_2 = \mathbf{q}$, and remove the Coulomb phase from the (dimensionally regularized) spin-nonflip amplitude \bar{T}

$$e^{-i n \alpha \theta_c} \bar{T}(\mathbf{p}, \mathbf{q}) = \frac{B_1}{|\mathbf{p}|} + B_2 \ln \frac{|\mathbf{p}|}{\mu_c} + \mathcal{T} + O(|\mathbf{p}|), \quad (\text{A.25})$$

where $n = 2$ for the scattering of two oppositely charged particles into two charged particles (example: $\pi^+ \pi^- \rightarrow \pi^+ \pi^-$), $n = 1$ for the transition of two charged particles into a pair of neutral particles or vice versa (example: $\pi^+ \pi^- \rightarrow \pi^0 \pi^0$) and $n = 0$ for the scattering of two neutral particles into two neutral particles (example: $\pi^0 \pi^0 \rightarrow \pi^0 \pi^0$). The (infrared–divergent) Coulomb phase is given by

$$\theta_c = \frac{\mu_c}{|\mathbf{p}|} \mu^{d-3} \left(\frac{1}{d-3} - \frac{1}{2} (\Gamma'(1) + \ln 4\pi) + \ln \frac{2|\mathbf{p}|}{\mu} \right), \quad (\text{A.26})$$

where μ stands for the scale of dimensional regularization.

The equation (A.25) defines the relativistic threshold amplitude \mathcal{T} in all cases of interest.

A.6 Real part of the threshold amplitudes

In particular cases, it turns out convenient to introduce the threshold amplitude \mathcal{A} , which coincides with \mathcal{T} (or the real part thereof) up to a normalization constant. Below we give the normalization for all amplitudes needed (for a general scattering process $1 + 2 \rightarrow \bar{1} + \bar{2}$ the notation $\mathcal{N}^{-1} = 8\pi(m_1 + m_2)$ is used, where m_1 and m_2 stand for the mass of the particles 1 and 2, respectively). The ellipses stand for the isospin breaking corrections.

– Pionium

Scattering channels:

$$\pi^+\pi^- \rightarrow \pi^+\pi^- (c) / \pi^+\pi^- \rightarrow \pi^0\pi^0 (x)$$

$$\begin{aligned} \mathcal{A}_c &= \frac{1}{32\pi} \text{Re } \mathcal{T}_c = \frac{1}{6} (2a_0 + a_2) + \dots, \\ \mathcal{A}_x &= -\frac{3}{32\pi} \text{Re } \mathcal{T}_x = (a_0 - a_2) + \dots. \end{aligned} \quad (\text{A.27})$$

The scattering lengths a_0, a_2 are denoted by a_0^0, a_2^0 in Ref. [84].

– $\pi\mathbf{K}$ atom

Scattering channels:

$$K^+\pi^- \rightarrow K^+\pi^- (c) / K^+\pi^- \rightarrow \bar{K}^0\pi^0 (x)$$

$$\begin{aligned} \mathcal{A}_c &= \mathcal{N} \text{Re } \mathcal{T}_c = \frac{1}{3} (2a^{1/2} + a^{3/2}) + \dots, \\ \mathcal{A}_x &= -\mathcal{N} \text{Re } \mathcal{T}_x / \sqrt{2} = \frac{1}{3} (a^{1/2} - a^{3/2}) + \dots. \end{aligned} \quad (\text{A.28})$$

The scattering lengths are normalized as in Ref. [228].

– Pionic hydrogen

Scattering channels:

$$p\pi^- \rightarrow p\pi^- (c) / p\pi^- \rightarrow n\pi^0 (x) / n\pi^0 \rightarrow n\pi^0 (0) / n\pi^- \rightarrow n\pi^- (n)$$

$$\begin{aligned} \mathcal{A}_{c,0,n} &= \mathcal{N} \text{Re } \mathcal{T}_{c,0,n}, & \mathcal{A}_x &= \mathcal{N} \text{Re } \mathcal{T}_x / \sqrt{2}, \\ \mathcal{A}_c &= a_{0+}^+ + a_{0+}^- + \dots, & \mathcal{A}_0 &= a_{0+}^+ + \dots, \\ \mathcal{A}_n &= a_{0+}^+ - a_{0+}^- + \dots, & \mathcal{A}_x &= -a_{0+}^- + \dots. \end{aligned} \quad (\text{A.29})$$

The scattering lengths are normalized as in Refs. [2, 238].

– **Kaonic hydrogen**

Scattering channels:

$$pK^- \rightarrow pK^- (c) / pK^- \rightarrow n\bar{K}^0 (x) / n\bar{K}^0 \rightarrow n\bar{K}^0 (0) / nK^- \rightarrow nK^- (n)$$

$$\begin{aligned} \mathcal{A}_{c,0,n} &= \mathcal{N} \mathcal{T}_{c,0,n}, & \mathcal{A}_x &= \mathcal{N} \mathcal{T}_x, \\ \mathcal{A}_c &= \frac{1}{2} (a_0 + a_1) + \dots, & \mathcal{A}_0 &= \frac{1}{2} (a_0 + a_1) + \dots, \\ \mathcal{A}_n &= a_1 + \dots, & \mathcal{A}_x &= \frac{1}{2} (a_0 - a_1) + \dots. \end{aligned} \quad (\text{A.30})$$

The scattering lengths are normalized as in Ref. [157].

– **Pionic deuterium**

Scattering channels:

$$\pi^- d \rightarrow \pi^- d (c)$$

$$\mathcal{A}_c = \mathcal{N} \mathcal{T}_c = a_{\pi d} + \dots. \quad (\text{A.31})$$

– **Kaonic deuterium**

Scattering channels:

$$K^- d \rightarrow K^- d (c)$$

$$\mathcal{A}_c = \mathcal{N} \mathcal{T}_c = a_{\bar{K}d} + \dots. \quad (\text{A.32})$$

A.7 Two-particle phase space

In the text, we use the symbols

$$p_n^* = \frac{\lambda^{1/2}(E_n^2, m_1^2, m_2^2)}{2E_n}, \quad \lambda(x, y, z) = x^2 + y^2 + z^2 - 2xy - 2xz - 2yz, \quad (\text{A.33})$$

with E_n given in Eq. (A.2).

A.8 Panofsky ratio

The Panofsky ratio is defined by

$$P = \frac{\sigma(\pi^- p \rightarrow \pi^0 n)}{\sigma(\pi^- p \rightarrow \gamma n)}, \quad (\text{A.34})$$

evaluated at the $\pi^- p$ threshold. Its value is $P = 1.546 \pm 0.009$ [212] ($P = 1.546 \pm 0.010$ [213]). At the accuracy we are working, one does not need to consider electromagnetic corrections to the cross sections. P is a quantity of order $\delta^{-1/2}$.

B Generalized unitarity

Let \mathbf{H} be a (non-hermitian) Hamiltonian. We further write $\mathbf{H} = \mathbf{H}_{0R} + \mathbf{H}_I$, where \mathbf{H}_{0R} denotes one-particle Hamiltonian, which includes all relativistic corrections. Acting on the free two-particle states, it gives

$$\mathbf{H}_{0R}|\mathbf{q}_1, \mathbf{q}_2\rangle = (q_1^0 + q_2^0)|\mathbf{q}_1, \mathbf{q}_2\rangle, \quad (\text{B.1})$$

where $q_i^0 = \sqrt{M_i^2 + \mathbf{q}_i^2}$, $i = 1, 2$. Next, we define the free resolvent

$$\mathbf{G}_{0R}(z^\pm) = (z - \mathbf{H}_{0R} \pm i0)^{-1} \quad (\text{B.2})$$

and the T -operator

$$\begin{aligned} \mathbf{T}_{NR}(z) &= \mathbf{H}_I + \mathbf{H}_I \mathbf{G}_{0R}(z^+) \mathbf{T}_{NR}(z) = \mathbf{T}_{NR}(z) \mathbf{G}_{0R}(z^+) \mathbf{H}_I + \mathbf{H}_I, \\ \mathbf{T}_{NR}^\dagger(z) &= \mathbf{H}_I^\dagger + \mathbf{H}_I^\dagger \mathbf{G}_{0R}(z^-) \mathbf{T}_{NR}^\dagger(z) = \mathbf{T}_{NR}^\dagger(z) \mathbf{G}_{0R}(z^-) \mathbf{H}_I^\dagger + \mathbf{H}_I^\dagger. \end{aligned} \quad (\text{B.3})$$

The relation to the T -matrix elements, introduced in Eq. (3.10) is given by

$$\begin{aligned} \langle \mathbf{p}_1, \mathbf{p}_2 | \mathbf{T}_{NR}(z) | \mathbf{q}_1, \mathbf{q}_2 \rangle &= -(2\pi)^3 \delta^3(\mathbf{p}_1 + \mathbf{p}_2 - \mathbf{q}_1 - \mathbf{q}_2) T_{NR}(\mathbf{p}_1, \mathbf{p}_2; \mathbf{q}_1, \mathbf{q}_2), \\ z &= p_1^0 + p_2^0 = q_1^0 + q_2^0. \end{aligned} \quad (\text{B.4})$$

Express now the Hamiltonian through the T -operator

$$\begin{aligned} \mathbf{H}_I &= \mathbf{T}_{NR}(z) \left(1 + \mathbf{G}_{0R}(z^+) \mathbf{T}_{NR}(z) \right)^{-1}, \\ \mathbf{H}_I^\dagger &= \left(1 + \mathbf{T}_{NR}^\dagger(z) \mathbf{G}_{0R}(z^-) \right)^{-1} \mathbf{T}_{NR}^\dagger(z). \end{aligned} \quad (\text{B.5})$$

Subtracting these two equations and using the identity

$$\mathbf{G}_{0R}(z^+) - \mathbf{G}_{0R}(z^-) = -2\pi i \delta(z - \mathbf{H}_{0R}), \quad (\text{B.6})$$

we finally arrive at the generalized unitarity relation for the T -operator.

$$\begin{aligned} \mathbf{T}_{NR}(z) - \mathbf{T}_{NR}^\dagger(z) &= -2\pi i \mathbf{T}_{NR}^\dagger(z) \delta(z - \mathbf{H}_{0R}) \mathbf{T}_{NR}(z) \\ &+ \left(1 + \mathbf{T}_{NR}^\dagger(z) \mathbf{G}_{0R}(z^-) \right) \left(\mathbf{H}_I - \mathbf{H}_I^\dagger \right) \left(1 + \mathbf{G}_{0R}(z^+) \mathbf{T}_{NR}(z) \right). \end{aligned} \quad (\text{B.7})$$

On the other hand, let us consider the non-relativistic multichannel scattering with hermitian Lagrangian. Unitarity condition in this case takes the form

$$\mathbf{T}_{ii}(z) - \mathbf{T}_{ii}^\dagger(z) = -2\pi i \sum_k \mathbf{T}_{ik}^\dagger(z) \delta(z - \mathbf{H}_{0R}) \mathbf{T}_{ki}(z), \quad (\text{B.8})$$

where $\mathbf{T}_{ii}(z) = \mathbf{T}_{NR}(z)$ describes the scattering in the elastic channel. From comparison of the above two equations it becomes clear that the term in Eq. (B.7), which contains $\mathbf{H}_I - \mathbf{H}_I^\dagger$, describes the ‘‘flow of the probability’’ into the shielded channels $i \neq k$. These channels are therefore encoded in the imaginary parts of the couplings in the Lagrangian Eq. (3.6).

C Matching and unitarity

Here we express of the coupling constants g_1 and e_1 – introduced in subsection 10.3 – through the threshold scattering amplitudes. The couplings g_1, e_1 enter the expression for the energy shift and width of πH at next-to-leading order, see Eq. (10.23). Taking the real and imaginary parts of this equation, we get

$$\begin{aligned}\Delta E_n^{\text{str}} &= -\frac{\alpha^3 \mu_c^3}{\pi n^3} \text{Re} (g_1 + 4\gamma_n^2 e_1 - g_1^2 \langle \bar{\mathbf{g}}_C^{n0}(E_n) \rangle) + o(\delta^4), \\ \Gamma_n &= \frac{2\alpha^3 \mu_c^3}{\pi n^3} \text{Im} (g_1 + 4\gamma_n^2 e_1 - g_1^2 \langle \bar{\mathbf{g}}_C^{n0}(E_n) \rangle) + o(\delta^{9/2}).\end{aligned}\quad (\text{C.1})$$

For the real part, the procedure is straightforward since, as it can be checked, $\text{Re } e_1 = O(1)$ that means that the contribution, proportional to $\text{Re } e_1$, does not emerge at the accuracy we are working. It is now clear that the answer – after adjusting the normalization accordingly – is given by Eq. (4.36),

$$\text{Re } g_1 = \frac{\text{Re } \mathcal{T}_c}{4m_p M_\pi} \left\{ 1 + \frac{\alpha \mu_c^2}{2\pi} \left(\Lambda(\mu) + \ln \frac{4\mu_c^2}{\mu^2} - 1 \right) \frac{\text{Re } \mathcal{T}_c}{4m_p M_\pi} \right\} + o(\delta). \quad (\text{C.2})$$

Matching of the imaginary parts of g_1 and e_1 is more complicated, because these break the naive counting rules in δ . A most straightforward way to address this problem is to use unitarity. The key observation is that, although the counting rules are modified, the modification at this order comes only from one term, namely the contribution of the $\pi^0 n$ intermediate state, which can be easily singled out.

An additional (technical) complication, which arises here, is related to the fact that we have to consider the unitarity condition at threshold in the presence of photons and to subtract the infrared-singular pieces in accordance to the definition of the threshold amplitude. Most easily, this problem can be circumvented by using the trick described in Ref. [45]: one analytically continues the unitarity condition for the negative values of the CM momentum squared \mathbf{p}^2 and approaches the threshold from below. We shall explain below, how this can be achieved.

At the first step, it is necessary to establish the singularity structure of the physical amplitudes, when the threshold is approached from below (note that previously we have defined the threshold amplitudes through the limiting procedure, when the threshold is approached from above). To this end it will be again useful to invoke the non-relativistic effective theory, which gives an analytic representation of the amplitude in the vicinity of the threshold in terms of a finite number of simple loop integrals. In the following, we discard the transverse photons as well as non-minimal couplings of the Coulomb photons completely. The reason is that these do not affect the matching of $\text{Im } g_1$ at $O(\delta^{3/2})$ and $\text{Im } e_1$ at $O(\delta^{-1/2})$, which suffices at the accuracy we are working.

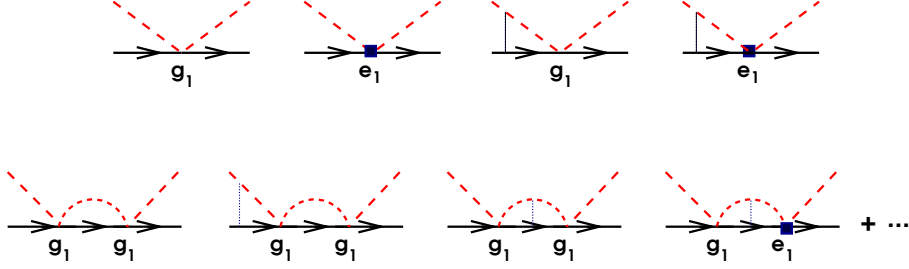


Figure C.1: Representative diagrams that describe the behavior of the non-relativistic spin-nonflip $\pi^- p \rightarrow \pi^- p$ amplitude near threshold, see Eq. (C.5). The vertex correction corresponds to V_c and the bubbles with and without Coulomb photons give J_c and B_c , respectively. The ellipses stand for diagrams with two and more pion bubbles. These do not contribute to the matching condition at the accuracy we are working. The vertex corrections in the final state are not shown.

We start with the non-relativistic amplitude for the $\pi^- p$ elastic scattering near threshold and remove the one-photon exchange contribution. In this manner, one obtains the counterpart of the amplitude \bar{T}_{NR} , defined in the scalar case by Eq. (4.32). In our case, the scattering amplitude contains the spin-nonflip as well as spin-flip parts. In the CM frame it is given by

$$\bar{T}_{\sigma'\sigma}(\mathbf{p}, \mathbf{q}) = \delta_{\sigma'\sigma} \bar{F}(\mathbf{p}, \mathbf{q}) + i \boldsymbol{\sigma}_{\sigma'\sigma} \cdot [\mathbf{q} \times \mathbf{p}] \bar{G}(\mathbf{p}, \mathbf{q}), \quad (\text{C.3})$$

where \mathbf{p} and \mathbf{q} denote the CM 3-momenta for the outgoing/incoming pion-nucleon pair. For determining the coupling constants g_1, e_1 it suffices to consider the spin-nonflip part of the amplitude and to project out the S -wave component

$$\bar{F}(\mathbf{p}, \mathbf{q}) = \frac{1}{2} \sum_{\sigma} \bar{T}_{\sigma\sigma}(\mathbf{p}, \mathbf{q}), \quad \bar{F}_0(\mathbf{p}^2) = \frac{1}{2} \int_{-1}^1 d \cos \theta \bar{F}(\mathbf{p}, \mathbf{q}), \quad (\text{C.4})$$

where θ is the angle between the vectors \mathbf{p} and \mathbf{q} .

Discarding all but Coulomb photons, one is left with only a few diagrams that determine the behavior of $\bar{F}_0(\mathbf{p}^2)$ at very small momenta, see Fig. C.1. At order α one obtains

$$\bar{F}_0(\mathbf{p}^2) = (1 - 2V_c) \left(g_1 - 4\mathbf{p}^2 e_1 + (g_1 - 4\mathbf{p}^2 e_1)^2 (J_c + B_c) + \dots \right). \quad (\text{C.5})$$

Note that, in order to keep the expressions as transparent as possible, we did not further expand Eq. (C.5) in δ and \mathbf{p}^2 , retaining some higher-order terms as well.

The loop integrals, entering Eq. (C.5), are given by

$$\begin{aligned}
V_c &= -\frac{\alpha\mu_c}{(-\mathbf{p}^2)^{1/2}} \mu^{d-3} \left(\frac{1}{d-3} - \frac{1}{2} (\Gamma'(1) + \ln 4\pi) + \frac{1}{2} \ln \frac{-4\mathbf{p}^2}{\mu^2} \right) \\
&\quad + O(|\mathbf{p}|, d-3), \\
J_c &= -\frac{\mu_c}{2\pi} (-\mathbf{p}^2)^{1/2} + O(|\mathbf{p}|^3, d-3), \\
B_c &= \bar{B}_c - \frac{\alpha\mu_c^2}{2\pi} \ln \frac{-\mathbf{p}^2}{\mu_c^2} + O(|\mathbf{p}|, d-3), \\
\bar{B}_c &= -\frac{\alpha\mu_c^2}{2\pi} \left(\Lambda(\mu) - 1 + \ln \frac{4\mu_c^2}{\mu^2} \right), \tag{C.6}
\end{aligned}$$

where $\mathbf{p}^2 < 0$. Further, the quantity J_c corresponds to the single loop with the proton and the charged pion, no photons. The quantities V_c and B_c are similar to the quantities defined in section 4 and correspond to the vertex correction and to the internal exchange of the Coulomb photon, respectively.

In Eq. (C.5) we now multiply both sides by $(1 + 2V_c)$ (remember that the quantity V_c is real below threshold) and calculate the imaginary part. Using explicit expressions for the loop integrals, we see that the following is valid below threshold,

$$\begin{aligned}
(1 + 2V_c) \text{Im } \bar{F}_0(\mathbf{p}^2) &= \left(h_0 + h'_0 \ln \frac{-\mathbf{p}^2}{\mu_c^2} \right) + |\mathbf{p}| \left(h_1 + h'_1 \ln \frac{-\mathbf{p}^2}{\mu_c^2} \right) \\
&\quad + |\mathbf{p}|^2 \left(h_2 + h'_2 \ln \frac{-\mathbf{p}^2}{\mu_c^2} \right) + o(\mathbf{p}^2), \tag{C.7}
\end{aligned}$$

where the coefficients h_i, h'_i can be expressed in terms of g_1, e_1 . We shall further assume that $\text{Im } g_1 = O(\delta^{1/2})$, $\text{Im } e_1 = O(\delta^{-1/2})$ (these assumptions will be verified *a posteriori*). To determine the constants g_1, e_1 from the matching, we need following relations, which can be established from Eqs. (C.5), (C.6) and (C.7),

$$h_0 = \text{Im} (g_1 + g_1^2 \bar{B}_c) + o(\delta^{3/2}), \quad h_2 = -4 \text{Im } e_1 + o(\delta^{-1/2}). \tag{C.8}$$

Let us now use the matching condition, which relates the imaginary part of the quantity $\bar{F}_0(\mathbf{p}^2)$ to the (one-photon exchange-removed) relativistic spin-nonflip amplitude, defined in accordance with Eq. (A.24). We denote the latter quantity as T_c , where the subscript ‘‘c’’ corresponds to the elastic channel $\pi^- p \rightarrow \pi^- p$. In the CM frame the matching condition reads

$$(1 + 2V_c) \text{Im } \bar{F}_0(\mathbf{p}^2) = \frac{1}{2} \int_{-1}^1 d \cos \theta \frac{(1 + 2V_c)}{2w_\pi(\mathbf{p}) 2w_p(\mathbf{p})} \text{Im } \bar{T}_c(\mathbf{p}, \mathbf{q}), \tag{C.9}$$

where $w_\pi(\mathbf{p})$ and $w_p(\mathbf{p})$ are the relativistic energies of the charged pion and the proton in the CM frame, respectively. Further, one may replace \bar{T}_c by the full spin-nonflip amplitude T_c , since the one-photon exchange piece is real.

We further use unitarity in the relativistic theory to evaluate the imaginary part of T_c near threshold. Since the threshold is approached from below, the elastic contribution from the $\pi^- p$ intermediate state, as well as $\pi^- p$ plus any number of photons do not contribute. Then, at the order of accuracy we are working, only the contributions from $n\pi^0$ and $n\gamma$ intermediate states should be retained. Substituting the result in Eq. (C.9), we finally get

$$(1 + 2V_c) \text{Im } \bar{F}_0(\mathbf{p}^2) = p^*(\mathbf{p}^2)H(\mathbf{p}^2) + p_\gamma^*(\mathbf{p}^2)H_\gamma(\mathbf{p}^2) + \dots, \quad (\text{C.10})$$

with

$$\begin{aligned} p^*(\mathbf{p}^2) &= \frac{\lambda^{1/2}(s(\mathbf{p}^2), m_n^2, M_{\pi^0}^2)}{2\sqrt{s(\mathbf{p}^2)}}, & p_\gamma^*(\mathbf{p}^2) &= \frac{\lambda^{1/2}(s(\mathbf{p}^2), m_n^2, 0)}{2\sqrt{s(\mathbf{p}^2)}}, \\ s(\mathbf{p}^2) &= (w_p(\mathbf{p}) + w_\pi(\mathbf{p}))^2, \end{aligned} \quad (\text{C.11})$$

and $H(\mathbf{p}^2)$, $H_\gamma(\mathbf{p}^2)$ denote the pertinent angular integrals containing the scattering amplitudes into various intermediate states. We do not display the explicit expressions for $H(\mathbf{p}^2)$ and $H_\gamma(\mathbf{p}^2)$ here. The threshold behavior of $F_0(\mathbf{p}^2)$ is determined by

$$\begin{aligned} p^*(\mathbf{p}^2) &= p^*(0) + (p^*(0))'\mathbf{p}^2 + O(\mathbf{p}^4), & p_\gamma^*(\mathbf{p}^2) &= p_\gamma^*(0) + O(\mathbf{p}^2), \\ H(\mathbf{p}^2) &= \left(k_0 + k'_0 \ln \frac{-\mathbf{p}^2}{\mu_c^2} \right) + O(|\mathbf{p}|), & H_\gamma(\mathbf{p}^2) &= H_\gamma(0) + O(|\mathbf{p}|). \end{aligned} \quad (\text{C.12})$$

Note that at this order in δ there are no logarithms in $H_\gamma(\mathbf{p}^2)$. Various coefficients count as

$$\begin{aligned} p^*(0) &= O(\delta^{1/2}), & (p^*(0))' &= O(\delta^{-1/2}), & p_\gamma^*(0) &= O(1), \\ k_0 &= O(1), & H_\gamma(0) &= O(\delta). \end{aligned} \quad (\text{C.13})$$

The main property of the above representation is that the expansion coefficients in $H(\mathbf{p}^2)$, $H_\gamma(\mathbf{p}^2)$ are not enhanced in δ -counting to the order we are working. At this order, $\sim \delta^{-1/2}$ behavior in e_1 comes solely from the derivative $(p^*(0))'$. The matching therefore gives

$$\begin{aligned} \text{Im}(g_1 + g_1^2 \bar{B}_c) &= p^*(0)k_0 + p_\gamma^*(0)H_\gamma(0) + o(\delta^{3/2}), \\ -4 \text{Im } e_1 &= (p^*(0))'k_0 + o(\delta^{-1/2}). \end{aligned} \quad (\text{C.14})$$

From the above expression one may readily verify the power counting $\text{Im } g_1 = O(\delta^{1/2})$ and $\text{Im } e_1 = O(\delta^{-1/2})$. Further, for the particular combination of the

low-energy constants g_1 and e_1 , which enters the expression for the decay width Eq. (C.1), we get

$$\begin{aligned} \text{Im}(g_1 + g_1^2 \bar{B}_c + 4\gamma_n^2 e_1) &= (p^*(0) - (p^*(0))' \gamma_n^2) k_0 + p_\gamma^*(0) H_\gamma(0) + o(\delta^{3/2}) \\ &= \left(1 + \frac{1}{P}\right) p^*(-\gamma_n^2) k_0 + o(\delta^{3/2}). \end{aligned} \quad (\text{C.15})$$

In the above expression P denotes the Panofsky ratio which, at the order of accuracy we are working, is

$$P = \frac{\sigma(\pi^- p \rightarrow \pi^0 n)}{\sigma(\pi^- p \rightarrow \gamma n)} \Big|_{\text{thr}} = \frac{p^*(0) k_0}{p_\gamma^*(0) H_\gamma(0)} + O(\delta^{1/2}). \quad (\text{C.16})$$

Further, note that the net effect of the effective-range term at this order is to merely shift the argument of the phase space factor to the correct bound-state value $p_n^* = p^*(-\gamma_n^2)$, since $\sqrt{s(-\gamma_n^2)} = E_n + O(\delta^4)$.

In order to evaluate the width at the required accuracy, it suffices to determine the coefficient k_0 . To this end, we recall that the quantity $H(\mathbf{p}^2)$ is defined as an angular integral over $|T_x|^2 = \{\text{Re } T_x\}^2 + \{\text{Im } T_x\}^2$, where $T_x(\mathbf{p}, \mathbf{q})$ denotes the scattering amplitude for the process $\pi^- p \rightarrow \pi^0 n$. Thus, at lowest order, k_0 must be proportional to $\{\text{Re } \mathcal{T}_x\}^2$. Further, the imaginary part of the amplitude gives the correction at $O(\delta)$ to this result. To find this correction, one may invoke unitarity once again and make sure that at this order only $\pi^0 n$ intermediate state contributes. We skip all details here and display the final result,

$$k_0 = \frac{1}{32\pi m_p M_\pi (m_p + M_\pi)} \left\{ \text{Re } \mathcal{T}_x \right\}^2 \left\{ 1 + \left(\frac{p^*(0)}{8\pi(m_p + M_\pi)} \text{Re } \mathcal{T}_0 \right)^2 \right\} + o(\delta). \quad (\text{C.17})$$

From this equation we get

$$\text{Im}(g_1 + g_1^2 \bar{B}_c + 4\gamma_n^2 e_1) = \frac{4\pi p^*(-\gamma_n^2)}{\mu_c} \left(1 + \frac{1}{P}\right) \mathcal{A}_x^2 \left\{ 1 + (p^*(0) \mathcal{A}_0)^2 \right\} + o(\delta^{3/2}), \quad (\text{C.18})$$

where we have used Eq. (A.29) in order to rewrite the above expression in terms of the real amplitudes \mathcal{A}_c , \mathcal{A}_x and \mathcal{A}_0 . Finally, using Eqs. (C.18), (C.1) and (10.28), we arrive at the complete expression for the decay width, displayed in Eq. (10.26).

Remark: Although the modification of the counting rules, which was considered in this appendix, seems a bit complicated at a first glance, it is in fact just a remnant of the unitary cusp effect. This effect has nothing to do with photons and can be established in the purely strong non-relativistic theory. Consider, for

example, the two-channel model like the one used for ponium (without transverse photons). The coupling constants c_1, c_2, c_3 in this model obey the usual counting rules. Construct now an effective one-channel Hamiltonian, integrating out the neutral channel and expressing new effective couplings in terms of c_1, c_2, c_3 and the neutral bubble (see, e.g., Refs. [36, 42]). The reader is invited to check himself that exactly the above modified counting rules for the new effective couplings emerge in the one-channel theory. End of remark.

References

- [1] D. Sigg *et al.*, Phys. Rev. Lett. **75** (1995) 3245.
- [2] G. Höhler, *Pion Nucleon Scattering. Part 2: Methods and Results of Phenomenological Analyses*, in Landolt-Börnstein - Group I Elementary Particles, Nuclei and Atoms, vol. **9 b2**, ed. H. Schopper, Berlin: Springer-Verlag (1983), 601p.
- [3] R. Koch and E. Pietarinen, Nucl. Phys. A **336** (1980) 331.
- [4] R. Koch, Z. Phys. C **29** (1985) 597.
- [5] R. Koch, Nucl. Phys. A **448** (1986) 707.
- [6] R. A. Arndt, W. J. Briscoe, I. I. Strakovsky, R. L. Workman and M. M. Pavan, Phys. Rev. C **69** (2004) 035213 [arXiv:nucl-th/0311089].
- [7] E. Matsinos, W. S. Woolcock, G. C. Oades, G. Rasche and A. Gashi, Nucl. Phys. A **778** (2006) 95 [arXiv:hep-ph/0607080].
- [8] S. Deser, M. L. Goldberger, K. Baumann and W. Thirring, Phys. Rev. **96** (1954) 774.
- [9] S. Weinberg, Physica A **96** (1979) 327.
- [10] J. Bijnens, G. Colangelo, G. Ecker, J. Gasser and M. E. Sainio, Phys. Lett. B **374** (1996) 210 [arXiv:hep-ph/9511397].
- [11] J. Bijnens, G. Colangelo, G. Ecker, J. Gasser and M. E. Sainio, Nucl. Phys. B **508** (1997) 263 [Erratum-ibid. B **517** (1998) 639] [arXiv:hep-ph/9707291].
- [12] B. Ananthanarayan, G. Colangelo, J. Gasser and H. Leutwyler, Phys. Rept. **353** (2001) 207 [arXiv:hep-ph/0005297].
- [13] G. Colangelo, J. Gasser and H. Leutwyler, Phys. Lett. B **488** (2000) 261 [arXiv:hep-ph/0007112].

- [14] G. Colangelo, J. Gasser and H. Leutwyler, Nucl. Phys. B **603** (2001) 125 [arXiv:hep-ph/0103088].
- [15] I. Caprini, G. Colangelo, J. Gasser and H. Leutwyler, Phys. Rev. D **68** (2003) 074006 [arXiv:hep-ph/0306122].
- [16] S. Descotes-Genon, N. H. Fuchs, L. Girlanda and J. Stern, Eur. Phys. J. C **24** (2002) 469 [arXiv:hep-ph/0112088].
R. Kaminski, J. R. Pelaez and F. J. Yndurain, arXiv:0710.1150 [hep-ph].
- [17] T. Yamazaki *et al.* [CP-PACS Collaboration], Phys. Rev. D **70** (2004) 074513 [arXiv:hep-lat/0402025];
S. R. Beane, P. F. Bedaque, K. Orginos and M. J. Savage [NPLQCD Collaboration], Phys. Rev. D **73** (2006) 054503 [arXiv:hep-lat/0506013];
S. R. Beane, P. F. Bedaque, T. C. Luu, K. Orginos, E. Pallante, A. Parreno and M. J. Savage, Phys. Rev. D **74** (2006) 114503 [arXiv:hep-lat/0607036];
S. R. Beane, T. C. Luu, K. Orginos, A. Parreno, M. J. Savage, A. Torok and A. Walker-Loud, arXiv:0706.3026 [hep-lat].
- [18] H. Leutwyler, *Insights and puzzles in light quark physics*, talk given at: 42nd Rencontres de Moriond, March 14–17, 2007, La Thuile, Italy, in: electronic proceedings, Eds. E. Auge, B. Pietrzyk and J. Tran Thanh Van, arXiv:0706.3138 [hep-ph].
- [19] G. Colangelo, PoS **KAON** (2007) 038 [arXiv:0710.3050 [hep-ph]].
- [20] The literature on the pion–nucleon sigma term is very large - it is impossible to display all the relevant articles here. We display a lattice study, a study based on πN scattering data, and a short review.
M. Procura, T. R. Hemmert and W. Weise, Phys. Rev. D **69** (2004) 034505 [arXiv:hep-lat/0309020];
M. M. Pavan, I. I. Strakovsky, R. L. Workman and R. A. Arndt, PiN Newslett. **16** (2002) 110 [arXiv:hep-ph/0111066];
M. E. Sainio, PiN Newslett. **16** (2002) 138 [arXiv:hep-ph/0110413].
- [21] M. L. Goldberger, H. Miyazawa and R. Oehme, Phys. Rev. **99** (1955) 986.
- [22] T. E. O. Ericson, B. Loiseau and A. W. Thomas, Phys. Rev. C **66** (2002) 014005 [arXiv:hep-ph/0009312].
- [23] V. V. Abaev, P. Metsa and M. E. Sainio, Eur. Phys. J. A **32** (2007) 321 [arXiv:0704.3167 [hep-ph]].
- [24] Z. K. Silagadze, JETP Lett. **60** (1994) 689 [arXiv:hep-ph/9411382].

- [25] H. Jallouli and H. Sazdjian, Phys. Rev. D **58** (1998) 014011 [Erratum-ibid. D **58** (1998) 099901] [arXiv:hep-ph/9706450].
- [26] H. Sazdjian, Phys. Lett. B **490** (2000) 203 [arXiv:hep-ph/0004226].
- [27] H. Jallouli and H. Sazdjian, Eur. Phys. J. C **48** (2006) 561 [arXiv:hep-ph/0605253].
- [28] V. E. Lyubovitskij and A. Rusetsky, Phys. Lett. B **389** (1996) 181 [arXiv:hep-ph/9610217].
- [29] V. E. Lyubovitskij, E. Z. Lipartia and A. G. Rusetsky, Pisma Zh. Eksp. Teor. Fiz. **66** (1997) 747 [JETP Lett. **66** (1997) 783] [arXiv:hep-ph/9801215].
- [30] M. A. Ivanov, V. E. Lyubovitskij, E. Z. Lipartia and A. G. Rusetsky, Phys. Rev. D **58** (1998) 094024 [arXiv:hep-ph/9805356].
- [31] P. Labelle and K. Buckley, arXiv:hep-ph/9804201.
- [32] D. Eiras and J. Soto, Phys. Rev. D **61** (2000) 114027 [arXiv:hep-ph/9905543].
- [33] B. R. Holstein, Phys. Rev. D **60** (1999) 114030 [arXiv:nucl-th/9901041].
- [34] X. Kong and F. Ravndal, Phys. Rev. D **59** (1999) 014031.
- [35] X. Kong and F. Ravndal, Phys. Rev. D **61** (2000) 077506 [arXiv:hep-ph/9905539].
- [36] A. Gall, J. Gasser, V. E. Lyubovitskij and A. Rusetsky, Phys. Lett. B **462** (1999) 335 [arXiv:hep-ph/9905309].
- [37] W. E. Caswell and G. P. Lepage, Phys. Lett. B **167** (1986) 437.
- [38] H. Feshbach, Ann. Phys. **5** (1958) 357.
- [39] H. Feshbach, Ann. Phys. **19** (1962) 287.
- [40] J. Gasser, V. E. Lyubovitskij and A. Rusetsky, Phys. Lett. B **471** (1999) 244 [arXiv:hep-ph/9910438].
- [41] V. E. Lyubovitskij and A. Rusetsky, Phys. Lett. B **494** (2000) 9 [arXiv:hep-ph/0009206].
- [42] J. Gasser, V. E. Lyubovitskij, A. Rusetsky and A. Gall, Phys. Rev. D **64** (2001) 016008 [arXiv:hep-ph/0103157].
- [43] J. Gasser, M. A. Ivanov, E. Lipartia, M. Mojžiš and A. Rusetsky, Eur. Phys. J. C **26** (2002) 13 [arXiv:hep-ph/0206068].

- [44] J. Schweizer, Phys. Lett. B **587** (2004) 33 [arXiv:hep-ph/0401048];
 J. Schweizer, Eur. Phys. J. C **36** (2004) 483 [arXiv:hep-ph/0405034].
- [45] P. Zemp, *Deser-type formula for pionic hydrogen*, talk given at: Workshop “Hadronic Atoms”, October 13–17, 2003, ECT*, Trento, Italy, in: Proceedings “HadAtom03”, Eds. J. Gasser, A. Rusetsky, J. Schacher, p.18 [arXiv:hep-ph/0401204];
 P. Zemp, *Pionic Hydrogen in QCD+QED: Decay width at NNLO*, PhD thesis, University of Bern, 2004.
- [46] U.-G. Meißner, U. Raha and A. Rusetsky, Eur. Phys. J. C **35** (2004) 349 [arXiv:hep-ph/0402261].
- [47] U.-G. Meißner, U. Raha and A. Rusetsky, Eur. Phys. J. C **41** (2005) 213 [Erratum-ibid. C **45** (2006) 545] [arXiv:nucl-th/0501073]
- [48] U.-G. Meißner, U. Raha and A. Rusetsky, Phys. Lett. B **639** (2006) 478 [arXiv:nucl-th/0512035].
- [49] U.-G. Meißner, U. Raha and A. Rusetsky, Eur. Phys. J. C **47** (2006) 473 [arXiv:nucl-th/0603029].
- [50] G. V. Efimov, M. A. Ivanov and V. E. Lyubovitskij, Sov. J. Nucl. Phys. **44** (1986) 296 [Yad. Fiz. **44** (1986) 460];
 G. V. Efimov, M. A. Ivanov and V. E. Lyubovitskij, JETP Lett. **45** (1987) 672 [Pisma Zh. Eksp. Teor. Fiz. **45** (1987) 526];
 G. V. Efimov, M. A. Ivanov, V. E. Lyubovitskij and A. G. Rusetsky, Sov. J. Nucl. Phys. **51** (1990) 121 [Yad. Fiz. **51** (1990) 190].
- [51] A. A. Belkov, V. N. Pervushin and F. G. Tkebuchava, Yad. Fiz. **44** (1986) 466 [Sov. J. Nucl. Phys. **44** (1986) 300].
- [52] M. K. Volkov, Theor. Math. Phys. **71** (1987) 606 [Teor. Mat. Fiz. **71** (1987) 381].
- [53] E. A. Kuraev, Phys. Atom. Nucl. **61** (1998) 239 [Yad. Fiz. **61** (1998) 289].
- [54] H. W. Hammer and J. N. Ng, Eur. Phys. J. A **6** (1999) 115 [arXiv:hep-ph/9902284].
- [55] A. N. Ivanov, M. Faber, A. Hirtl, J. Marton and N. I. Troitskaya, Eur. Phys. J. A **18** (2003) 653 [arXiv:nucl-th/0306047].
- [56] A. N. Ivanov, M. Faber, A. Hirtl, J. Marton and N. I. Troitskaya, Eur. Phys. J. A **19** (2004) 413 [arXiv:nucl-th/0310027].

- [57] A. N. Ivanov, M. Cargnelli, M. Faber, J. Marton, N. I. Troitskaya and J. Zmeskal, *Eur. Phys. J. A* **21** (2004) 11 [arXiv:nucl-th/0310081].
- [58] A. N. Ivanov *et al.*, *Eur. Phys. J. A* **23** (2005) 79 [arXiv:nucl-th/0406053].
- [59] A. N. Ivanov *et al.*, *Eur. Phys. J. A* **25** (2005) 329 [arXiv:nucl-th/0505078].
- [60] A. N. Ivanov *et al.*, *J. Phys. G* **31** (2005) 769.
- [61] B. F. Irgaziev and B. A. Fayzullaev, arXiv:hep-ph/0404203.
- [62] S. Krewald, R. H. Lemmer and F. P. Sassen, *Phys. Rev. D* **69** (2004) 016003 [arXiv:hep-ph/0307288].
- [63] G. P. Lepage and B. A. Thacker, *Nucl. Phys. Proc. Suppl.* **4** (1988) 199.
- [64] N. Brambilla, A. Pineda, J. Soto and A. Vairo, *Rev. Mod. Phys.* **77** (2005) 1423 [arXiv:hep-ph/0410047].
- [65] N. Brambilla and A. Vairo, arXiv:0711.1328 [hep-ph].
- [66] T. E. O. Ericson and W. Weise, *Pions And Nuclei*, Oxford: Clarendon (1988), 479p.
- [67] F. Scheck, *Leptons, hadrons and nuclei*, Amsterdam: North-Holland (1983), 388p.
- [68] A. Deloff, *Fundamentals in hadronic atom theory*, River Edge, USA: World Scientific (2003), 352p.
- [69] C. J. Batty, E. Friedman and A. Gal, *Phys. Rept.* **287** (1997) 385.
- [70] Proceedings of International Conference on Exotic Atoms and Related Topics (EXA05), February 21 - 25, 2005, Vienna, Austria, Eds. A. Hirtl, J. Marton, E. Widmann, J. Zmeskal, Vienna: Austrian Acad. of Sciences Press, 2005.
- [71] W. Weise, *Deeply bound meson-nuclear states: Concepts and strategies*, talk given at: EXA05, February 21–25, 2005, Vienna, Austria, in: Ref. [70], [arXiv:nucl-th/0507058].
- [72] B. Adeva *et al.* [DIRAC Collaboration], CERN proposal CERN/SPSLC 95-1 (1995).
- [73] B. Adeva *et al.* [DIRAC Collaboration], *Nucl. Instrum. Meth. A* **515** (2003) 467 [arXiv:hep-ex/0305022].
- [74] F. Gomez *et al.* [DIRAC Collaboration], *Nucl. Phys. Proc. Suppl.* **96** (2001) 259.

- [75] B. Adeva *et al.* [DIRAC Collaboration], J. Phys. G **30** (2004) 1929 [arXiv:hep-ex/0409053].
- [76] D. Goldin [DIRAC Collaboration], Int. J. Mod. Phys. A **20** (2005) 321.
- [77] B. Adeva *et al.* [DIRAC Collaboration], Phys. Lett. B **619** (2005) 50 [arXiv:hep-ex/0504044].
- [78] B. Adeva *et al.*, *Lifetime measurement of $\pi^+\pi^-$ and $\pi^\pm K^\mp$ atoms to test low energy QCD. Addendum to the DIRAC proposal*, CERN-SPSC-2004-009 [SPSC-P-284 Add.4].
- [79] L. G. Afanasev *et al.*, Phys. Lett. B **338** (1994) 478.
- [80] Z. Halabuka, T. A. Heim, K. Hencken, D. Trautmann and R. D. Viollier, Nucl. Phys. B **554** (1999) 86.
- [81] L. Tauscher, PoS **KAON** (2007) 036.
- [82] N. H. Fuchs, H. Sazdjian and J. Stern, Phys. Lett. B **269** (1991) 183;
J. Stern, H. Sazdjian and N. H. Fuchs, Phys. Rev. D **47** (1993) 3814 [arXiv:hep-ph/9301244];
M. Knecht, B. Moussallam, J. Stern, and N. H. Fuchs, Nucl. Phys. B **457** (1995) 513 [hep-ph/9507319];
M. Knecht, B. Moussallam, J. Stern, and N. H. Fuchs, Nucl. Phys. B **471** (1996) 445 [hep-ph/9512404].
- [83] G. Colangelo, J. Gasser and H. Leutwyler, Phys. Rev. Lett. **86** (2001) 5008 [arXiv:hep-ph/0103063].
- [84] J. Gasser and H. Leutwyler, Ann. Phys. (N.Y.) **158** (1984) 142.
- [85] J. Gasser and H. Leutwyler, Nucl. Phys. B **250** (1985) 465.
- [86] L. L. Nemenov and V. D. Ovsyannikov, Phys. Lett. B **514** (2001) 247.
- [87] L. L. Nemenov, V. D. Ovsyannikov and E. V. Chaplygin, Nucl. Phys. A **710** (2002) 303.
- [88] J. R. Batley *et al.* [NA48/2 Collaboration], Phys. Lett. B **633** (2006) 173 [arXiv:hep-ex/0511056].
- [89] N. Cabibbo, Phys. Rev. Lett. **93** (2004) 121801 [arXiv:hep-ph/0405001].
- [90] N. Cabibbo and G. Isidori, JHEP **0503** (2005) 021 [arXiv:hep-ph/0502130].

- [91] E. Gamiz, J. Prades and I. Scimemi, Eur. Phys. J. C **50** (2007) 405 [arXiv:hep-ph/0602023].
- [92] G. Colangelo, J. Gasser, B. Kubis and A. Rusetsky, Phys. Lett. B **638** (2006) 187 [arXiv:hep-ph/0604084].
- [93] J. Gasser, B. Kubis and A. Rusetsky, in preparation.
- [94] B. Bloch-Devaux, *Recent results from NA48/2 on K_{e4} and $K^\pm \rightarrow \pi^\pm \pi^0 \pi^0$ decays - Interpretation in terms of $\pi\pi$ scattering lengths*, talk given at: PASCHOS06, September 10–16, 2006, Columbus, OH, USA.
- [95] J. Gasser, PoS **KAON** (2007) 033 [arXiv:0710.3048 [hep-ph]].
- [96] G. Colangelo, J. Gasser and A. Rusetsky, in preparation.
- [97] E. Barberio and Z. Was, Comput. Phys. Commun. **79** (1994) 291;
E. Barberio, B. van Eijk and Z. Was, Comput. Phys. Commun. **66** (1991) 115.
- [98] B. Bloch-Devaux, private communication.
- [99] A. Nehme, Eur. Phys. J. C **40** (2005) 367 [arXiv:hep-ph/0408104];
A. Nehme, Phys. Rev. D **69** (2004) 094012 [arXiv:hep-ph/0402007];
V. Cuplov and A. Nehme, arXiv:hep-ph/0311274;
A. Nehme, Nucl. Phys. B **682** (2004) 289 [arXiv:hep-ph/0311113].
- [100] S. Pislak *et al.* [BNL-E865 Collaboration], Phys. Rev. Lett. **87** (2001) 221801 [arXiv:hep-ex/0106071].
- [101] S. Pislak *et al.* [BNL-E865 Collaboration], Phys. Rev. D **67** (2003) 072004 [arXiv:hep-ex/0301040].
- [102] B. Bloch-Devaux, PoS **KAON** (2007) 035.
- [103] A. Roessl, Nucl. Phys. B **555** (1999) 507 [arXiv:hep-ph/9904230].
- [104] V. Bernard, N. Kaiser and U.-G. Meißner, Nucl. Phys. B **357** (1991) 129.
- [105] J. Bijnens, P. Dhonte and P. Talavera, JHEP **0405** (2004) 036 [arXiv:hep-ph/0404150].
- [106] P. Büttiker, S. Descotes-Genon and B. Moussallam, Eur. Phys. J. C **33** (2004) 409 [arXiv:hep-ph/0310283].
- [107] J. Schweizer, Phys. Lett. B **625** (2005) 217 [arXiv:hep-ph/0507323].

- [108] B. Ananthanarayan and P. Buettiker, Eur. Phys. J. C **19** (2001) 517 [arXiv:hep-ph/0012023].
- [109] D. Chatellard *et al.*, Phys. Rev. Lett. **74** (1995) 4157.
- [110] D. Sigg *et al.*, Nucl. Phys. A **609** (1996) 269.
- [111] D. Chatellard *et al.*, Nucl. Phys. A **625** (1997) 855.
- [112] P. Hauser *et al.*, Phys. Rev. C **58** (1998) 1869.
- [113] H. C. Schroder *et al.*, Phys. Lett. B **469** (1999) 25.
- [114] H. C. Schröder *et al.*, Eur. Phys. J. C **21** (2001) 473.
- [115] G. C. Oades *et al.*, *Measurement of the strong interaction width and shift of the ground state of pionic hydrogen*, PSI Proposal R-98-01 (1998), <http://pihydrogen.web.psi.ch>.
- [116] D. Gotta [Pionic Hydrogen Collaboration], Int. J. Mod. Phys. A **20** (2005) 349;
L. M. Simons [Pionic Hydrogen Collaboration], Int. J. Mod. Phys. A **20** (2005) 1644.
- [117] D. Gotta, Prog. Part. Nucl. Phys. **52** (2004) 133.
- [118] L. M. Simons [Pionic Hydrogen Collaboration], *Pionic hydrogen*, talk given at: International Workshop on Exotic Hadronic Atoms, Deeply Bound Kaonic Nuclear States and Antihydrogen: Present Results, Future Challenges, June 19–24, 2006 Trento, Italy, in: Miniproceedings, Eds. C. Curceanu, A. Rusetsky and E. Widmann, p.8 [arXiv:hep-ph/0610201];
D. Gotta [Pionic Hydrogen Collaboration], *Pionic hydrogen*, talk given at: International Workshop on Precision Physics of Simple Atomic Systems (PSAS 2006), June 12–16, 2006, Venice, Italy, to appear in the proceedings.
- [119] See homepage of the Pionic Hydrogen Collaboration at PSI, <http://pihydrogen.web.psi.ch>
- [120] D. Gotta *et al.*, *Pionic Deuterium*, PSI Proposal R-06-03 (2006).
- [121] T. Strauch, *Pionic Deuterium*, talk given at: 11th International Conference on Meson-Nucleon Physics and the Structure of the Nucleon (MENU2007), September 10–14, 2007, Jülich, Germany, to appear in the proceedings.
- [122] I. R. Afnan and A. W. Thomas, Phys. Rev. C **10** (1974) 109.

- [123] T. Mizutani and D. S. Koltun, *Annals Phys.* **109** (1977) 1.
- [124] A. W. Thomas and R. H. Landau, *Phys. Rept.* **58** (1980) 121.
- [125] V. M. Kolybasov and A. E. Kudryavtsev, *Nucl. Phys. B* **41** (1972) 510.
- [126] A. Deloff, *Phys. Rev. C* **64** (2001) 065205 [arXiv:nucl-th/0104067].
- [127] V. V. Baru, A. E. Kudryavtsev and V. E. Tarasov, *Phys. Atom. Nucl.* **67** (2004) 743 [*Yad. Fiz.* **67** (2004) 764] [arXiv:nucl-th/0301021].
- [128] V. V. Baru and A. E. Kudryavtsev, *Phys. Atom. Nucl.* **60** (1997) 1475 [*Yad. Fiz.* **60** (1997) 1620].
- [129] V. V. Baru and A. E. Kudryavtsev, *PiN Newslett.* **12** (1997) 64.
- [130] V. E. Tarasov, V. V. Baru and A. E. Kudryavtsev, *Phys. Atom. Nucl.* **63** (2000) 801 [*Yad. Fiz.* **63** (2000) 871].
- [131] S. R. Beane, V. Bernard, T.-S. H. Lee and U.-G. Meißner, *Phys. Rev. C* **57** (1998) 424 [arXiv:nucl-th/9708035].
- [132] S. R. Beane, V. Bernard, E. Epelbaum, U.-G. Meißner and D. R. Phillips, *Nucl. Phys. A* **720** (2003) 399 [arXiv:hep-ph/0206219].
- [133] V. Lensky, V. Baru, J. Haidenbauer, C. Hanhart, A. E. Kudryavtsev and U.-G. Meißner, *Phys. Lett. B* **648** (2007) 46 [arXiv:nucl-th/0608042].
- [134] C. Hanhart, arXiv:nucl-th/0703028.
- [135] M. P. Valderrama and E. R. Arriola, arXiv:nucl-th/0605078.
- [136] L. Platter and D. R. Phillips, *Phys. Lett. B* **641** (2006) 164 [arXiv:nucl-th/0605024].
- [137] V. Baru, C. Hanhart, A. E. Kudryavtsev and U.-G. Meißner, *Phys. Lett. B* **589** (2004) 118 [arXiv:nucl-th/0402027].
- [138] V. A. Baru, J. Haidenbauer, C. Hanhart, A. Kudryavtsev, V. Lensky and U.-G. Meißner, arXiv:0706.4023 [nucl-th].
- [139] S. Weinberg, *Phys. Lett. B* **295** (1992) 114 [arXiv:hep-ph/9209257].
- [140] M. Döring, E. Oset and M. J. Vicente Vacas, *Phys. Rev. C* **70** (2004) 045203 [arXiv:nucl-th/0402086].
- [141] E. Epelbaum, *Prog. Part. Nucl. Phys.* **57** (2006) 654 [arXiv:nucl-th/0509032].

- [142] B. Borasoy and H. W. Griebhammer, *Int. J. Mod. Phys. E* **12** (2003) 65.
- [143] S. R. Beane and M. J. Savage, *Nucl. Phys. A* **717** (2003) 104 [arXiv:nucl-th/0204046].
- [144] S. Weinberg, *Phys. Rev. Lett.* **17** (1966) 616.
- [145] V. Bernard, N. Kaiser and U.-G. Meißner, *Int. J. Mod. Phys. E* **4** (1995) 193 [arXiv:hep-ph/9501384].
- [146] T. Becher and H. Leutwyler, *Eur. Phys. J. C* **9** (1999) 643 [arXiv:hep-ph/9901384].
- [147] J. Gasser, H. Leutwyler and M. E. Sainio, *Phys. Lett. B* **253** (1991) 252.
- [148] J. Gasser, H. Leutwyler, M. P. Locher and M. E. Sainio, *Phys. Lett. B* **213** (1988) 85.
- [149] R. Baldini *et al.* [DEAR collaboration], *DAΦNE exotic atom research: The DEAR proposal*, LNF-95-055-IR.
- [150] S. Bianco *et al.* [DEAR Collaboration], *Riv. Nuovo Cim.* **22N11** (1999) 1.
- [151] G. Beer *et al.* [DEAR Collaboration], *Phys. Rev. Lett.* **94** (2005) 212302.
- [152] J. Zmeskal *et al.*, *Nucl. Phys. A* **754** (2005) 369.
- [153] M. Iwasaki *et al.*, *Phys. Rev. Lett.* **78** (1997) 3067;
T. M. Ito *et al.*, *Phys. Rev. C* **58** (1998) 2366.
- [154] C. Curceanu-Petrascu *et al.*, *Eur. Phys. J. A* **31** (2007) 537.
- [155] M. Cargnelli, *Acta Phys. Slov.* **55** (2005) 7;
V. Lucherini, *Int. J. Mod. Phys. A* **22** (2007) 221.
- [156] N. Kaiser, P. B. Siegel and W. Weise, *Nucl. Phys. A* **594** (1995) 325 [arXiv:nucl-th/9505043].
- [157] E. Oset and A. Ramos, *Nucl. Phys. A* **635** (1998) 99 [arXiv:nucl-th/9711022].
- [158] B. Krippa, *Phys. Rev. C* **58** (1998) 1333 [arXiv:hep-ph/9803332].
- [159] J. A. Oller and U.-G. Meißner, *Phys. Lett. B* **500** (2001) 263 [arXiv:hep-ph/0011146].
- [160] B. Borasoy, R. Nißler and W. Weise, *Phys. Rev. Lett.* **94** (2005) 213401 [arXiv:hep-ph/0410305].

- [161] B. Borasoy, R. Nißler and W. Weise, Eur. Phys. J. A **25** (2005) 79 [arXiv:hep-ph/0505239].
- [162] B. Borasoy, R. Nißler and W. Weise, Phys. Rev. Lett. **96** (2006) 199201 [arXiv:hep-ph/0512279].
- [163] J. A. Oller, J. Prades and M. Verbeni, Phys. Rev. Lett. **95** (2005) 172502 [arXiv:hep-ph/0508081].
- [164] J. A. Oller, J. Prades and M. Verbeni, Phys. Rev. Lett. **96** (2006) 199202 [arXiv:hep-ph/0601109].
- [165] J. A. Oller, Eur. Phys. J. A **28** (2006) 63 [arXiv:hep-ph/0603134].
- [166] B. Borasoy, U.-G. Meißner and R. Nißler, Phys. Rev. C **74** (2006) 055201 [arXiv:hep-ph/0606108].
- [167] J. A. Oller, E. Oset and A. Ramos, Prog. Part. Nucl. Phys. **45** (2000) 157 [arXiv:hep-ph/0002193];
- [168] D. Jido, J. A. Oller, E. Oset, A. Ramos and U.-G. Meißner, Nucl. Phys. A **725** (2003) 181 [arXiv:nucl-th/0303062];
- [169] C. Garcia-Recio, M. F. M. Lutz and J. Nieves, Phys. Lett. B **582** (2004) 49 [arXiv:nucl-th/0305100];
- [170] J. Gasser and M. E. Sainio, *Sigma-term physics*, talk given at: 3rd Workshop on Physics and Detectors for DAΦNE (DAΦNE 99), November 16–19, 1999, Frascati, Italy, in: Proceedings "Frascati 1999, Physics and detectors for DAΦNE", Eds. S. Bianco *et al.*, p.659 [arXiv:hep-ph/0002283].
- [171] J. Gasser, *Kaonic atoms in QCD*, talk given at: Workshop on Physics at Meson Factories (DAΦNE 2004), June 7–11, 2004, Frascati, Italy, in: Proceedings "DAΦNE 2004: Physics at Meson Factories", Eds. F. Anulli *et al.*, p.317 [arXiv:hep-ph/0412393].
- [172] R. J. Eden, P. V. Landshoff, D. I. Olive and J. C. Polkinghorne, *The analytic S-matrix*, Cambridge, UK: Cambridge University Press (1966), 295p.
- [173] T. Kinoshita and M. Nio, Phys. Rev. D **53** (1996) 4909 [arXiv:hep-ph/9512327].
- [174] P. Labelle, Phys. Rev. D **58** (1998) 093013 [arXiv:hep-ph/9608491].
- [175] A. Pineda and J. Soto, Nucl. Phys. Proc. Suppl. **64** (1998) 428 [arXiv:hep-ph/9707481].

- [176] A. Pineda and J. Soto, Phys. Rev. D **58** (1998) 114011 [arXiv:hep-ph/9802365].
- [177] N. Brambilla, A. Pineda, J. Soto and A. Vairo, Nucl. Phys. B **566** (2000) 275 [arXiv:hep-ph/9907240].
- [178] M. Beneke and V. A. Smirnov, Nucl. Phys. B **522** (1998) 321 [arXiv:hep-ph/9711391].
- [179] A. Pineda and J. Soto, Phys. Rev. D **59** (1999) 016005 [arXiv:hep-ph/9805424].
- [180] A. Pineda and J. Soto, Phys. Lett. B **420** (1998) 391 [arXiv:hep-ph/9711292].
- [181] V. Antonelli, A. Gall, J. Gasser and A. Rusetsky, Annals Phys. **286** (2001) 108 [arXiv:hep-ph/0003118].
- [182] A. V. Manohar, Phys. Rev. D **56** (1997) 230 [arXiv:hep-ph/9701294].
- [183] A. Czarnecki, K. Melnikov and A. Yelkhovsky, Phys. Rev. A **59** (1999) 4316 [arXiv:hep-ph/9901394].
- [184] S. G. Karshenboim, Phys. Rept. **422** (2005) 1 [arXiv:hep-ph/0509010].
- [185] A. Gall, *Matching in nonrelativistic effective quantum field theories*, PhD thesis, University of Bern, 1999, arXiv:hep-ph/9910364.
- [186] D. B. Kaplan, M. J. Savage and M. B. Wise, Phys. Lett. B **424** (1998) 390 [arXiv:nucl-th/9801034].
- [187] D. B. Kaplan, M. J. Savage and M. B. Wise, Nucl. Phys. B **534** (1998) 329 [arXiv:nucl-th/9802075].
- [188] D. R. Yennie, S. C. Frautschi and H. Suura, Annals Phys. **13** (1961) 379.
- [189] J. Schwinger, J. Math. Phys. **5** (1964) 1606.
- [190] A. Nandy, Phys. Rev. D **5** (1972) 1531.
- [191] T. L. Trueman, Nucl. Phys. **26** (1961) 57.
- [192] J. L. Uretsky and T. R. Palfrey, Jr., Phys. Rev. **121** (1961) 1798.
- [193] S. M. Bilenky, Van Kheu Nguyen, L. L. Nemenov and F. G. Tkebuchava, Sov. J. Nucl. Phys. **10** (1969) 469.
- [194] R. Urech, Nucl. Phys. B **433** (1995) 234 [arXiv:hep-ph/9405341].

- [195] M. Knecht and R. Urech, Nucl. Phys. B **519** (1998) 329 [arXiv:hep-ph/9709348].
- [196] U.-G. Meißner, G. Müller and S. Steininger, Phys. Lett. B **406** (1997) 154 [Erratum-ibid. B **407** (1997) 454] [arXiv:hep-ph/9704377].
- [197] H. Neufeld and H. Rupertsberger, Z. Phys. C **71** (1996) 131 [arXiv:hep-ph/9506448];
H. Neufeld and H. Rupertsberger, Z. Phys. C **68** (1995) 91.
- [198] M. Knecht, H. Neufeld, H. Rupertsberger and P. Talavera, Eur. Phys. J. C **12** (2000) 469 [arXiv:hep-ph/9909284].
- [199] J. Blomqvist, Nucl. Phys. B **48** (1972) 95.
- [200] D. Eiras and J. Soto, Phys. Lett. B **491** (2000) 101 [arXiv:hep-ph/0005066].
- [201] G. E. Pustovalov, JETP **5** (1957) 1234.
- [202] S. G. Karshenboim, Can. J. Phys. **76** (1998) 169.
- [203] S. G. Karshenboim, U. D. Jentschura, V. G. Ivanov and G. Soff, Eur. Phys. J. D **2** (1998) 209.
- [204] J. Gasser, A. Rusetsky and I. Scimemi, Eur. Phys. J. C **32** (2003) 97 [arXiv:hep-ph/0305260].
- [205] J. Bijnens and J. Prades, Nucl. Phys. B **490** (1997) 239 [arXiv:hep-ph/9610360].
- [206] B. Moussallam, Nucl. Phys. B **504** (1997) 381 [arXiv:hep-ph/9701400].
- [207] B. Ananthanarayan and B. Moussallam, JHEP **0406** (2004) 047 [arXiv:hep-ph/0405206].
- [208] S. Descotes-Genon and B. Moussallam, Eur. Phys. J. C **42** (2005) 403 [arXiv:hep-ph/0505077].
- [209] A. Pineda, Phys. Rev. C **71** (2005) 065205 [arXiv:hep-ph/0412142].
- [210] J. Gegelia, Eur. Phys. J. A **19** (2004) 355 [arXiv:nucl-th/0310012].
- [211] H. A. Bethe and E. E. Salpeter, *Quantum Mechanics of One- and Two-Electron Atoms*, Berlin: Springer-Verlag (1957), 368p.
- [212] J. Spuller *et al.*, Phys. Lett. B **67** (1977) 479.
- [213] T. Flügel, *The pion beta decay experiment and a remeasurement of the Panofsky ratio*, PhD thesis, ETHZ, 1999.

- [214] L. Afanasyev *et al.*, *Lifetime measurement of $\pi^+\pi^-$ and $\pi^\pm K^\mp$ atoms to test low energy QCD*, Letter of intent of the experiment at Japan Proton Accelerator Research Complex, DIRAC/J-PARC, Japan, 2002.
- [215] L. Afanasyev *et al.*, *Letter of intent for lifetime measurement of $\pi^+\pi^-$ and $\pi^\pm K^\mp$ atoms to test low energy QCD at the new international research facility at the GSI laboratory*, DIRAC/GSI, GSI, 2004.
- [216] A. C. Betker *et al.*, Phys. Rev. Lett. **77** (1996) 3510.
- [217] L. L. Nemenov, Sov. J. Nucl. Phys. **41** (1985) 629 [Yad. Fiz. **41** (1985) 980].
- [218] L. G. Afanasev *et al.*, Phys. Lett. B **308** (1993) 200.
- [219] M. Knecht and A. Nehme, Phys. Lett. B **532** (2002) 55 [arXiv:hep-ph/0201033].
- [220] J. Gasser, M. A. Ivanov and M. E. Sainio, Nucl. Phys. B **745** (2006) 84 [arXiv:hep-ph/0602234].
- [221] J. Bijnens and F. Cornet, Nucl. Phys. B **296** (1988) 557.
- [222] U. Burgi, Nucl. Phys. B **479** (1996) 392 [arXiv:hep-ph/9602429].
- [223] A. Nehme, Eur. Phys. J. C **23** (2002) 707 [arXiv:hep-ph/0111212].
- [224] B. Kubis and U.-G. Meißner, Phys. Lett. B **529** (2002) 69 [arXiv:hep-ph/0112154].
- [225] B. Kubis and U.-G. Meißner, Nucl. Phys. A **699** (2002) 709 [arXiv:hep-ph/0107199].
- [226] A. Nehme and P. Talavera, Phys. Rev. D **65** (2002) 054023 [arXiv:hep-ph/0107299].
- [227] B. Kubis, *Strong interactions and electromagnetism in low-energy hadron physics*, Dissertation Bonn Univ. (2002). Berichte des Forschungszentrums Jülich, **4007** ISSN 0944-2952.
- [228] V. Bernard, N. Kaiser and U.-G. Meißner, Phys. Rev. D **43** (1991) 2757.
- [229] G. Rasche and W. S. Woolcock, Nucl. Phys. A **381** (1982) 405.
- [230] D. Sigg, A. Badertscher, P. F. A. Goudsmit, H. J. Leisi and G. C. Oades, Nucl. Phys. A **609** (1996) 310.
- [231] G. C. Oades, G. Rasche, W. S. Woolcock, E. Matsinos and A. Gashi, Nucl. Phys. A **794** (2007) 73 [arXiv:hep-ph/0702258].

- [232] K. Melnikov and T. van Ritbergen, Phys. Rev. Lett. **84** (2000) 1673 [arXiv:hep-ph/9911277];
 R. Rosenfelder, Phys. Lett. B **479** (2000) 381 [arXiv:nucl-th/9912031];
 I. Sick, Phys. Lett. B **576** (2003) 62 [arXiv:nucl-ex/0310008];
 H.-W. Hammer and U.-G. Meißner, Eur. Phys. J. A **20** (2004) 469 [arXiv:hep-ph/0312081].
- [233] G. J. M. Austen and J. J. de Swart, Phys. Rev. Lett. **50** (1983) 2039.
- [234] N. Fettes, U.-G. Meißner and S. Steininger, Phys. Lett. B **451** (1999) 233 [arXiv:hep-ph/9811366].
- [235] N. Fettes and U.-G. Meißner, Nucl. Phys. A **693** (2001) 693 [arXiv:hep-ph/0101030].
- [236] N. Fettes, U.-G. Meißner and S. Steininger, Nucl. Phys. A **640** (1998) 199 [arXiv:hep-ph/9803266].
- [237] G. Müller and U.-G. Meißner, Nucl. Phys. B **556** (1999) 265 [arXiv:hep-ph/9903375].
- [238] T. Becher and H. Leutwyler, JHEP **0106** (2001) 017 [arXiv:hep-ph/0103263].
- [239] V. Bernard, Prog. Part. Nucl. Phys. **60** (2008) 82 [arXiv:0706.0312 [hep-ph]].
- [240] U.-G. Meißner, PoS **LAT2005** (2005) 009 [arXiv:hep-lat/0509029].
- [241] P. Büttiker and U.-G. Meißner, Nucl. Phys. A **668** (2000) 97 [arXiv:hep-ph/9908247].
- [242] V. Bernard, N. Kaiser and U.-G. Meißner, Nucl. Phys. A **615** (1997) 483 [arXiv:hep-ph/9611253].
- [243] E. Epelbaum, W. Glöckle and U.-G. Meißner, Eur. Phys. J. A **19** (2004) 125 [arXiv:nucl-th/0304037].
- [244] M. C. M. Rentmeester, R. G. E. Timmermans and J. J. de Swart, Phys. Rev. C **67** (2003) 044001 [arXiv:nucl-th/0302080].
- [245] D. R. Entem and R. Machleidt, Phys. Rev. C **68** (2003) 041001 [arXiv:nucl-th/0304018].
- [246] U.-G. Meißner and S. Steininger, Phys. Lett. B **419** (1998) 403 [arXiv:hep-ph/9709453].

- [247] J. Gasser and H. Leutwyler, Phys. Rept. **87** (1982) 77.
- [248] A. M. Bernstein, Phys. Lett. B **442** (1998) 20 [arXiv:hep-ph/9810376].
- [249] N. Fettes and U.-G. Meißner, Phys. Rev. C **63** (2001) 045201 [arXiv:hep-ph/0008181].
- [250] V. E. Lyubovitskij, Th. Gutsche, A. Faessler and R. Vinh Mau, Phys. Lett. B **520** (2001) 204 [arXiv:hep-ph/0108134].
- [251] V. E. Lyubovitskij, Th. Gutsche, A. Faessler and R. Vinh Mau, Phys. Rev. C **65** (2002) 025202 [arXiv:hep-ph/0109213].
- [252] T. E. O. Ericson and A. N. Ivanov, Phys. Lett. B **634** (2006) 39 [arXiv:hep-ph/0503277].
- [253] J. D. Davies *et al.*, Phys. Lett. B **83** (1979) 55.
- [254] M. Izycki *et al.*, Z. Phys. A **297** (1980) 11.
- [255] P. M. Bird *et al.*, Nucl. Phys. A **404** (1983) 482.
- [256] D. A. Whitehouse, Phys. Rev. Lett. **63** (1989) 1352.
- [257] T. S. H. Lee, J.A. Oller, E. Oset and A. Ramos, Nucl. Phys. A **643** (1998) 402 [arXiv:nucl-th/9804053].
- [258] R. H. Dalitz and S. F. Tuan, Ann. Phys. **8** (1959) 100.
- [259] R. H. Dalitz and S. F. Tuan, Ann. Phys. **10** (1960) 307.
- [260] A. Deloff and J. Law, Phys. Rev. C **20** (1979) 1597.
- [261] V. Bernard, N. Kaiser and U.-G. Meißner, Z. Phys. C **70** (1996) 483 [arXiv:hep-ph/9411287].
- [262] A. M. Bernstein, E. Shuster, R. Beck, M. Fuchs, B. Krusche, H. Merkel and H. Ströher, Phys. Rev. C **55** (1997) 1509 [arXiv:nucl-ex/9610005].
- [263] A. D. Martin, Nucl. Phys. B **179** (1981) 33.
- [264] A. Gal, Int. J. Mod. Phys. A **22** (2007) 226 [arXiv:nucl-th/0607067].
- [265] J. H. Hetherington and L. H. Schick, Phys. Rev. **137** (1965) B935.
- [266] M. Torres, R. H. Dalitz and A. Deloff, Phys. Lett. B **174** (1986) 213.
- [267] A. Deloff, Phys. Rev. C **61** (2000) 024004.
- [268] R. C. Barrett and A. Deloff, Phys. Rev. C **60** (1999) 025201.

- [269] A. Bahaoui, C. Fayard, T. Mizutani and B. Saghai, Phys. Rev. C **68** (2003) 064001 [arXiv:nucl-th/0307067].
- [270] A. Nogga and C. Hanhart, Phys. Lett. B **634** (2006) 210 [arXiv:nucl-th/0511011].
- [271] E. Epelbaum, W. Glöckle and U.-G. Meißner, Nucl. Phys. A **671** (2000) 295 [arXiv:nucl-th/9910064].
- [272] G. Fäldt, Phys. Scripta **16** (1977) 81.
- [273] S. Weinberg, Trans. New York Acad. Sci. **38** (1977) 185.
- [274] R. M. Rockmore, Phys. Lett. B **356** (1995) 153.
- [275] S. Weinberg, Phys. Rev. Lett. **17** (1966) 616.
Y. Tomozawa, Nuovo Cim. **46A** (1966) 707.
- [276] V. Baru, *Pion-deuteron Scattering Length in Chiral Perturbation Theory up to order $\chi^{3/2}$* , talk given at: 11th International Conference on Meson-Nucleon Physics and the Structure of the Nucleon (MENU2007), September 10–14, 2007, Jülich, Germany, to appear in the proceedings.
- [277] A. Rusetsky, *The theory of pionic deuterium: status and perspectives*, talk given at: International Workshop “Exotic hadronic atoms, deeply bound kaonic nuclear states and antihydrogen: present results, future challenges” June 19–24, 2006, ECT*, Trento, Italy, in: Miniproceedings, Eds. C. Curceanu, A. Rusetsky, E. Widmann, p.11 [arXiv:hep-ph/0610201].
- [278] V. Baru, private communication.
- [279] S. S. Kamalov, E. Oset and A. Ramos, Nucl. Phys. A **690** (2001) 494. [arXiv:nucl-th/0010054].
- [280] R. Chand and R. H. Dalitz, Annals Phys. **20** (1962) 1.
- [281] E. Epelbaum, private communication.
- [282] A. Sibirtsev, M. Büscher, V. Y. Grishina, C. Hanhart, L. A. Kondratyuk, S. Krewald and U.-G. Meißner, Phys. Lett. B **601** (2004) 132 [arXiv:nucl-th/0406061].
- [283] V. Y. Grishina, L. A. Kondratyuk, M. Büscher and W. Cassing, Eur. Phys. J. A **21** (2004) 507 [arXiv:nucl-th/0402093].
- [284] A. Partensky and M. Ericson, Nucl. Phys. B **1** (1967) 382.
- [285] E. Lambert, Helv. Phys. Acta **42** (1969) 667.

- [286] G. Rasche and W. S. Woolcock, *Helv. Phys. Acta* **49** (1976) 455.
- [287] G. Rasche and W. S. Woolcock, *Helv. Phys. Acta* **49** (1976) 557.
- [288] H. Pilkuhn and S. Wycech, *Phys. Lett. B* **76** (1978) 29.
- [289] U. Moor, G. Rasche and W. S. Woolcock, *Nucl. Phys. A* **587** (1995) 747.
- [290] A. Gashi, G. Rasche, G. C. Oades and W. S. Woolcock, *Nucl. Phys. A* **628** (1998) 101 [arXiv:nucl-th/9704017].
- [291] A. Gashi, G. C. Oades, G. Rasche and W. S. Woolcock, *Nucl. Phys. A* **699** (2002) 732 [arXiv:hep-ph/0108116].
- [292] G. Rasche, *The derivation of Deser's formula and electromagnetic corrections to the pionium lifetime*, talk given at: International Workshop on Hadronic Atoms and Positronium in the Standard Model, May 26–31, 1998, in: *Proceedings*, Eds. M. A. Ivanov *et al.*, p.66 [arXiv:hep-ph/9807564];
G. Rasche, *Electromagnetic corrections to the lifetime of pionium*, talk given at: HADATOM01 Workshop, October 11–12, 2001, Bern, Switzerland, in: *Proceedings*, Eds. J. Gasser, A. Rusetsky, J. Schacher, p.11 [arXiv:hep-ph/0112293].
- [293] W. B. Kaufmann and W. R. Gibbs, *Phys. Rev. C* **35** (1987) 838.
- [294] T. E. O. Ericson, B. Loiseau and S. Wycech, *Nucl. Phys. A* **721** (2003) 653 [arXiv:hep-ph/0211433].
- [295] T. E. O. Ericson, B. Loiseau and S. Wycech, arXiv:hep-ph/0310134.
- [296] T. E. O. Ericson and L. Tauscher, *Phys. Lett. B* **112** (1982) 425.
- [297] A. Gashi, G. Rasche and W. S. Woolcock, *Phys. Lett. B* **513** (2001) 269 [arXiv:hep-ph/0104059].
- [298] P. Suebka and Y. Yan, *Phys. Rev. C* **70** (2004) 034006.
- [299] I. Amirkhanov, I. Puzynin, A. Tarasov, O. Voskresenskaya and O. Zeinalova, *Phys. Lett. B* **452** (1999) 155 [arXiv:hep-ph/9810251].
- [300] J. Kulpa and S. Wycech, *Acta Phys. Polon. B* **27** (1996) 941.
- [301] G. F. Chew and M. L. Goldberger, *Phys. Rev.* **75** (1949) 1637.
- [302] E. Lipartia, V. E. Lyubovitskij and A. Rusetsky, *Phys. Lett. B* **533** (2002) 285 [arXiv:hep-ph/0110186].

- [303] B. H. Bransden and C. J. Joachain, *Physics of atoms and molecules*, London and New York: Longman (1983), 686p.
- [304] M. J. Zuilhof and J. A. Tjon, *Phys. Rev. C* **22** (1980) 2369.
- [305] F. Gross, *Eur. Phys. J. A* **17** (2003) 407 [arXiv:nucl-th/0209088].